Studies on redox associated molecular changes under salt stress in rice (*Oryza sativa* L.)

By

Manish Pandey

(LIFE01201504006)

Bhabha Atomic Research Centre, Mumbai

A thesis submitted to the

Board of Studies in Life Sciences

In partial fulfillment of requirements

for the Degree of

DOCTOR OF PHILOSOPHY

of

HOMI BHABHA NATIONAL INSTITUTE

June, 2021

Homi Bhabha National Institute[1]

Recommendations of the Viva Voce Committee

As members of the Viva Voce Committee, we certify that we have read the dissertation prepared by **Manish Pandey**entitled "**Study of redox associated molecular changes under salt stress in rice (*Oryza sativa* L.)**" and recommend that it may be accepted as fulfilling the thesis requirement for the award of Degree of Doctor of Philosophy.

Chairman	Dr. T. R. Ganapathi		**Date: 04/06/2021**
Guide / Convener	Dr. P. Suprasanna		**Date: 04/06/2021**
External Examiner	Dr. Alok K. Sinha		**Date: 04/06/2021**
Member 1	Dr. (Smt.) Hema Rajaram		**Date:** 04/06/2021
Member 2	Dr. A. Saini		**Date:** 04/06/2021

Final approval and acceptance of this thesis is contingent upon the candidate's submission of the final copies of the thesis to HBNI.

I/We hereby certify that I/we have read this thesis prepared under my/our direction and recommend that it may be accepted as fulfilling the thesis requirement.

Date: 04/06/2021
Place: Mumbai

Dr. P. Suprasanna
Guide

[1] This page is to be included only for final submission after successful completion of viva voce

STATEMENT BY AUTHOR

This dissertation has been submitted in partial fulfillment of requirements for an advanced degree at Homi Bhabha National Institute (HBNI) and is deposited in the Library to be made available to borrowers under rules of the HBNI.

Brief quotations from this dissertation are allowable without special permission, provided that accurate acknowledgement of source is made. Requests for permission for extended quotation from or reproduction of this manuscript in whole or in part may be granted by the Competent Authority of HBNI when in his or her judgment the proposed use of the material is in the interests of scholarship. In all other instances, however, permission must be obtained from the author.

Manish Pandey

DECLARATION

I, hereby declare that the investigation presented in the thesis has been carried out by me. The work is original and has not been submitted earlier as a whole or in part for a degree / diploma at this or any other Institution / University.

Manish Pandey

List of Publications arising from the thesis

Papers in refereed journal:

1. Pandey M, Paladi RK, Srivastava AK, Suprasanna P. Thiourea and hydrogen peroxide priming improved K^+ retention and source-sink relationship for mitigating salt stress in rice. Sci Rep. 2021; 11(3000).

Conferences:

1. Pandey M, Paladi RK, Thakur A, Srivastava AK, Suprasanna P. Application of thiourea and hydrogen peroxide as ROS modulators in mitigating salt stress in rice. Presented at LSS-2018 on "Frontier in Sustainable Agriculture", 26-28 April 2018 held at BARC, Anushaktinagar, Mumbai, India.
2. Pandey M, Paladi RK, Talla A, Srivastava AK, Suprasanna P. Ameliorative potential of thiourea and hydrogen peroxide to mitigate salt stress induced damage and boost plant growth in rice. Presented at India-EMBO Symposium on "Sensing and signaling in plant stress response" 15– 17, April 2019 held at New Delhi, India.

Manish Pandey

Dedicated to.....

..... My Parents

ACKNOWLEDGEMENTS

As I write this page, I would like recollect the memories from years that have rolled back and register my sincere gratitude for those with whom I was associated and who have helped me in some or the other way. At the outset, I am highly indebted to my research guide Dr. P. Suprasanna, Ex Head, Nuclear Agriculture and Biotechnology Division (NA&BTD), Bhabha Atomic Research Centre (BARC) for his excellent guidance, constructive criticism, and valuable suggestions. It is his vast experience, continuous encouragement and untiring involvement that have brought the present work into a good shape. I would like to express my sincere gratitude to all the members of my doctorial committee Dr. T.R. Ganapathi, Dr. Hema Rajaram and Dr. Ajay Saini- for their suggestions and critical evaluation.

It is my pleasure to express my heartfelt sincere gratitude to Dr. Ashish Kumar Srivastava for his encouragement and youthful attitude. It was a privilege being associated with him and I was greatly benefited by his thorough knowledge, constructive ideas and fine tips on research.

I fall short of words to express my gratitude to Pooja, Radhakrishna, Laxmi, Jincy and Surve ji for all the support they have given me during the past years. I had a wonderful time while working in the laboratory with them as a coworker. I am also grateful to Tejshree, Abhiram, Jayant, Ankita, Amruta and other colleagues of NABTD for their invaluable help and sincere support.

I am also sincerely thankful to Dr. Shantanu Sengupta, Institute of Genomics and Integrative Biology (IGIB), New Delhi for extending the facility for iTRAQ analysis of differential protein expression. I would also like to thank Dr. Sandeep Sharma (Central Salt and Marine Chemicals Research Institute (CSIR–CSMCR),

Bhavnagar, Gujrat for helping me in the analysis of GC-MS based metabolic profiling. My sincere thanks are due to Dr. Sahayog Jamdar, Dr. Shashidhar R, Dr. Jitendra Kumar and Dr. Sachin Hajare, for encouraging and helping me time to time. Special thanks to my close friends Priya, Alka, Bhanu and Manish, who were available and provided their help in every possible way.

I am deeply indebted to my parents for their unconditional love, encouragement and all the moral support. Heartiest thanks are due to my wonderful family and wife Gayatri for tolerating my mood swings related to success and difficulties encountered during all these years. I would like to thank my daughters Gauri and Riddhi. It is their innocence and pranks that kept me lively even during the gloomiest times. They have been my pillar of strength throughout my life. Above all, I thank GOD everyday in my prayer for such wonderful people around me and for HIS GRACE due to which I was able to complete this task.

CONTENTS

Summary

Salt stress is envisaged as one of the major abiotic constrains responsible for limiting the crop productivity worldwide. Various breeding, agronomic and genomics-based approaches have been adopted to manage and/or thrive salt tolerance in economical important crops. One such approach is to use the low-dose application of plant bioregulators (PBRs) to boost the *built-in* defense and confer stress tolerance in plants. Considering this, in the present study, the relative significance of two redox based PBRs including thiourea (TU, non-physiological thiol-based ROS scavenger) and H_2O_2 (a physiologically produced ROS), was evaluated for their capacity to impart salt tolerance.

In spite of having the opposite mode of regulation on ROS levels, both TU and H_2O_2 were able to induce the reducing redox status as indicated by the higher levels of Trolox equivalent and higher fluorescence intensity of redox-sensitive dyes. Besides, better K^+ retention and increased activities of enzymatic antioxidants, such as glutathione reductase, were also observed. All these changes together contributed the invigoration of plant growth under NaCl+TU (NT) and NaCl+H_2O_2 (NH) treatments relative to NaCl alone treatment. Using medium-supplementation approach at seedling stage, it was established that TU and H_2O_2 pre-treatments activated the expression levels of key salt-stress responsive genes like *OsHAK* and *OsLEA*. In addition, the levels of photosynthesis related proteins in the leaf tissue were also increased under NH and NT treatments, as compared to those under NaCl treatment. GC-MS based metabolomics data indicated activation of the salicylic acid signaling and GABA-shunt pathways under NH as well as H_2O_2 alone treatments, whereas shikimic acid and Mal-Asp shunt pathways were found to be activated under NT and TU alone

treatments. The analysis at gene, protein and metabolite levels, identified specific as well as common components associated with NH and NT treatment regulated amelioration of NaCl stress in rice.

Further, in order to establish the agronomic feasibility of TU and H_2O_2 applications, the foliar supplementation approach was applied on field-grown rice plants. A positive upregulation of source-sink equilibrium along with improved yield associated parameters were observed in the plants subjected to TU and H_2O_2 spray, under control as well as NaCl stress. Taken together, the findings concluded that both TU and H_2O_2 can maintain the reduced redox status that serve as "core" regulator for enhancing plant growth and minimizing yield gap, under both lab as well as field conditions.

LIST OF FIGURES

LIST OF TABLES

LIST OF ABBREVIATIONS

1	EC	Electrical conductivity
2	PBRs	Plant bioregulators
3	TU	Thiourea
4	NT	NaCl + Thiourea
5	NH	NaCl + H_2O_2
6	e^-	Electron
7	ROS	Reactive oxygen species
8	FTR	Ferrodoxin dependent thioredoxin reductase
9	NTR	NADPH dependent thioredoxin reductase
10	PC	Protein carbonyl
11	ETC	Electron transport chain
12	PS	Photosystem
13	NPQ	Non photochemical quenching
14	F_v/F_m	Maximum quantum yield
15	SD	Standard deviation
16	iTRAQ	Isobaric tag for relative and absolute quantification
17	GC-MS	Gas chromatography-mass spectrometry
18	ETR	Electron transport rate
19	PS-II	Photosystem -II
20	PS-II Yield	Quantum yield of photosystem -II
21	PCA	Principal component analysis

Chapter 1

Introduction

and

Review of Literature

The rapidly increasing population, concomitant with shrinking of cultivable land, is one of the key challenges for global food security [1]. Further, the erratic climatic conditions-mediated losses in agricultural produce intensify the risk to food security [2]. Considering these factors, the global food production needs to be increased by about 70% of current production rate by the end of 2050 [3]. Salinity is a major environmental factor that constraints the agricultural productivity worldwide [4]. Salinity affects about 20% of global irrigated land which can extended up to 50% by the middle of the century [5]. Salinization of the arable land is a continuous process affected by harsh climatic conditions, poor quality of irrigation water and uneven rainfall pattern [6]. Different approaches including breeding (conventional and mutation), marker assisted selection, biotechnological (transgene-driven approach) as well as agronomical (application of plant bioregulator) have been employed by researchers worldwide to reduce the yield gap under salt stress. Although breeding is considered as the most economical approach, it depends on inherent exploitable genetic variation in germplasm and long-term commitment.

The inherent genetic variation barrier can be overcome by the use of induced mutations which has led to generation of novel variants in the process of damage/repair of the DNA. Mutation breeding has led to development and release of 3364 new crop varieties in different crops for yield, biotic and abiotic stress tolerance (FAO/IAEA; https://mvd.iaea.org/20-03-2021). Additionally, genetic engineering with the aid of transgenic and genome editing tools, has generated some potential salt tolerant lines. At present, however, there are no reports for the field-testing and commercial release of transgenic lines [7].

The application of plant bioregulators (PBRs) has emerged as a complementary approach for traditional as well as newly developed varieties in realistic field conditions. Application of PBRs can capacitate the inbuilt defence system without manipulating the plant

genetic makeup. Most of the PBRs work on the principal of priming, where predisposition of the plant with a mild stressor tunes the whole plant system towards severe stress [8].

Increased ROS production and subsequent disturbances in redox homeostasis are the key components responsible for stress induced damages. Towards this, it can be hypothesised that fine-tuning of the redox homeostasis with the aid of PBRs may ameliorate the stress induced damage. Previous studies in our group have evaluated the ameliorative potential of Thiourea (TU, a "-SH" containing, redox active non physiological ROS scavenger) toward various abiotic stresses [8]. Based on the field trials, the methods of seed soaking and foliar spray of TU are recommended for crop plants (Table 1.3) and a detailed mechanism has been established [8]. On the other hand, Hydrogen peroxide (H_2O_2) initially recognised to be a toxic by-product of aerobic metabolism may also coordinate various important physiological processes in plants under controlled production. Similarly, the exogenous application of hydrogen peroxide (H_2O_2) has been well documented as PBR, showing its potential application towards array of stresses and crop systems (Table 1.4). Since, both of these PBRs belongs to different chemical categories; TU (a redox active, ROS scavenger; Depriming agent) and H_2O_2 (a known ROS, Priming agent), it is interesting to evaluate their effect on ameliorative efficiency towards salt stress and yield enhancement and, further identify the common /discrete component(s) of their mode of action. In the present thesis, a preliminary experiment was carried out using the TU and H_2O_2 supplementation under rice hydroponics system. The results revealed an improved ionic homeostasis and antioxidant capacity under both the treatments. A comparative proteome and metabolome study was also performed to get a mechanics insight of TU and H_2O_2 mediated salt stress amelioration. Further, the study was extended towards small scale pot study for analysing the effect of treatments over source-sink relation. Source-sink relationship defines the metabolic status and equilibrium in source leaf (photoassimilate/sucrose synthesis) and developing sinks (Sucrose utilisation and

storage). This thesis highlights the mechanistic cue for salinity stress amelioration and yield enhancement. The thesis also supports the idea of fine tuning of redox homeostasis prior to stress imposition for boosting the plant's inbuilt defence system.

In this chapter, different aspects of soil salinity, its deleterious effects, and approaches to enhance the salinity tolerance in crop plants are discussed. The sensing, signalling and adaptive mechanisms towards salt stress along with brief information about the plant system and applied bioregulators (TU and H_2O_2) are also summarized. In the end the chapter concludes with the aims and objectives of the present thesis.

1.1. A general introduction to soil salinity

Soil salinity in agricultural terms can be referred as excess deposition of soluble salts in soil. Alternatively, soil salinization can also be referred as a process of increasing the salt index in soil to toxic level for plants [9]. The chlorides of Na^+, Ca^{2+} and Mg^{2+}, and to lower degree, the sulphates and carbonates are mainly responsible for soil salinization [10]. Salinization of the irrigated land is a natural phenomenon and associated with inappropriate agricultural practises like the use of poor-quality water for irrigation, improper drainage, superficial irrigation etc. [10]. Further, the erratic climatic conditions like increase in temperature and associated evaporation rate along with rise in sea level, intensifies the problem of salinization [10]. Soil salinization poses a serious environmental threat for sustainability of land, water and food resources globally, especially within the arid and semi-arid regions [11].

1.1.1. Status of soil salinity in world and India

About 1 billion hectare of total land area [12], with one-fifth of irrigated area globally was reported to be under the influence of salinization [13]. In India, 6.73 Mha area which accounts for 2.1% of the total geographical area, is affected with soil salinity. In India,

salinity affected areas have been grouped into four major agriculturally important regions (Fig 1.1) [9];

1. Semi-arid zone (Indo-Gangetic basin Punjab, Bihar, Haryana, Uttar Pradesh, Delhi, and West Bengal)
2. Arid and semi-arid zone (Gujarat, Maharashtra, Rajasthan and Madhya Pradesh)
3. Peninsular region (Maharashtra, Andhra Pradesh, Orissa, Tamil Nadu and Karnataka)
4. Coastal-alluvial region (Maharashtra, Gujarat, Orissa, Andhra Pradesh, Karnataka, Kerala, Tamil Nadu and Andaman & Nicobar Islands)

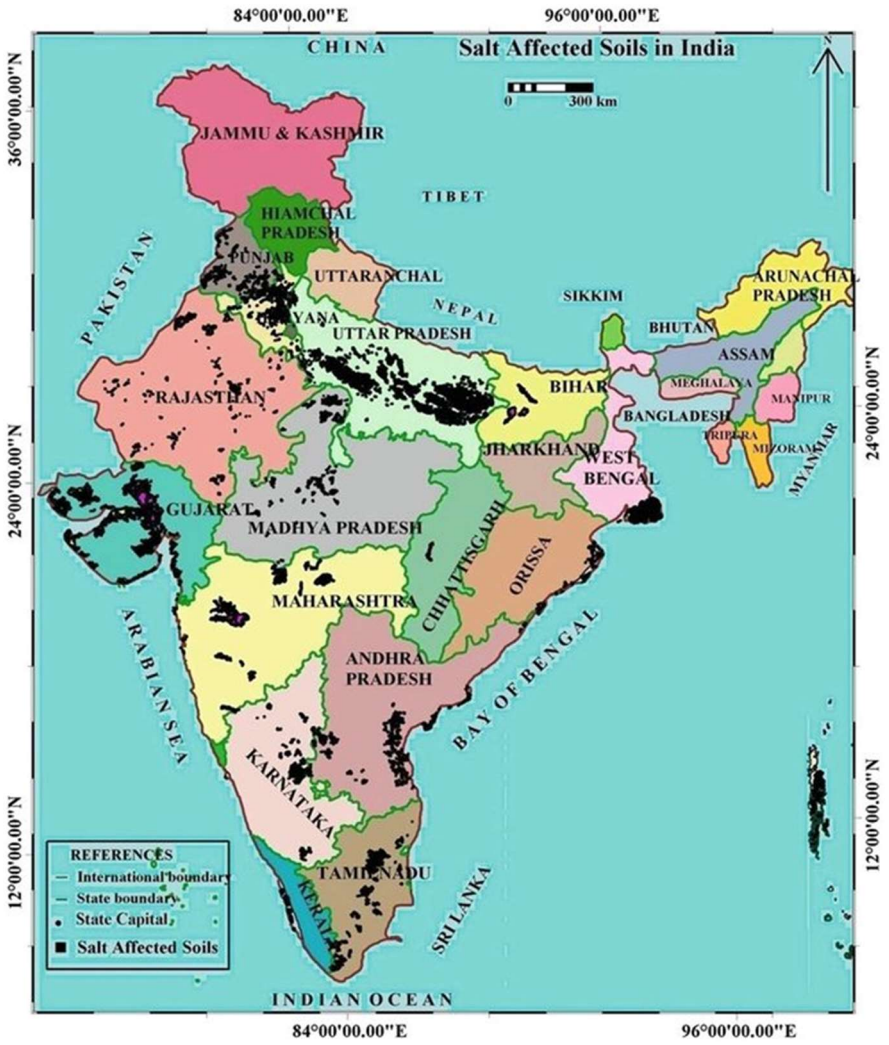

Fig. 1.1: Distribution of soil salinity in India (Adopted; https://cssri.re.in/extent-and-distribution-of salt-affected-soils-in-India/)

Majority of the salt-affected areas (75%) in India are reported to be confined in 5 states; Gujarat (2.23 Mha) being the largest, followed by Uttar Pradesh (1.37 Mha), Maharashtra (0.61Mha), West Bengal (0.44 Mha), and finally Rajasthan (0.38 Mha) [14].

1.1.2. Measurement of soil salinity

The most common method of soil salinity quantification is based on the measurement of electrical conductivity, which is given as deciSiemens per metre (dS/m). Soil showing an EC value of greater than 4 dS/m (corresponding to 40 mM NaCl) along with exchangeable sodium ratio (ESR) < 15%, is defined as saline. The saline soil showing EC value of 4 dS/m is known to create a cellular osmotic pressure equal to 0.2 MPa, imposing an osmotic stress to the plants [10].

1.1.3. Factors responsible for soil salinity

Although parental weathering of the rock is the natural phenomenon associated with salinization of water and land resources, anthropogenic activity mediated secondary salinization is primarily responsible for salinization of irrigated lands. Among the various contributors of secondary salinization, poor quality of irrigation water and agricultural practices (shallow irrigation, improper drainage) leads to increase the salt content in fertile land over a period of time rendering it saline. Additionally, salt precipitation and tidal movement in coastal region also contributes to salinization process [10].

1.2. Effects of soil salinity at plant productivity

Soil salinity is regarded as one of the key challenges to global agricultural production; up to 50-80% yield reduction was reported under moderate salt stress (EC 4-8 dS/m) for most of the important crops [15]. The osmotic and ionic components of salinity negatively affect the water and nutrient balance of the plant, resulting in growth and yield penalty. In cereals, salinity primarily affects various morphological attributes including plant height, tiller number and spikelet sterility [16]. Further, accumulation of toxic ions led to photosynthetic

inhibition, chlorosis and senescence in leaves resulting in yield reduction in crops [17]. The secondary ion specific toxic effects of salt stress are more prominent in older leaves due to inability of vacuole expansions mediated ionic dilution. Premature senescence of older leaves was also considered to be a salt tolerance strategy to save the growing young tissues by sacrificing toxic ion loaded old leaves [18]. The balance of old leaves disposal and young leaf emergence expansion decide the overall photosynthetic capacity and growth of the plant, particularly under salt stress [10].

1.3. Sodium uptake and transport in plants

Presence of excess Na^+ in soil favours the passive transport of Na^+ in root cytoplasm downstream to an established electrochemical gradient. Although, non-selective cation channels (NSCCs) in root plasma membrane contributes a major port of Na^+ entry in plant [19]. Na^+ can also enter through high affinity potassium transporters (HKTs and HAKs) [17]. Additionally, recent reports implicate aquaporins to be to be involved in cellular uptake of Na^+ [20]. After getting its entry in root epidermis, symplastic/apoplastic transport route followed for loading of Na^+ in xylem vessels. Further, the presence of apoplastic barrier including, the casparian strips present within the root endodermis, facilitated the symplastic movement of selective ions towards stele [21]. In rice, the Na^+ might also move across the endodermis via the apoplastic pathway through a bypass in the region showing under developed apoplastic barriers like root tips, origin site of lateral roots as well as young roots [22]. Upon reaching the stele area, xylem loading of Na^+ occurs. Thereafter Na^+ enters and moves across the transpiration stream for its long-distance root- to shoot translocation, finally entering into the leaves (Fig.1.2).

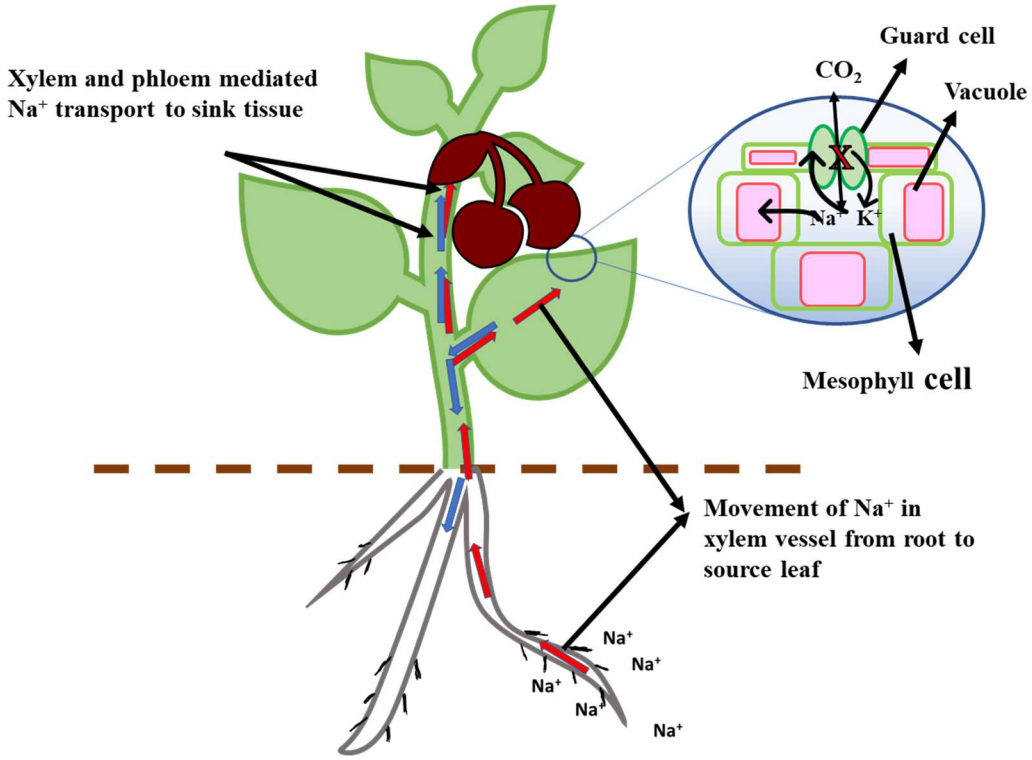

Fig. 1.2: Schematic representation showing entry of Na^+ from soil to plants. Red arrow shows the movement of Na^+ in xylem whereas blue arrow shows the phloem translocation.

Plants are equipped with an efficient system for Na^+ retrieval in xylem tissue with the help of high affinity potassium transporters (HKT) to prevent its long-distance movement in above ground tissue [23]. The overexpression of *HKT* was reported to improve the K^+/Na^+ balance in *Arabidopsis* [24] and rice [25]. In leaves, selective accumulation of Na^+ in vacuoles and epidermis helps in maintaining the photosynthetic efficiency by reducing the cytotoxic Na^+ concentration (Fig. 1.2). Na^+-compartmentalization into vacuoles is mediated by Na^+/H^+ exchangers (NHXs). The over-expression of NHX1 was reported to enhance the salinity tolerances in *Gossypium* [26], *Arabidopsis* [27] and rice [28]. The influx of the Na^+ into guard cell, associated with the K^+ efflux regulating the turgor pressure of guard cell and thereby stomatal conductance [29]. Further, Na^+ enters in the developing sink organs via xylem stream and phloem translocation from source leaves. The accumulation of the Na^+ in

developing sink was reported to decrease the size and strength of sinks, owing to inhibition of cell division and metabolic activities [30].

1.4. Osmotic and ionic imbalance and associated effects on plant physiology

The osmotic stress under salinity imposes the growth inhibition by decreasing the stomatal conductance and water uptake. Further the slow accumulation of Na^+ in the cytosol with concomitant efflux of K^+ disturbs the ionic homeostasis of the cell [29]. Although both Na^+ and K^+ are the most abundant monovalent cations in living organism, Na^+ is a stronger chaotropic agent owing to its smaller ionic and larger hydrated radius [31]. The osmotic stress signalling leads to increased accumulation of osmoprotectants for maintaining the cellular osmotic potential to ensure water availability to plant. On the other hand, the ionic stress specific signalling entails Na^+ extrusion/sequestration from the cytoplasm to ensure plant survival under salt stres**s.** Failure of each of these mechanisms can result in impaired plant growth and survival (Fig. 1.3). The toxic effect of salinity is usually associated with increased accumulation of Na^+ which disrupt the ionic homeostasis (K^+/Na^+) of plant. Intracellular K^+ homeostasis is crucial as it regulates the plant's physiological status like chloroplast development, osmoregulation, stomatal conductance, phloem translocation, cytosolic pH regulation and stabilization of membrane potential [32]. Various enzymes of the carbon metabolism like pyruvate-kinase, ADP-glucose starch synthase and phosphofructokinase, along with protein translation are activated by K^+ [33]. This has highlighted that carbon metabolism is a potential target for Na^+ mediated competitive inhibition. Due to its broad-spectrum regulation over various aspects of physiological and developmental processes, the maintenance of a high K^+/Na^+ ratio in the cytoplasm is recognized as the master switch for salinity tolerance [34].

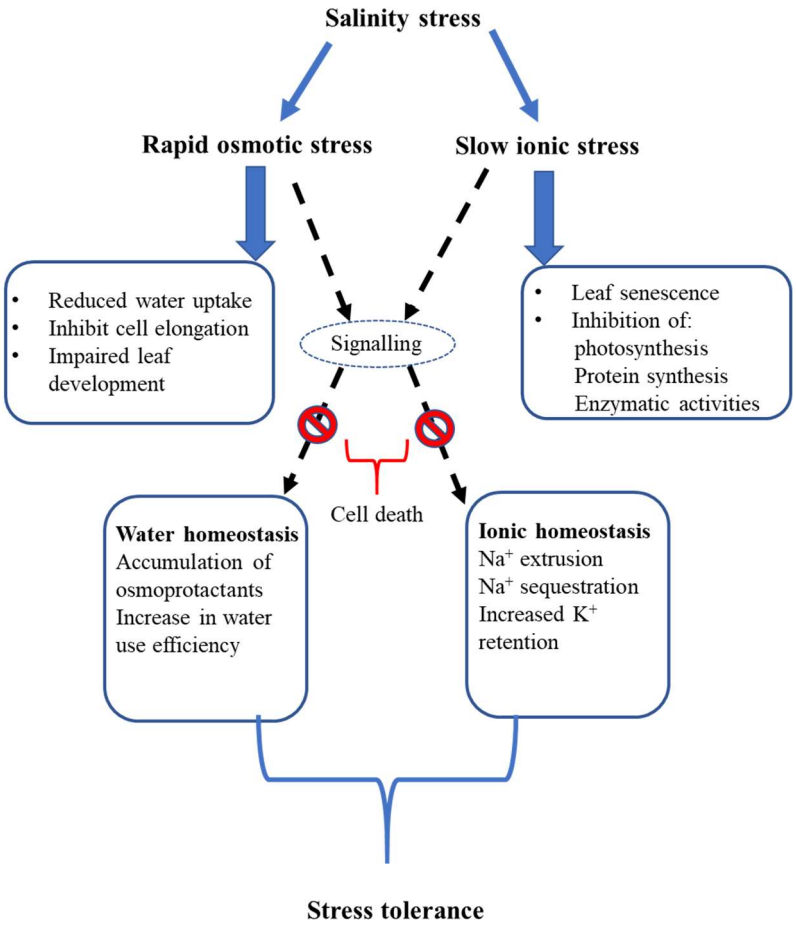

Fig. 1.3: Effects of osmotic and ionic component of salinity on plant physiology

This optimal K^+/Na^+ ratio, especially under stress relies over efficient uptake and xylem loading of K^+ with restricted efflux. Similarly, restricted uptake and xylem loading of Na^+, concomitant with increased efflux from root and vacuolar sequestration are known to improve the ionic homeostasis and thereby salinity tolerance in plants [32].

1.5. Salt stress perception, signalling and adaptations

Plants can sense salt stress by turgor pressure change (HK as osmosensor) with the help of Na^+ specific sensor Glycosyl-inositol phosphorylceramide (GIPC) [35]. Plants can perceive both components of salinity stress with the mediation of intracellular Ca^{+2} oscillations, with higher spike for salt stress than equimolar osmotic stress [36]. Further, salinity mediated increase in ROS and ABA production plays a key role in regulating the damage /repair processes in plants. Thus, co-ordinated action of Ca^{+2}, ABA and ROS

signalling together is involved in the perception and activation of salt tolerant mechanisms (Fig. 1.4). Salinity mediated Ca^{+2}oscillations can be sensed by SOS3 (CBL-4), which then interacts with the protein kinase SOS2 (CIPK- 21; a Ca^{+2} decoder). The formation of SOS3-SOS2 complex, phosphorylates the plasma-membrane localized SOS1 (Na^+/H^+ antiporter), facilitating the Na^+ exclusion from the cytoplasm. The whole process of change in Ca^{+2} oscillation, sensing, decoding and activation of effector protein is very quick and completed within 20 s of salinity exposure [37].

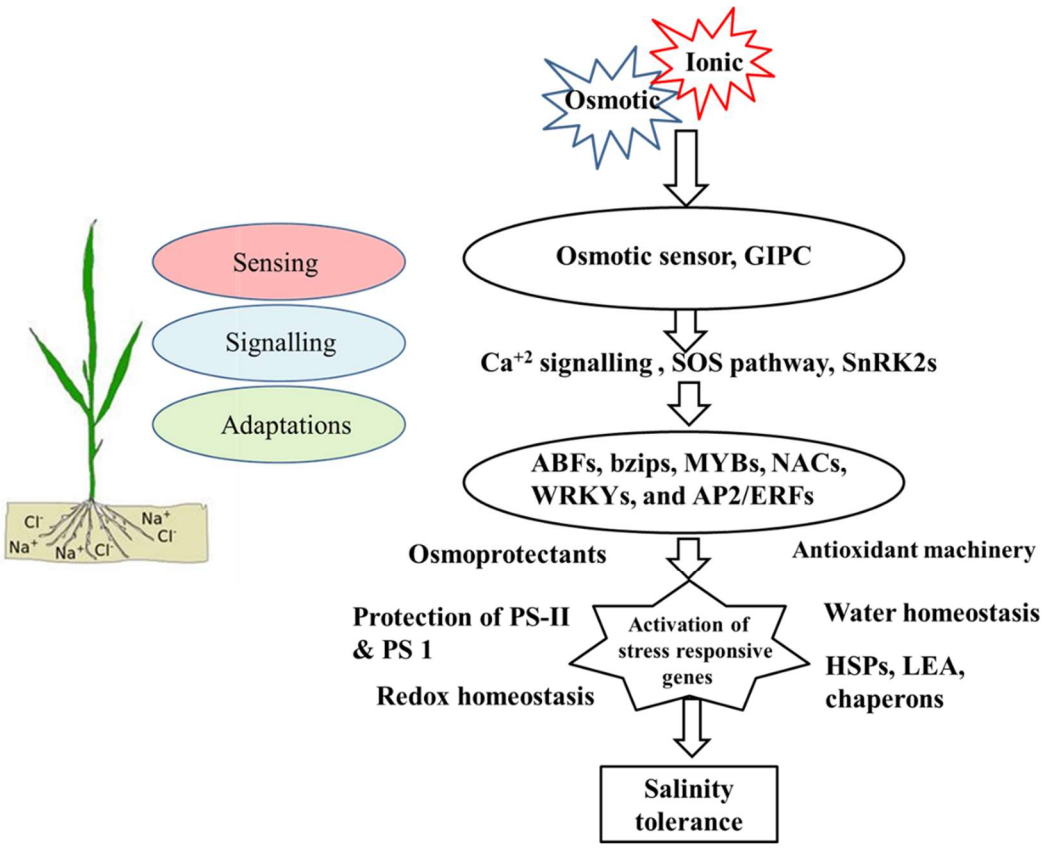

Fig. 1.4: Various processes involved in the sensing, signalling and adaptations of plant towards salt stress

The increased accumulation of ABA under salt stress is an integrative signalling process which involves signal perception, complex signal transduction along with regulation of various stress responsive genes including genes involved in ABA metabolism. The complex signal transduction downstream to salinity perception involves the

participation of various protein kinases like mitogen activated protein kinase (MAPK), SNF1-related protein kinases (SnRKs), calcineurin B-like-interacting protein kinase (CIPK), families along with ABA-responsive transcription factors (TFs), including MYB, NAC, AP2/ERF, WRKY, bZIP for the activation of stress responsive genes [38]. These signalling mediators are involved in boosting the salinity tolerance mechanism by regulating water, antioxidant and ion homeostasis along with activation of defence genes like heat shock protein HSPs, late embryogenic protein (LEA) and chaperones [39].

1.6. Reactive oxygen species (ROS) generation and salt stress responses

Redox homeostasis is recognized as the central regulator controlling plant metabolism, physiology and various developmental processes. The complex interplay of ROS generation and ROS scavenging, regulates the cellular redox homeostasis [40]. Salinity-induced increase in ROS production effectively disrupts the redox homeostasis of plant by shifting the cellular redox status towards oxidising end. The change in cellular redox signal acts as a cellular messenger, showing its affiliation with Ca^{+2}/ABA signalling pathway for activation of salt responsive genes [41]. However, due to the complexity and intermittent cross-talk of different signalling pathways, understanding of redox specific signalling in plant under the changing environmental conditions is currently limited [42].

1.6.1. General introduction to ROS

About 2.7 billion years ago, primitive photosynthetic organisms introduced molecular oxygen (O_2) to the reducing environment of the earth, out-turning with the inevitable ROS production under aerobic metabolism [43]. It has been estimated that about 1 - 2% of total O_2 used in plant's metabolism is redirected for ROS production in different subcellular compartments [44]. Atmospheric O_2 in its ground state (triplet oxygen, $^3O_2$) is less reactive due to parallel spins of unpaired electrons in different molecular orbitals. However additional energy mediated spin transition in electron spins led to initiate the process of ROS

production. The additional energy for this transition is supplied by biochemical reactions, electron transport chains (ETC), and radiations [45]. The different ROS members are subsequently formed as products of O_2 reduction depicted in Fig 1.5.

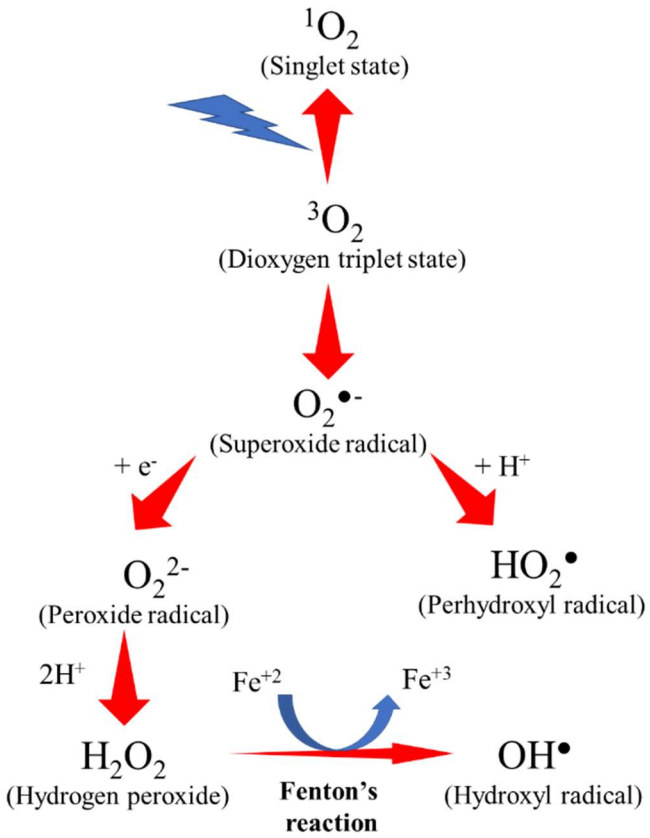

Fig. 1.5: ROS generation by energy and electron transfer (Source; [44])

In the biological systems, superoxide radicals ($O_2^{\bullet-}$) are originated as the primary ROS by single electron transfer to molecular O_2. Further, a series of reactions which include reduction, protonation and dismutation of intermediated species led to formation of various ROS [44]. Additionally, transition metal induced formation of hydroxyl radical ($OH^{\bullet}$) by Fenton-type reactions complement the ROS production. The different members of the ROS family have different characteristics Table 1.1.

Table-1.1: Characteristics of ROS (Source; [44])

ROS	Half life	Distance travelled	Origin	Reactivity			Attenuating system
				DNA	Proteins	Lipids	
Singlet oxygen ($^1O2$)	1-4 μs	30 nm	Chloroplast Mitochondria Membranes	Reacts with G-residue	Reacts with Trp, His, Tyr, Met and Cys	PUFA	Carotenoids and Tocopherols
Superoxides ($O_2^{\bullet-}$)	1-4 μs	30 nm	Chloroplast Mitochondria Membranes Cytoplasm Peroxisomes	No	Reacts Fe-S centres	very low	Superoxide dismutases
Hydroxyls ($OH^{\bullet}$)	1 μs	1 nm	Chloroplast Mitochondria Membranes	Very high	Very high	Very high	Flavonoids and Proline
Hydrogen peroxide (H_2O_2)	1 ms	1 μm	Chloroplast Mitochondria Peroxisomes Membranes	No	Cys	Very low	Catalase, Peroxidases and Flavonoids

1.6.2. ROS disrupts redox homeostasis and induces oxidative stress

Cellular energetic of a living organism is regulated by various redox reactions (e^- transfer reactions) particularly in chloroplast, mitochondria and peroxisomes [46] resulting in ROS production. Although ROS are originated as the toxic by-product of these redox reactions, their basal level is indispensable for normal growth and signalling [47]. The low level of ROS is reported to be involved in redox signalling for activating signalling cascades for maintaining normal plant physiology. On the other hand, a high level of ROS is linked

with increased oxidative damage. Thus, a delicate balance between the ROS production and antioxidant capacity defines the plant's behaviour towards normal physiology or stress specific response (Fig. 1.6). The insufficient antioxidant capacity mediated increase in intracellular ROS destabilises the cellular function by inducing oxidation of lipid, DNA, proteins and carbohydrates [45].

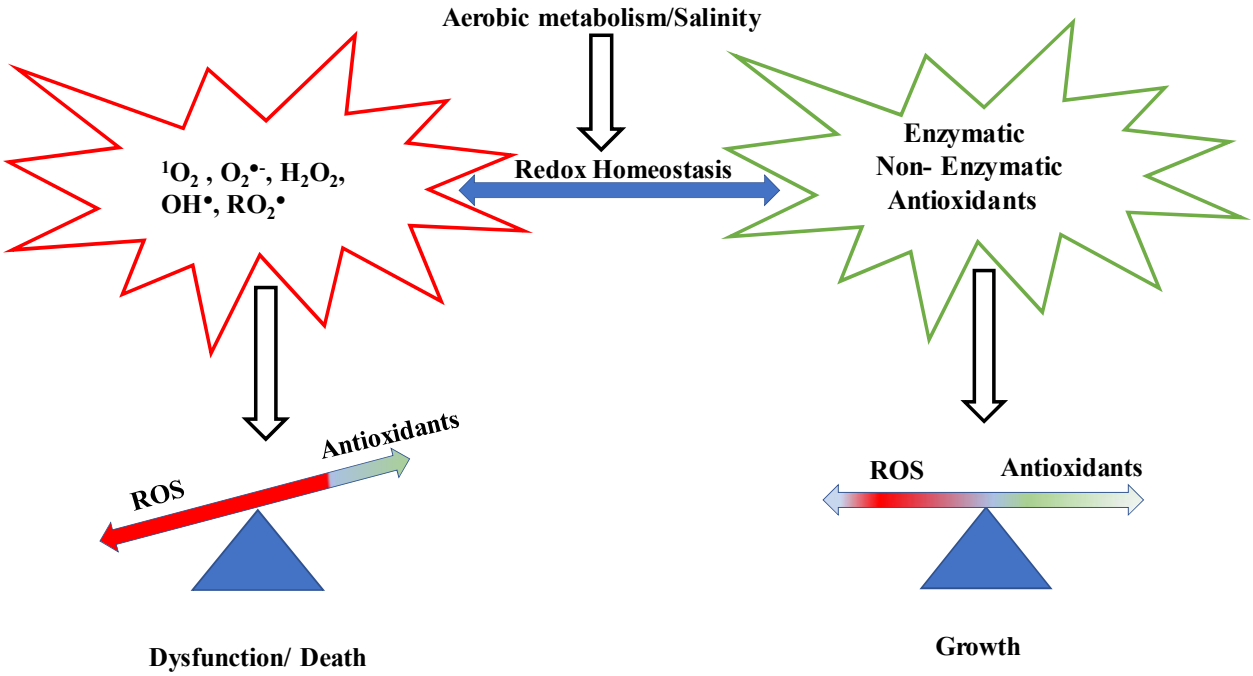

Fig. 1.6: Schematic representation of redox homeostasis. Salinity disturbs the equilibrium between antioxidant and ROS production and antioxidant systems causing oxidative stress.

1.6.3. Lipids as ROS target

Lipid as a major constituent of the plasma membrane assembly, are involved in adaptation towards changing environments. Increased ROS level under stress initiates the formation of lipid peroxides by lipid peroxidation reaction. The double bond between C atoms (unsaturated fatty acids) and the ester linkage between glycerol and fatty acids are the potential target site of ROS for the formation of lipid peroxides. The accumulation of lipid peroxidation products like acrolein, malondialdehyde (MDA) and 4-hydroxy-(E)-2-nonenal (HNE) in plant mediated their toxic effects due to their high affinity towards proteins [48].

The HNE mediated inhibition of the mitochondrial respiration [49] and MDA mediated deregulations of the Oxygen evolving complex have been reported [50]. Further, the free movement of the lipid peroxidation products across the membrane facilitate the covalent modification of the proteins throughout the cell. Identification of 39 oxidatively modified proteins in different subcellular organelles in *Arabidopsis* was also reported under salt stress [51]. The various protein targets of the lipo-oxidation are listed in the following table (Table 1.2).

Table-1.2: Summary of proteins targets of lipid-oxidation under salt stress (source: [51])

Proteins	**Plant**
Oxygen evolving complex (OEC33)	*S. oleracea*
Light harvesting complex proteins (LHCP)	*A. thaliana*
Luminal binding protein	*A. thaliana*
α- keto glutarate dehydrogenase	*S. tuberosum*
Pyruvate dehydrogenase complex	*S. tuberosum*
NAD- malic enzyme	*S. tuberosum*
Triose phosphate isomerase	*A. thaliana*
Phosphoglucomutase	*A. thaliana*
Cysteine synthase	*A. thaliana*
Ascorbate peroxidase	*A. thaliana*
Peroxidase	*A. thaliana*
Heat shock protein (Hsp 70)	*A. thaliana*
Cyclophilins	*A. thaliana*
Nucleoside diphosphate kinase	*A. thaliana*
Germin like protein	*A. thaliana*
Leucine aminopeptidase	*A. thaliana*

1.6.4. Proteins as ROS target

Under oxidative stress, the increased level of ROS can also target proteins with oxidation of any proteinogenic amino acid. Although, ROS can oxidise any amino acid, the functional consequences depend on the type of amino acids oxidised like cysteine (Cys) modification has more detrimental effect compared to methionine (Met) modification [52]. The ROS mediated post translational modifications of proteins (nitrosylation, carboxylation, glutathiolation and disulphide bond formation) are reported to regulate the activity of various enzymes under stress condition. Such modifications under stress conditions can also mediate loss of protein functions involved in regulation of metabolic, transport and regulatory pathways [52]. Under severe oxidative stress, accumulation of toxic protein aggregates can also induce programmed cell death [53]. A reversible/irreversible Cys modification under stress regulates the downstream signalling towards adaptation or programmed cell death. The reversible Cys modification constitutes an important mechanistic approach for regulating the protein activity with redox buffering capacity. Additionally, ROS mediated protein carbonylation (PC) results in drastic change in physiochemical properties of the proteins [54] leading to their inactivation. The oxidation of the side chains of amino acids, especially proline, threonine, lysine and arginine, is thought of as a primary protein carbonylation reaction, generating products detectable with 2,4-dinitrophenylhydrazine. By contrast, the addition of aldehydes produced during lipid peroxidation results in 'Secondary protein carbonylation' reaction. Addition of reactive carbonyl group in the protein chain alters protein characteristics like intermolecular cross linking, functionality and degradation kinetics. ROS mediated increase in level of protein carbonylation has been reported under various abiotic stresses including salinity [51].

1.6.5. DNA as ROS target

Although oxidative damage to DNA is well established in animal systems, the genetic complexity and efficient DNA repair system of the plants contribute towards minimising the oxidative stress [55]. Abiotic stresses mediated nucleic acid oxidation has been reported under various biotic and abiotic stresses [56]. Increased ROS level (particularly $OH^{\bullet}$) mediated oxidation of deoxyribose sugar, along with accumulation of toxic products of nucleotide base oxidation products destabilised the integrity of DNA and promote irreparable cross-linking, leading to programmed cell death in plants [45]. The activation of the plant antioxidant defense systems in different subcellular compartments like peroxisomal catalase and cytosolic ascorbate peroxidase have been shown to work in tandem with the nuclear glutathione and peroxiredoxin to minimise the ROS load and in maintaining integrity of plant genome [45].

1.7. ROS defense machinery

Plants are well equipped with very efficient endogenous defense mechanisms for ROS detoxification [44, 45]. The detoxification of ROS, employing enzymatic/non-enzymatic approaches together constitute plant's antioxidant machineries (Fig. 1.7). Antioxidants, are the compounds having an inherent capability to donate its electron to ROS, thereby neutralising it. The oxidised products of the antioxidant formed during ROS attenuation processes are either less reactive or can be reduced back to its original form with a set of complex reactions. Ascorbate and glutathione are the chief water-soluble antioxidants found in almost all compartment of the plant cells along with phenolics and flavonoids**.** Similarly, carotenoids and α-tocopherols (vitamin E) are known to be the lipid-soluble antioxidants in plants. On the other hand, various enzymes like catalase (CAT), superoxide dismutase (SOD), monodehydroascorbate reductase (MDHAR), ascorbate peroxidase (APX), dehydroascorbate reductase (DHAR), glutathione reductase (GR), glutathione S-transferase

(GST), glutathione peroxidase (GPx), peroxiredoxins, (Prxs), thioredoxins (Trxs) glutaredoxin (Grx) etc., together constitute the enzymatic antioxidant defense. The upregulation of both non enzymatic and enzymatic antioxidant defences under stress is considered as protective mechanism for neutralising the damaging effect of ROS under oxidative stress.

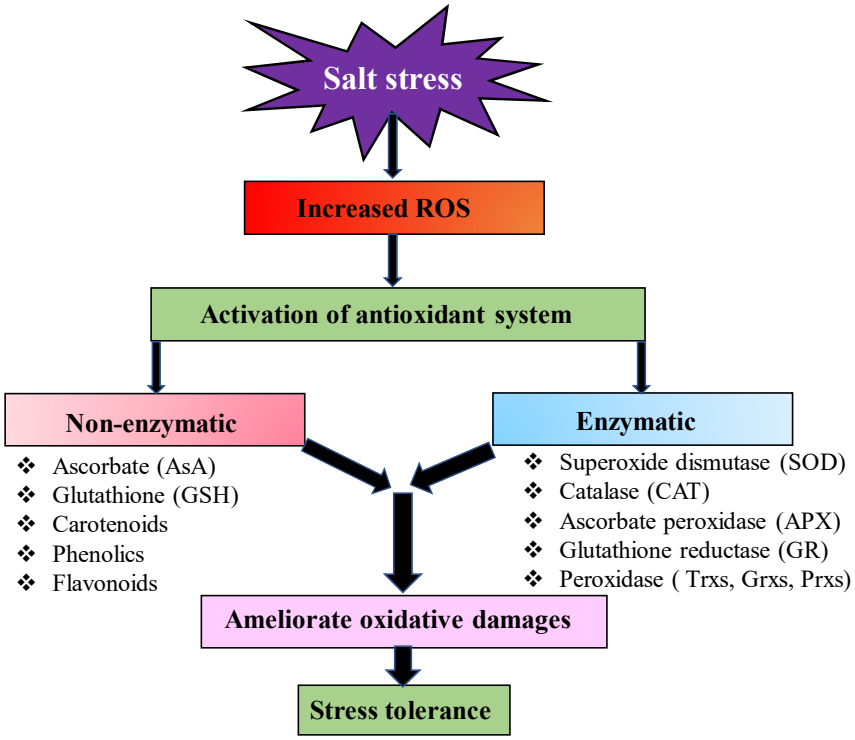

Fig. 1.7: Schematic depiction of activation of enzymatic/non-enzymatic antioxidant machinery under salt stress

1.7.1. Enzymatic antioxidant systems

1.7.1.1. Superoxide dismutase (EC 1.15.1.1)

Superoxide dismutases (SODs), the ubiquitous metalloenzymes, constitute the first barrier of enzymatic protection against ROS. These are involved in detoxification of superoxide radicals by dismutating it into H_2O_2 and limiting the $OH^{\bullet}$ production via Haber–Weiss reaction [57]. The metallic cofactor present in the active site guides the further classification of SODs into three main groups (Cu/Zn-SOD, Mn-SOD and Fe-SOD). Cu/Zn-

SOD is considered to be the most abundant isoform present within various cellular compartments including the chloroplast, mitochondria, cytosol, peroxisomes and apoplast. On the contrary, Fe-SOD and Mn-SODs are reported to be localised specifically in chloroplast and mitochondria respectively [58]. In rice, the over expression of *Mn-SOD* [59] and *Cu/Zn SOD* [60] was shown to confer drought and salinity tolerance. Similarly, priming mediated salinity amelioration in rice was also correlated with efficient activation of antioxidant enzymes including SOD [61].

1.7.1.2. Catalase (CAT: EC 1.11.1.6)

Catalase is a tetrameric heme-containing enzyme which works in co-ordination with SODs for quick disintegration of H_2O_2, generating harmless products like H_2O and O_2. Catalase, is an important enzyme of the enzymatic antioxidant system due to its ubiquitous presence, non-dependency for reducing equivalents and showing higher turnover rate for H_2O_2 decomposition (26 x $10^6 s^{-1}$) [62]. Various cellular compartments like peroxisomes, mitochondria, and cytosol are enriched with CAT activity [63]. A fine regulation of H_2O_2 level and downstream signalling in plant cells is achieved through the synchronized activity of CAT and APX, constituting main component of H_2O_2 scavenging system. Differential expression and affinity of CAT and APX in plant cells; CAT (peroxisomal; high K_m) and APX (diverse subcellular compartments; low K_m) have been shown to mediate the stress responses [64]. Catalase activity is a known to be essential for the protection of photosynthetically-active cells from oxidative stress triggered by various abiotic stresses, including salt stress [65]. Overexpression of *E. coli CAT* gene in rice has been reported to increase the salinity tolerance in rice [66]. The activation of catalase activating STRK1 protein has also been reported to lower accumulation of H_2O_2 with increased salinity tolerance in rice [67].

1.7.1.3. Ascorbate peroxidase (EC: 1.11.1.11)

Akin to catalase, ascorbate peroxidase (APX) also contributes towards detoxification of H_2O_2 in various cellular compartments. Although both the enzymes share their functionality, differences exist in term of affinity toward H_2O_2 and use of reducing equivalent as electron donors. Ascorbate peroxidase acts as a bridge for enzymatic/nonenzymatic antioxidant machinery with the mediation of "ascorbate-glutathione (AsA-GSH) cycle". Briefly, this cycle entails the direct involvement of AsA as an electron donor for APX activity is accompanied with re-reduction of resultant dehydroascorbate (DHA) with glutathione and glutathione reductase [68]. Activation of AsA-GSH cycle has been reported to be a predominant pathway of ROS detoxification in photosynthetically-active cells, through the mediation of the water-water cycle. The electron leaking at PSI photosystem led to formation of $O2^{\cdot-}$, which subsequently got dismutated into H_2O_2 and finally water with the mediation of chloroplastic SOD and APX [69].

In plants, ascorbate peroxidases are specified by small gene families, their expression being regulated by expression spatial and developmental cues, in addition to diverse environmental factors [70]. The rice *APX* gene family consists of eight members, each subcategory [cytosolic (*cAPX*), microsomal (*mAPX*), mitochondrial (*mitAPX*) and chloroplastic], each having two members, with one member being associated with chloroplastic stroma (*sAPX*) and one present as bound to thylakoids (*tAPX*)] [71]. Earlier studies highlighted the importance of APX in maintaining the redox homeostasis under various abiotic stresses. Over-expression of the cytosolic *APX* [72] and thylakoid bound *APX* in tobacco confers tolerance towards osmotic and salt stress [73].

1.7.1.4. Glutathione reductase (GR: EC 1.8.1.7)

Glutathione reductase is a homodimeric enzyme (110 kDa) of NADPH-dependent oxidoreductase family having FAD as prosthetic group. It is ubiquitously present in all living

organisms and subcellular compartments including chloroplasts, cytosol, and mitochondria [74]. Nevertheless, in the photosynthetic tissues more than 80% activity is contributed by its chloroplastic isoform [74]. Glutathione reductase, as an important player of the AsA-GSH cycle is known to play a crucial role in the reactivation of antioxidant pools (AsA and GSH) utilising NADPH as reductant. Glutathione as a central regulator of the redox homeostasis is involved in maintenance of GSH/GSSG and AsA/DHA ratio. Further the redox status mediated change in GR conformations regulates the catalytic activity of GR. In the absence of thiols, GR tends to form higher order forms, including tetramers. Although these higher order forms exhibit catalytic activity, under cellular conditions GSH keeps the enzyme as a dimer [75]. Further studies on GR indicate that GR exhibits an increased activity under various abiotic stresses across plant species [76]. Suppression of chloroplastic *GR* was also associated with an increased sensitivity to compounds such as methyl viologen, cadmium stress and UV-B stress in transgenic tobacco [77]. Overexpression of *S. lycopersicum NAC2* transcription factor (*SlNAC*$_2$) in *Arabidopsis* enhanced the salinity tolerance by positive regulation of GR activity [78].

1.7.1.5. Thioredoxins and Glutaredoxins

In plants, thioredoxins (Trx) and glutaredoxins (Grx) are reported to be the components of a redox system which regulates the dithiol-disulfide exchanges of target proteins (Fig. 1.8); thereby mediating important roles in redox signalling during plant development and adaptation to various stresses [79]. Plant thiols, redox state and regulation of cysteinyl thiol groups in proteins including signalling components such as transcription factors, are emerging as core components during plant stress adaptation. The plant Trxs and Grxsare associated with regulation of plant metabolism, development, phytohormone responses, and stress adaptations [79]. These proteins are encoded by large gene families, and their enormous diversity suggests either functional specialization or extensive redundancy. So far,

about 50 genes encoding Trx and Trx-like proteins and approximately 30 Grxs encoding genes have been identified in higher plants. In plants, the regeneration of oxidized Trxs and Grxs is achieved via distinct pathways (Fig.1.8). While most Grxs utilize reduced glutathione as an electron donor, Trxs reduction is more complicated and subject to their cellular localization. Cytosolic and mitochondrial Trxs are known to be reduced by NADPH-thioredoxin reductases (NTR), which contain a double Cys motif in their catalytic centres and use a flavine cofactor. On the other hand, an iron-sulfur (Fe–S) protein, the ferredoxin-dependent thioredoxin reductase (FTR) which moves electrons from PS I to thiol reducing cascades, reduces the chloroplastic Trxs in a light-dependent manner.

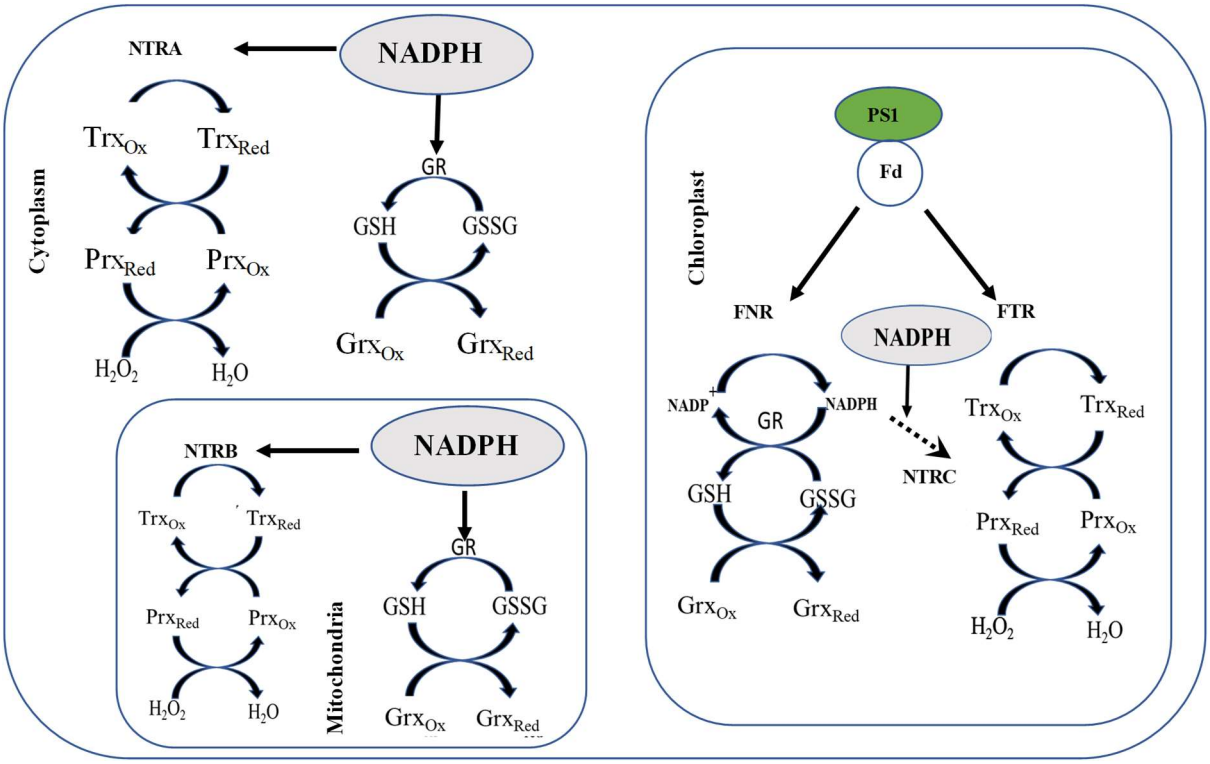

Fig.1.8: Thioredoxin (Trx) and Glutaredoxin (Grx) systems in various subcellular compartments (Source; [80])

Reduced thioredoxin, in turn supplies the reducing power to various peroxidases involved in the protein modification via disulphide-reductase (S-S to SH), removal of toxic

lipid peroxidation products and reversal of RNS mediated protein nitrosylation [80]. The thioredoxin dependent peroxidases form an import family of redox regulatory protein known as peroxiredoxins (Prxs). The Prxs targeted processes are thought to regulate gene expression, post-transcriptional and post-translational regulation, as well as modulation of metabolic pathways in plants [81]. In all higher plants, a set of six Prxs are known to be expressed, including 1-CysPrx (implicated in plant embryogenesis), Prx Q and 2-Cys Prx (plastidial) and one each of cytosolic, mitochondrial, and plastidial type II Prxs [82]. In *Arabidopsis*, proteomic analysis identified mitochondrial Prx IIF and cytosolic Prx IIE and IIB as S-nitrosylation targets in plants exposed to gaseous NO [83]. In tobacco, the 2-Cys Prx, was shown to be essential for H_2O_2 scavenging, thereby protecting photosynthetic function [84] under high light and drought stress respectively. Similarly, glutathione dependent peroxidases bridge the non-enzymatic /enzymatic pathway of redox homeostasis.

Cytosolic NADPH-dependent thioredoxin reductases (*NTRA*), have been shown to regulate cellular ROS levels in plants, resulting in improved tolerance to drought and oxidative stress [85]. Treatment with methyl viologen, which induces oxidative stress by promoting ROS accumulation, was shown to upregulate the expression of *NTRA*. Moreover, Overexpression of *NTRA* resulted in reduced ROS and consequently higher survival rate in plants when exposed to oxidative stress, relative to wild-type and knockout lines.

1.7.2. Non-enzymatic antioxidant system

Ascorbate and glutathione mediated scavenging of ROS constitute an important non enzymatic antioxidant system in plants [86]. A relative high concentration (mM range) was reported in *A. thaliana*, with the highest AsA (22.8 mM) and GSH (14.9 mM) concentrations in peroxisome and mitochondria respectively [86]. Further, AsA mediated redox buffering capacity in the apoplast, influences the signalling and growth response under oxidative stress [87]. Moreover, regeneration of α-tocopherol (vitamin E) from tocopheroxyl radical was also

reported to be AsA-dependent and thereby protecting the plasma membranes from ROS mediated destabilisation [45]. Carotenoids as an antioxidant system, contributes towards maintaining the structural integrity of the photosystems, including light harvest complex and thylakoid membrane. The presence of carotenoids in the photosystem facilitates its active participation towards light harvesting, ROS scavenging and excess energy dissipation by non-photochemical quenching [88]. Increased expression of key regulator of the AsA-GSH cycle and isoprene synthesis (carotenoids biosynthesis) was reported to enhance the plant performance under stress conditions [86]. Additionally, flavonoid and phenolics (secondary metabolites of the plant's metabolism) have also been shown to have great potential of ROS scavenging and reducing the ROS mediated damages [89]. The salinity tolerance with upregulation of the genes associated with flavonoid biosynthesis in *Nicotiana* [90] along with increased accumulation of phenolic content in tolerant rice cultivars under salt stress [91] signifies the importance of secondary metabolites for ameliorating salt stress in plants.

1.8. Redox homeostasis in Chloroplast

In plants, chloroplasts are the prime site for ROS productions may contribute to several times higher production rate compared to mitochondria [45]. Salinity mediated rapid closure of stomata limit the CO_2 diffusion and fixation in leaf measophyll tissue. Impairment of the photosynthetic CO_2 fixation under salt stress is coupled with overreduction of chloroplastic ETC and increased ROS production [92]. The overreduction of chloroplastic ETC facilitates the leaking of electrons from PS1 reaction centre to $O_2$and generates $O2^{\bullet-}$ (Fig. 1.9). The redox homeostasis in the chloroplast is maintained by Cu-Zn superoxide dismutase, peroxiredoxin (2Cys-Prx), APX and ascorbate pool in the vicinity of PS-I, converting the $O2^{\bullet-}$ back to H_2O (water -water cycle) [45].

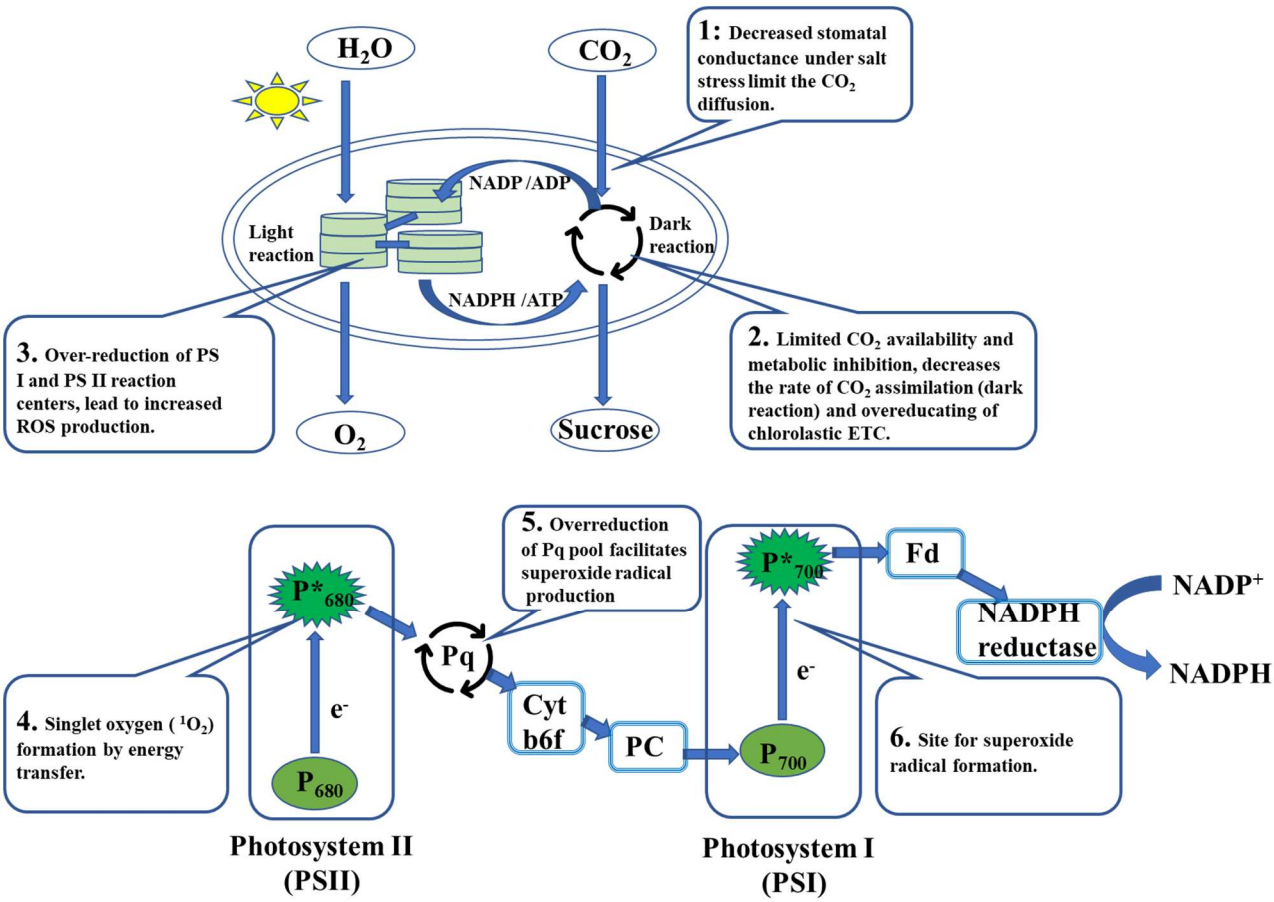

Fig. 1.9: Schematic depiction of ROS production in chloroplast (Number corresponds to series of event under salt-stress)

In the PSII, release of electrons from plastoquinone (Pq) electron acceptors is responsible for the generation of $O_2^{\bullet-}$ [69]. The subsequent electron transfer in the series of ROS formation can transform $O_2^{\bullet-}$ into other toxic intermediates form like $OH^{\bullet}$ with the mediation of H_2O_2 intermediate and Fenton reaction at the Fe-S centres. Similarly, over-reduced electron transport chain (ETC) under stress conditions facilitated the generation of the singlet oxygen ($^1O_2$) by transfer of excitation energy at the PS-II reaction centre. Singlet oxygen ($^1O_2$) can cause extensive tissue damage by lipid peroxidation and damage membrane proteins posing PS II reaction centre at risk [93, 42]. The nonphotochemical quenching mediated excess energy dissipation along with positive regulation of The H_2O_2 produced in the "Mehler-reaction" regulated the production of ROS at PSII reaction centre. Non-efficient

chloroplastic ROS scavenging mechanisms enhance the salt sensitivity in plants [94], while maintenance of the ROS homeostasis has been shown to be an important target for salinity tolerance in plant. Various chloroplastic proteins involved in the light reaction, such as LHC chlorophyll a-b binding proteins (LHC-CAB), PS II chlorophyll-binding protein 47 (CP47) and Oxygen evolving complex (OEC) have been shown to play an important role towards coping with the salinity stress and regulating the activity of PSII [95]. Increased expression of the OEC and CP47 was also correlated well with decreased degradation of D1 protein to ensure optimal PSII functions [96].

1.9. ROS homeostasis in mitochondria

Mitochondria harness the energy of fixed carbon resources via cellular respiration. Being actively involved in the aerobic respiration, mitochondria encounter an increased risk of ROS production [97]. Although mitochondria contribute to relatively less ROS production compared to chloroplast and peroxisome, however it turned to be the major site for ROS production in non-green tissues or under dark conditions [98]. In general, complex 1 and complex III of the Mt ETC are known to be the major sites for generation of ROS (Fig. 1.10). Formed at complexes I and III, the ubisemiquinone intermediate serves as the principal electron donor to oxygen, and primary determinant of the mitochondrial functioning [99]. Increased energy input for the management of salinity mediated imbalance in ROS, ionic and osmotic homeostasis affect the mitochondrial functioning [100].

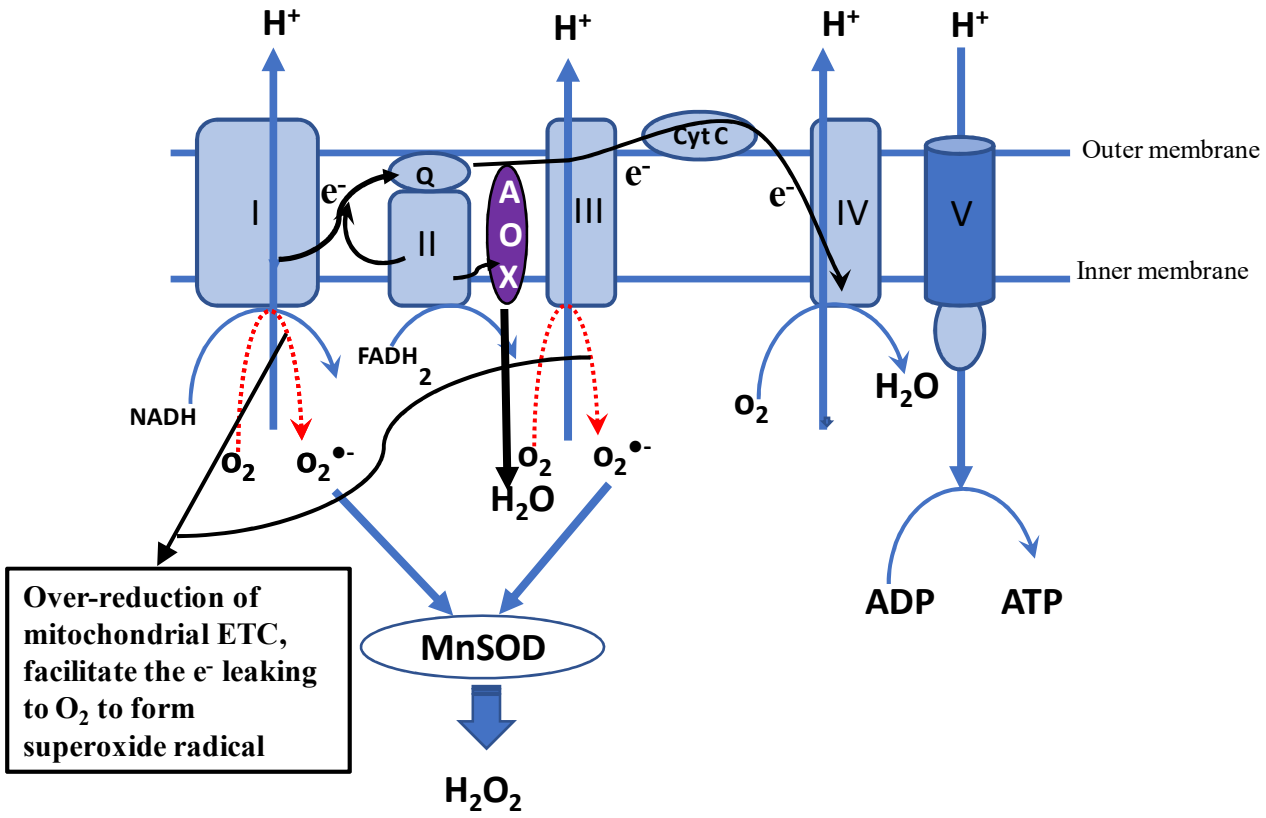

Fig. 1.10: Schematic depiction of ROS generation in mitochondria

Salinity mediated increased expression of Mn-SOD [59], alternative oxidase (AOX) along with constituents of F1Fo ATP synthase complex have been reported to maintain the mitochondrial functioning and improve salinity tolerance in plant system [40]. Mitochondrial AOX can prevent over-reduction of the Mt ETC by transferring electrons from reduced ubiqunone to O_2. As a result, complex III along with complex IV are rescued from overreduction and excess ROS production [101]. Alternate oxidase transfers electrons from ubiquinol to molecular oxygen and serve as an alternative electron exit of the ETC. This permits the exclusion of, complexes III, IV precluded from respiratory electron transport. Increased expression of *AOX* was also reported to enhance the salinity tolerance and photosynthetic efficiency in pea [102], *Arabidopsis* [103]. In rice, the increased expression of *F1F0* of the *ATP synthase* was shown to improve the plant tolerance to osmotic and salt stress [104]. Besides, an active involvement of thioredoxins and peroxiredoxins also

regulated the mitochondrial redox homeostasis in plant system [105]. Akin to ROS, NO was also reported to regulate the activity of several mitochondrial proteins like ATP synthase β subunit, HSP90 and peroxiredoxins Prx II F [106].

1.10. ROS homeostasis in peroxisomes

Under the conditions of decreased stomatal conductance, the lower CO_2/O_2 ratio activates the oxygenase property of Ribulose 1,5 bis phosphate carboxylase/ oxygenase (Rubisco) leading to photorespiration [107]. Since, peroxisomes are the site for glycolate oxidation; their active involvement was registered under stresses affecting the stomatal conductance and photosynthesis [108]. Peroxisomes are enriched with ascorbate peroxidases (APX) and catalase (CAT) to neutralise H_2O_2 generation at the site of production [109]. Additionally, xanthine oxidase mediated $O2^{\bullet-}$ production was also reported in leaf peroxisomes.

1.11. Effect of salinity on central carbon metabolism

Salinity negatively affects chloroplast CO_2 fixation due to stomatal/metabolic limitations. Various photosynthesis associated proteins, such as carbonic anhydrase, Rubisco small and large subunits, Rubisco activase, Rubisco binding proteins along with Calvin cycle-specific enzymes including fructose bisphosphatase (FBP), phosphoribulokinase (PRK) and sedoheptulose-1,7 bisphosphatase (SBPase) are reported to be negatively affected under salt stress [110]. The altered metabolism in the chloroplast channelized the metabolite flux in different subcellular compartments for pentose phosphate pathway; photorespiration and mitochondrial respiration can also activate the various shuttle systems (GABA shunt, malate /oxaloacetate). Long-term salt exposure mediated co-induction of the glycolysis and sucrose metabolism was reported to decrease cytosolic sugar content in barley [111] and *O. sativa* [112]. The decrease in sugar can be attributed to its utilisation for increased respiration (glycolysis) and osmotic adjustment [113]. Downstream pyruvate metabolism was also

negatively affected under salt stress, leading to feedback inhibition of glycolysis [114] and its oxidation in TCA cycle.

Salinity mediated increase in mitochondrial respiration can be attributed to temporary adjustment mechanism to meet the requirement of enhanced energy [115]. The uninterrupted energy generation through mitochondrial respiration was dependent on uncomplicated fluxing of various TCA cycle intermediates (particularly organic acids). Increased availability of such intermediary organic acids is related to the plant's ability to sustain or enhance yield under stressful environment [116]. In contrast, salinity mediated reduced pyruvate transport and inhibition of pyruvate dehydrogenase complex in mitochondria, correlated well with that of substrates availability (most notably citrate and isocitrate) to sustain the TCA cycle in wheat [114], barley [111] and rice [112]. In wheat, long term salinity led to an increased accumulation of amino acids like proline, lysine, GABA and alanine [114] and similar to, barley [116] and sugarbeet [117]. The TCA cycle intermediates 2-oxoglutarate, oxaloacetate and pyruvate are required for the synthesis of these amino acids, following the metabolic inhibition of regulatory enzymes [111]. The differential metabolome profile in rice root showed reduced TCA cycle intermediates and grater accumulation of amino acids in tolerant cultivars [118].

The salinity mediated inhibition of the key regulatory enzymes of TCA facilitated the activation of alternate pathways like GABA shunt and Asp-malate pathway for maintaining the mitochondrial respiration [119]. The glutamate produced via the GABA shunt moves form the cytosol to the mitochondria where it is further catabolized [120]. The impairment of glycolysis and TCA cycle under stress activates the malate-aspartate shuttle for transporting cytosolic and mitochondrial reducing power for energy production in mitochondrial ETC. Similarly, the existence of malate valve in chloroplast can be assumed as an alternate

pathway for supply chloroplastic reducing equivalent to mitochondria with the mediation of malate dehydrogenase [121].

1.12. Source-sink relationship under salt stress

Salinity negatively affects the yield potential of crops by negatively affecting both the source and sink strength (Fig 1.11). In the mature plant, the site of photoassimilate production and export are referred as source tissue, while the site of its import and consumption are referred as sink tissue [122]. In general, leaf and other photosynthetically active green tissues are the source tissue, whereas seeds/fruits/roots and developing tubers are the sink. The transfer of photoassimilate from source to sink (source sink metabolic homeostasis) is a highly coordinated process influenced by both environment and tissue's metabolic status [123].

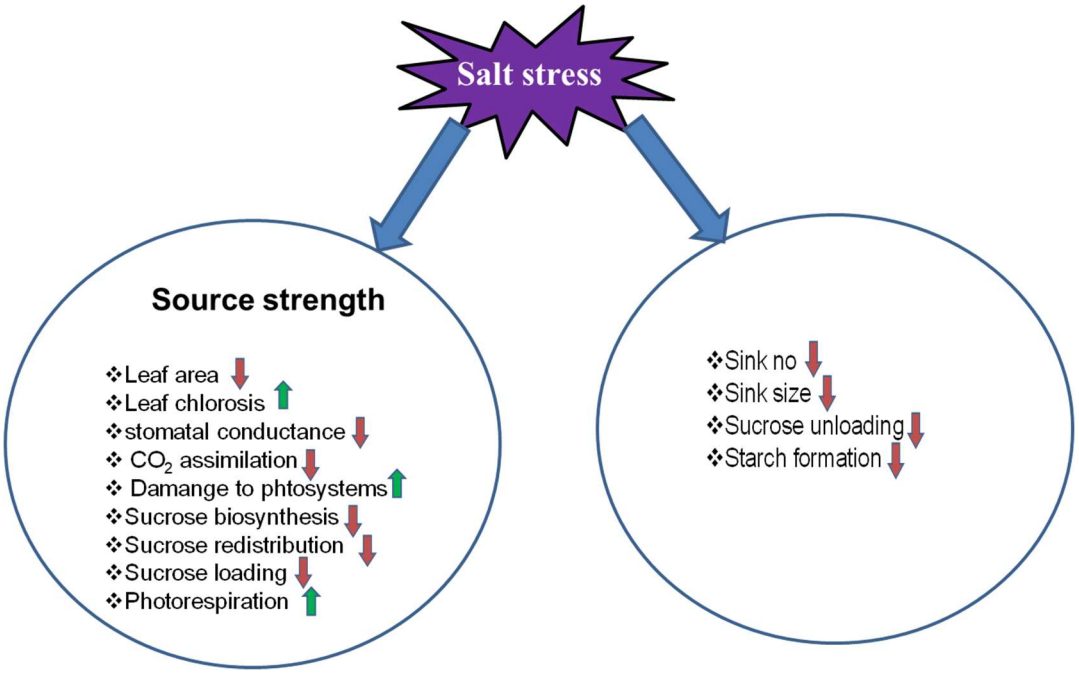

Fig. 1.11: Effect of salt stress at source- sink metabolic homeostasis in mature plants.

The green and red arrows represent the increase and decrease respectively.

Plant's metabolic effort to adapt and sustain its growth under salinity is the main cause of reduced photosynthesis and crop yield [124]. Both the components (osmotic and ionic) of salinity differentially influence the plant growth. Osmotic stress predominates the short-term

salinity response, affecting the stomatal conductance, thereby decreasing the dynamic leaf photosynthesis without affecting steady state photosynthesis in *S. lycopersicum* [125]. The osmotic stress also negatively affects the overall shoot growth, leaf emergence and expansion and thereby improving the water use efficiency of the plant. The toxic Na^+ accumulation under long term salt stress is known to create the ionic imbalance mediated decrease in leaf area, chlorosis, sucrose synthesis and metabolic inhibition to Calvin cycle enzymes such as Rubisco, FBPase, ribulose-5-phosphate kinase (Ru5P kinase), phosphoenol pyruvate carboxylase (PEPC) and glyceraldehyde-3-phosphate dehydrogenase. Salinity mediated decrease in stomatal conductance and metabolic limitations impaired the flow of e^- through photosystems resulting in excess ROS generation at PS II ($^1O_2$) and in the reducing side of the PSI ($O_2^{\bullet -}$ and H_2O_2) [93, 42]. Excess ROS mediated damage to PS was reflected as a decrease in maximum quantum yield (F_v/F_m), electron transfer rate (ETR), quantum yield of photosystem-II (PS-II yield), along with increase in the non-photochemical quenching (NPQ) [126]. The relative maintenance of these parameters under salinity defines the salinity tolerance behaviour in rice [126]. The activation of NPQ under abiotic stresses is a protective mechanism to avoid photoinhibition of PSII. NPQ regulates the excitation energy transfer towards photochemical reaction by dissipating excess energy through non radiative process in the pigment matrices of PS II reaction centre. Mutants showing impaired NPQ activation are reported to be more sensitive to photoinhibition [127]. Contrary to this, the rice lines overexpressing NPQ regulatory gene (*PsbS*) exhibited improved photosynthetic efficiency and yield [128]. Further the premature senescence of the photosynthetic source tissues and reduction in the growth and number of harvestable sink organs are the prime factors responsible for yield loss under salt stress [129].

Sucrose metabolism has a critical regulatory role in defining plant growth, yield potential, and stress responses [130]. Sucrose synthesis and redistribution in source leaves

along with sucrose utilization in the sink are the key steps which define energy sustainability of a plant under stress [122]. In higher plants, photosynthesis entails the fixation of CO_2 as triose phosphates (triose-P) in the chloroplasts via the Calvin cycle. The triose-P/phosphate transporter transports the triose-P moieties to the cytosol, whereupon these serve as substrates for aldolases to yield fructose 1,6-bisphosphate (F1,6BP). The combined activity of cytosolic fructose 1,6-bisphosphatase (FBPase) and sucrose phosphate synthase (SPS) converts F1,6BP into sucrose phosphate (Sucrose-P). The latter is dephosphorylated into sucrose by the activity of sucrose phosphate phosphatase. Sucrose is the primary form of assimilated carbon which gets transported from the photosynthetic (source) tissues to non-photosynthetic (sink) tissues, via phloem [131]. The non-structural carbohydrates like sucrose, starch and hexoses along with inorganic phosphate (Pi), can cause feedback inhibition of photosynthesis, by regulating the triose-P utilisation and thereby limiting the source strength [132]. The relative concentration of triose-P and Pi are the key regulators for maintaining the source sink metabolic homeostasis in the photosynthetically active leaves. Starch formation in chloroplast and sucrose formation in the cytoplasm both share triose-P as their initial substrate. Intracellular communication between these two compartments is mediated via triose-P/Pi antiporter system that is located at chloroplast membrane. A low concentration of cytosolic orthophosphate restricts the export of triose-P from chloroplast, directing the triose-P pool towards starch synthesis instead. Conversely, higher cytosolic Pi promotes the triose P export from the chloroplast and sucrose biosynthesis in cytosol. The ratio of the triose-P/Pi regulates the activity of various regulatory enzymes in the sucrose and starch biosynthetic pathways. A high chloroplastic triose-P/Pi ratio activates ADP-glucose-pyrophosphorylase (positive modulator for starch biosynthesis), whereas a low cytosolic ratio of triose–P/Pi stimulates/boosts the formation of Fructose 2,6-bisphosphate by activating Phosphofructokinase-2 (negative modulator of sucrose biosynthesis).

The rate of sucrose biosynthesis in the leaves (source capacity) is mediated primarily by SPS and FBPase and under tight feedback regulation of the leaf sucrose content. Photosynthesis and yield impairment with SPS null mutant was reported in *A. thaliana* [133]. On the other hand, SPS overexpression in sugarcane [134] increased the source leaf capacity for sucrose production and yield. Akin to SPS, cytoplasmic FBPase also contributed towards regulating the complex network which coordinates assimilation of CO_2 and biosynthesis of sucrose and starch. An increased expression of FBPase was linked to enhanced sucrose synthesis in the leaves of *A. thaliana* [135] and transgenic leaf oil crop [136]. Feedback inhibition of SPS also co-ordinately decreased the activity of FBPase by activating fructose phosphate kinase which resulted in the formation of fructose2,6 bis phosphate and increased the hexose P pool [137] and facilitated the transient starch formation in leaf chloroplast.

Further, sucrose redistribution in the cytosol mediated via invertase and sucrose synthase (SuSy) regulates the feed forward sucrose synthesis in the cytosol via SPS activity. A decrease in sucrose metabolizing enzymes SPS, vacuolar acid invertase (AI), and neutral invertase (NI) in cotton was reported to be correlated well with that of yield reduction [138]. Sink strength (capacity to drag sucrose) is defined by phloem loading at production site, phloem translocation and sucrose unloading at newly developed sink areas. The unloaded sucrose in the sink tissue was metabolized by NI, SuSy, and AI. This provides the hexose pool required for the cellular biosynthesis of carbohydrates, both structural and non-structural. For instance, sucrose is irreversibly hydrolysed into its constituent monomers (glucose and fructose) via the action of invertases. On the other hand, SuSy uses uridine diphosphates (UDP) to catalyse the reversible cleavage of sucrose, producing fructose and Uridine diphosphate glucose (UDPG). The importance of the AI was also evident for the expansion of cotton fibre and *Arabidopsis* root elongation [139]. Recently *Os*Vin2-1 mutant was also reported to have reduced seed size and grain weight as a consequence of impaired

sink strength [140]. The activity of SuSy in sink is considered to be a biochemical marker for sink strength. In maize, mutations in SuSy, resulted in shortage of basis substrates like UDPG (for cellulose synthesis) and glucose (starch synthesis), leading to a shrunken seed phenotype [141]. In another study, over-expression of SuSy in cotton resulted in invigorations of the seeds with increased fibre content [142]. The enhancement of the Susy and VIN activity in the sink tissue were associated with effective utilization of the sucrose in the sink tissue, suggested by increased starch and less sucrose content in the grain. The NI was reported to present in various intracellular organelles like cytoplasm, chloroplast, mitochondria and nucleus. Mitochondrial NI was also reported to maintain the ROS homeostasis in coordination with mitochondrial hexose kinase [143].

Although most of the chloroplastic proteins involved in the CO_2 assimilation were found to be redox regulated, metabolic regulation pre-dominated the fate of sucrose biosynthesis in cytoplasm. Thioredoxin mediated direct activation of major Calvin cycle enzymes, including phosphoribulokinase (PRK), glyceraldehyde-3-phosphate dehydrogenase (GAPDH), fructose-1,6-bisphosphate aldolase (FBPase) and sedoheptulose-1,7-bisphosphatase (SBPase) have been reported [144].

Transport of sucrose via plasmodesmata in phloem has been reported to show redox dependent behaviour in *Arabidopsis* [145]. The cellular redox status mediated increased translocation by sucrose transporter (SUT-1) was reported in potato [146]. Further the unloaded sucrose in the sink tissue was channelized to support the metabolism and growth of sink tissue. The sucrose to starch conversion in the sink tissue was also reported to be under redox control. The first committed and final polymerizing steps toward starch biosynthesis by ADPG and starch synthase both showed a redox dependent activation by NADPH-thioredoxin reductase C (NTRC) system. RNA interference mediated downregulation of the

NTRC was reported to decrease the activity of ADPG and sucrose synthase and resulted in the formation of small and lighter fruits in tomato [147].

1.13. Strategies to improve salt-tolerance in crops

In order to minimise the yield gap under salt stress, numerous studies aimed at improving salt tolerance of economically important plants are currently underway. Majority of these efforts are focused towards boosting the acclimation efficiency of the plants under salt stress, which include early perception, signalling and efficient activation of stress tolerance mechanisms. The various approaches to improve the resilience against salt stress are given below;

1.13.1. Breeding for salt tolerance

Plant breeding is the conventional approach which has long been used to develop high yielding and/or stress-tolerant crops. This approach relies on the careful exploitation of inherent genetic variation, either by direct selection or marker-assisted selection for quantitative trait loci (QTL) [148]. Plant breeders utilise the naturally existing intergeneric and intra& inter-specific genetic variation in crop germplasms to develop salt-tolerant lines. Some new salt-tolerant varieties of wheat and rice were successfully developed with the aid of traditional breeding approach [149]. The advent of next generation sequencing and associated technological advancements have enriched crop genomic resources and accelerated the identification of QTLs associated with stress tolerance [150]. The new age approaches of molecular breeding exploits molecular markers for tagging and evaluation of QTLs for desired phenotype and their introgression via a marker-assisted approach [151].

Though plant breeding is still the preferred approach for developing improved varieties, the absence/shortage of desired genetic variation among existing germplasm, or the presence of reproductive barrier [152] can severely limit its potential. Mutation breeding is an alternative approach which entails the generation of desired genetic variation by treatment of

propagules to mutagenic agents, followed by their direct or indirect usage in breeding programs. Since the methodology only increases the natural mutation rate within a short timeframe, mutant/ mutant derived varieties enjoy the same regulatory and public acceptance as conventionally developed varieties [153]. Till date, 3364 mutant crop varieties have been released for improved biotic/abiotic stress resistance, yield potential and nutritional quality (https://mvd.iaea.org/20-03-2021).

1.13.2. Transgenics for improved salt tolerance

Conventional breeding approaches are impeded by a number of practical (time consuming, labour intensive) and technical hurdles (reproductive barrier, linkage drag). Genetic engineering circumvents these issues by exploiting known salt-responsive genes, including transcription factors, ion channels and enzymes associated with ROS detoxification and osmolyte synthesis [39]. Genetic engineering is associated with cloning and transfer of candidate genes for improving tolerance traits to cultivated salt-sensitive varieties along with modulation in the expression of inherent genes. For instance, overexpression of effectors genes involved in osmolyte accumulation (GB, P5CS), ion exclusion (NHX) and antioxidant machinery (DHAR, SOD, CAT) conferred improved salt tolerance in target crops [154]. Salt-responsive transcription factors have also emerged as good candidates for engineering salt tolerance in plant. Depending upon their relative position in a stress-signalling cascade, transcription factors can regulate a broad or specific set of genes, which permits design of a flexibility and tailored approach. For instance, the overexpression of TF, like NAC, AP2/ERF, MYB, and WRKY were reported to increase the tolerance towards various abiotic stresses including salinity [155]. However, the controlled experimental conditions which are used for candidate gene studies are vastly different from the real field scenario characterized by a complex interplay of multiple environmental factors. In addition, the molecular cross talk between different gene regulatory networks is poorly understood. Thus, exploiting

individual genes for transgenic development can lead to unforeseen metabolic imbalances and associated growth penalties, which reduces the power of this approach [156]. The release of superior performing transgenic is also restricted by lack of regulatory approval and/or public acceptance. This necessitates the development and usage of alternative approaches for improving salt tolerance.

1.13.3. Plant bioregulators for crop protection

In contrast with the breeding and transgenic approaches which rely over the genetic reconstitution, the use of plant bioregulator is an entirely agronomic approach for improving salinity tolerance in plants. Plant bioregulators are chemicals of natural or synthetic origin whose exogenous application can boost built-in defence system of the plant [8]. The application of hormone based PBR like salicylic acid, gibberellic acid brassinosteroids has been reported to impart salinity tolerance in various crops. Similarly, a broad group of the chemical based PBR show their protective effects towards various abiotic stresses [8]. Though most PBRs have been reported to exert their protective effects by modulating redox homeostasis, the exact mechanism of salinity tolerance is specific to applied PBR. The application of PBRs was shown to increase the efficacy of the plant system by reprogramming the sensing, signalling and activation of the salt responsive genes. Thus, PBR based strategy is a coordinated approach for salinity tolerance through transcriptional/metabolic regulations without manipulating the genetic constitution.

1.14. About the plant system: Rice (*Oryza sativa* L.)

Rice (*Oryza sativa*) is a founding crop of the agrarian system. The evolution of rice, from a wild Asian grass to a preferred staple crop of human consumption almost matches with the pace of human civilization. The agricultural practises of rice cultivation date back to about 8000-6000 BC in the Eastern, South-Eastern and Southern-Asia regions. With the advent of time about 2000 BC, Yangtze River basins (China) emerged as the central hub for

domestication and global spread of rice [157]. Rice belongs to the Poaceae family with a genome size of 430 Mb. It is a diploid (2n=24), annual, short-day, self-pollinated plant with determinate inflorescence. More than 50% of world's population is reported to be dependent on the rice to meet their nutritional requirements. Although rice is grown in more than 100 countries, 90% of the total global production comes from Asia [158]. *Oryza sativa* (Asian rice) is the most dominant species of rice particularly with reference to area under cultivation. On the other hand, *Oryza glaberrima* (African rice), has very confined cultivation in some areas of the Africa. Indian contribution to world rice production currently stands at 25%, second only to China [159]. India has about 192 MHa of the total cropped area, of which 45 MHa is under rice cultivation, with an average yield of 2.85 t/ha. Rice is the most salt sensitive crop (glycophyte) showing a reduction of 50% at EC 6.9 [160]. Earlier studies reported the yield penalty of upto 1 t/ha in rice, with poor quality water (EC >2 dS/m) irrigation [161].

1.15. Thiourea: thiol-based redox regulator

Thiourea [$(NH_2)_2OS$]is an organo-sulfur compound whose structure resembles urea [$(NH_2)_2OC$], except the substitution of oxygen by sulphur. The presence of S-atom, together with isomeric transition between thiol-thione isoforms renders thiourea into a redox-active compound. As a consequence, TU has an immense potential for scavenging ROS and improving redox homeostasis [8]. In plants, thiourea was first used as a dormancy breaking agent [162] at low doses and it was shown to inhibit catalase; this facilitatedH_2O_2 mediated oxidation of NADPH, a common oxidant in metabolic pathways, including the pentose phosphate pathway. Multiple reports have substantiated that the application of TU as plant bioregulator increases the yield potential and stress amelioration under different abiotic stresses including salinity (Table 1.3).

Table-1.3: Thiourea dose, mode of application and effects on crop plants

Crop-plants	Applied dose	Application method	Experimental conditions	Protective effects	Ref.
Mustard	7.5 mM	Foliar spray	Normal field conditions	Increased yield and oil content	[131]
Maize	6.5 mM	Seed priming + Foliar spray	Salinity	Maintaining the ionic and water homeostasis	[163]
Wheat	2.5 and 5 mM	Foliar spray	Drought	Increased synthesis of phenolics and flavonoids	[164]
Wheat	6.5 mM	Foliar spray	Drought	Improved water use efficiency	[165]
Wheat	6.5 mM	Seed priming + Foliar spray	Salinity	Improved nutrient uptake, photosynthetic machinery	[166]
Wheat	2.6 and 5.2 mM	Foliar spray	Boron	Reduced oxidative stress	[167]
Rice	6.5 mM	Seed priming + Foliar spray.	Arsenic	Decreased arsenic load in grain	[168]
Rice	6.5 mM	Seed priming + Foliar spray	Arsenic	Improved growth, yield with reduced arsenic load in grain	[169]
Rice	6.5 mM	Seed priming + Foliar spray	Arsenic	Improved antioxidant capacity and total S content in plant	[170]

1.16. Hydrogen peroxide (H_2O_2): pro-oxidant for plant defence

Hydrogen peroxide is a toxic by-product of aerobic metabolism in living organisms [8]. Its relative stability, ability to cross the plasma membrane and conversion to even more toxic hydroxyl radicals ($OH^{\bullet}$), makes it extremely damaging [171]. Although elevated H_2O_2levels are detrimental to physiological processes, basal level is required for normal plant growth. Various plant processes like cell elongation, activation of defence system, oxidative burst against pathogen and programmed cell death are differentially regulated, subject to H_2O_2 levels [172]. The H_2O_2 priming imposes a mild stress to the plant resulting in the activation

of ROS dependent signalling network and defence proteins [173]. The prior activation of this machinery was shown to perform efficiently under subsequent stress exposure. Priming with H_2O_2 improved various plant water use efficiency [174], antioxidant capacity [175, 176], and photosynthesis protection [177, 178]. The exogenous application of $H_2O_2$was shown to enhance crop tolerance and productivity under different stress conditions (Table 1.4).

Table-1.4: Hydrogen peroxide dose, mode of application and effects on crop plants

Crop-plants	Applied dose	Application method	Experimental conditions	Protective effects	Ref.
Soybean	1 mM	Foliar spray	Drought	Improved water use efficiency	[174]
Rice	100 μM	Pretreatment	Temperature	Maintained the redox homeostasis	[175]
Cucumber	1.5 mM	Foliar spray	Drought	Improved antioxidant system and photosynthesis	[177]
Mustard	100 μM	Pretreatment	Cadmium	Activated antioxidant defense and glyoxalase systems	[179]
Pea	1 mM and 2mM	Foliar spray	Cadmium	Improved photosynthetic pigments and tolerance towards	[180]
Sunflower	0.1 mM -100 mM	seed priming	Salinity	Improved ionic homeostasis and antioxidant defense	[181]
Wheat	1 mM	seed priming	Salinity	Improved tolerance to salt stress	[182]
Maize	10 mM	Foliar spray	Salt stress	Maintained integrity and functionality of chloroplasts	[178]

In the present study, two redox-based PBRs-thiourea (TU, a thiol-based non-physiological ROS scavenger) and H_2O_2 (a pro-oxidant and ROS signalling molecule), with contrasting effects on ROS levels have been evaluated to understand whether these impose an overlapping or independent effect(s) on plant growth and productivity under salt stress. To

assess the impact of TU and H_2O_2 on antioxidant and ionic equilibrium, young rice seedlings were supplemented with TU and H_2O_2 in a hydroponics setup. The molecular determinants of TU and H_2O_2 mediated salinity tolerance were investigated using expression profiling of salt responsive genes, along with coordinated information from proteomic and metabolomics datasets. The impact of TU and H_2O_2 on overall plant productivity was demonstrated by assessment of source-sink relationship and yield attributes in foliar-supplemented field-grown plants, Both TU and H_2O_2 were shown to maintain the cellular redox status in the reduced state; the redox status then functions as a "core" regulator, improving the ion homeostasis (K^+ retention), photosynthetic efficiency as well as source-sink strength. Together, these effects lead to improved plant growth and ultimately, enhanced yield under both control conditions and NaCl stress.

1.17. Aims and objectives

1: To demonstrate the ameliorative potential of TU and H_2O_2 treatments under salinity stress in rice.

2. To study the molecular mechanism of TU and H_2O_2 mediated salinity tolerance.

3. To study photosynthetic efficiency, source sink relationship and grain yield under TU and H_2O_2 treatment conditions.

Chapter 2

Materials and Methods

2.1. Chemicals

Chemicals like sodium chloride (NaCl), thiourea (TU), hydrogen peroxide (H_2O_2), polyvinyl pyrrolidone (PVP), thiobarbituric acid (TBA), potassium dihydrogen ortho phosphate (KH_2PO_4), dihydrogen ortho phosphate (K_2HPO_4), oxidized glutathione (GSSG), ascorbic acid , α-bypyridal, ferric chloride, fructose 6 Phosphate, glucose, ADP-glucose, phenyl methanesulphonyl fluoride (PMSF), agarose, NADPH, triton X-100, MOPS buffer, ethylene diamine tetra acetic acid (EDTA), Bradford reagent, nitroblue tetrazolium (NBT), oxalo acetic acid (OAA), glutamic acid (L-Glu), α-keto glutaric acid (α-KG), γ-aminobutyric acid (GABA), GABase (G7509) diethyl pyrocarbonate (DEPC), 2X PCR ready mix, SYBR Green 2X master mix, , ethidium bromide, individual components of Yoshida medium, Tri reagent were purchased form Sigma Chemical Company, USA. Additionally, kits used in the quantification of protein carbonyls (OxyBlot Protein Oxidation Detection Kit; S7150), Starch (STA-20) and sucrose (SCA-20) were also procured from Sigma Chemical Company. The various reagents used in differential proteomics study included; spin column for concentrating protein preparations (Amicon® ultra; 3KD cutoff, Millipore), The 8–plex labeling kit (iTRAQ® Reagent – 8 Plex, Sigma), sequencing grade Trypsin (Roche). The oligo dT-primer was obtained from Novagen, USA. HPLC grade purity reagents like methanol, chloroform, BSTFA [Bis(trimethylsilyl)trifluoroacetamide], Ribitol were procured for GC-MS based metabolite analysis. The first strand reverse transcription-polymerase chain reaction (RT-PCR) kit was procured from Invitrogen, USA. The specific gene primers for RT-PCR were made to order from Metabion International. The deionized water from a Millipore Milli-Q system was used to

prepare reagent solutions shortly before the use. All the other chemicals used in the study were procured from reputed local manufacturers/suppliers considering highest accessible available purity

2.2. Plant material, growth- and treatment-conditions

The entire study was performed on Indian rice (*Oryza sativa* L.) var. IR-64. The seeds were surface sterilized using 30% ethanol for 3 min followed by repeated washing with distilled water to remove traces of ethanol. The seeds were allowed to germinate in a shaker incubator (100 rpm; 32°C), with adequate water level sufficient enough to provide aerobic conditions to germinating seeds. Following the overnight incubation, seeds were spread over moistened filter paper under dark conditions for germination. After 4 days, germinated seedlings were transplanted onto customized small polypropylene floats of dimension (4 cm x 3.5 cm) having the capacity to hold 16 seedlings. The floats were placed in 100 mL beaker of containing ½ strength Yoshida medium [183] and transferred into a plant growth chamber (Sanyo, Japan) with growth conditions like; 14h photoperiod, day/night temperatures (25/22°C), photon flux density (150 µE $m^{-2}s^{-1}$), and relative humidity (65-75%).

Table-2.1: Composition of Yoshida medium

Stock No.	**Elements**	**Reagents (Analytical grade)**	**Stock (g/L)**
Stock 1	N	NH_4NO_3	114.3
	P	$NaH_2PO_4.H_2O$	50.4

	K	K_2SO_4	89.3
Stock 2	Ca	$CaCl_2.2H_2O$	110.8
Stock 3	Mg	$MgSO_4.7H_2O$	40.5
Stock 4	Si	$Na_2SiO_3.9H_2O$	47.6
Stock-5	Fe	$FeSO_4.7H_2O$ $EDTA.Na_2$	4.63 6.28
Stock 6 (Minor nutrients)	Mn	$MnCl_2.4H_2O$	1.875
	Mo	$(NH_4)_6Mo_4.2H_2O$	0.0925
	Bo	H_3Bo_3	1.1675
	Zn	$ZnSO_4.7H_2O$	0.04375
	Cu	$CuSO_4.5H_2O$	0.03875

The plants were maintained under controlled conditions for 2 weeks. Further, two independent approaches were opted out for evaluating the ameliorative potential of TU and towards NaCl stress. The first approach, involved the supplementation of TU and H_2O_2 in nutrient medium under hydroponics. Briefly, 14 days old hydroponically grown seedlings were subjected to different treatments including control (Yoshida medium), NaCl (50 mM), H_2O_2 (1 µM) and NaCl (50 mM) + H_2O_2 (1 µM), TU (7.5 µM), NaCl (50 mM) + TU (7.5 µM). The

treatments like NaCl + H_2O_2 and NaCl + TU treatments were symbolized as NH and NT, respectively. A pre-treatment of 1 µM H_2O_2 (H_2O_2 and NH) and 7.5 µM TU (TU and NT) was also given for 24 h (Fig. 2.1). In shoots, time dependent alteration in the enzymatic antioxidant activities and Na^+ and K^+ accumulation pattern was carried out in a time course extending from 1, 6, 24 and 48 h after stress imposition. Further, expression levels of selected salt responsive genes were analyzed after 6 h of the treatments. Various studies related to quantification of oxidative stress (protein carbonyl and MDA, thiol staining) along with proteomic, metabolomic and activity estimation of enzymes related to tricarboxylic acid cycle (TCA) cycle under different treatments were conducted at 24 h stress impositions. Eventually, the qualitative and quantitative phenotyping along with measurement of antioxidant capacity was carried out, at 7 days post-stress (Fig. 2.1).

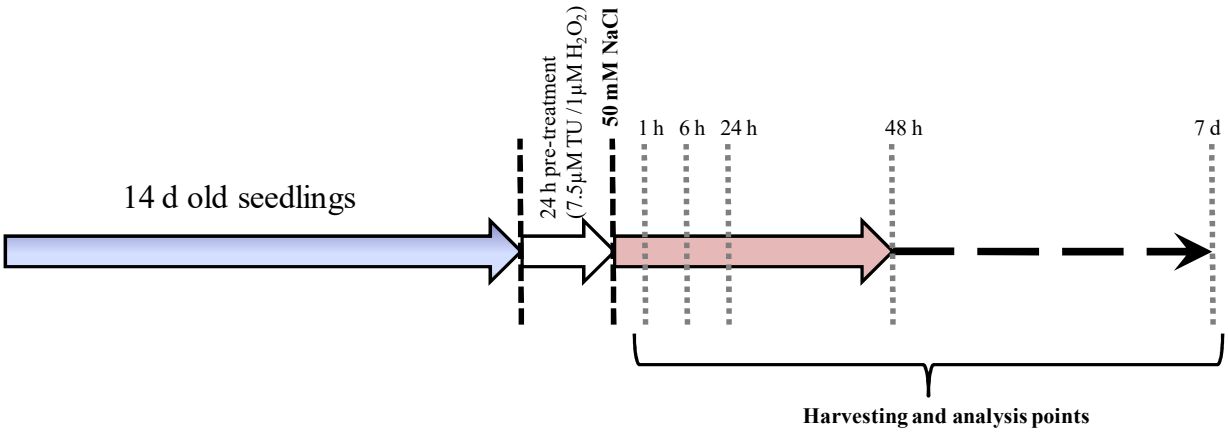

Fig. 2.1: Schematic representation of approach 1 (supplementation study under hydroponic system).

In the second approach, which basically dealt with foliar application of TU and H_2O_2, 30 days old hydroponically grown seedlings (4 in numbers) were transplanted in plastic pots having 14 kg of soil, under the net-house conditions at Bhabha Atomic Research Centre, Mumbai (India). The fertigation and agronomic practices were followed for growing rice plants, viz. application of basal fertilizer dose of N:P:K (50:50:50 kg/ha), which was achieved by adding 4 g of suphala-fertilizer (15:15:15) for 14 kg of soil/pot. Additionally, a split dose of urea (0.72 g per pot) was introduced at 40 and 60 d post-transplantation. All of the pots were maintained to 3-4 cm standing top water till maturity, with weakly irrigation. Overall, three foliar applications of TU and H_2O_2 were given at vegetative (40 days post-transplantation), early anthesis (55 days post-transplantation), and grain filling (72 days post-transplantation) stages. At 5 days post 3rd-foliar spray, various parameters related to phenotypic differences, photosynthetic efficiency, ion accumulation, and source sink relation were studied. Yield and yield associated parameters were quantified at the maturity phase (Fig. 2.2).

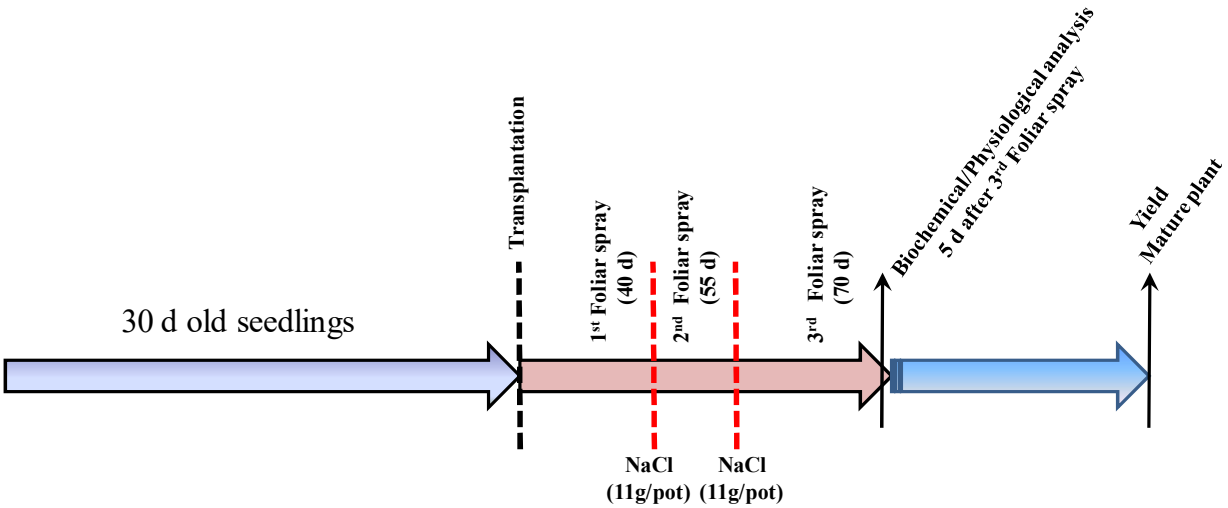

Fig. 2.2 Schematic representation of approach 2 (foliar spray under pot study).

A total six subsets of treatments were included in the study. Group-1 plants which included NaCl treated plants; NaCl was applied as split dose in two batches of 11 g /pot each at 42- and 57-days post-transplantation. The dose optimization of NaCl i.e., 22g NaCl /pot was calculated considering field capacity of 14 kg paddy soil (4.6 L) as well as amount of the top-water (1.4 L) and corresponded to ~ 62 mM NaCl concentration. The group-2 and -3 plants were treated with foliar applications of TU (6.5 mM TU + 0.01% Tween-20) and (1 mM H_2O_2 + 0.01% Tween20), respectively. Group-4 and -5 plants were subjected to combined treatment of NaCl + TU (NT) and NaCl + H_2O_2 (NH) treatments, respectively. Group-6 plants were devoid of any treatments and given a foliar-spray of water (three times at 40-, 55- and 72- days post-transplantation) and considered as control.

2.3. Measurement of antioxidant enzymes activities

Plant leaf tissue from different treatments (250 mg) were homogenized in 0.8mL, 100 mM ice cold potassium phosphate buffer (pH 7.0) encompassing 1 mM EDTA, 1 mM phenylmethylsulfonyl fluoride (PMSF) and 1% polyvinyl pyrrolidone (w/v) at 4ºC. After squeezing the homogenate through layered cheese cloth, the debris free extract was further centrifuged at 15,000 rpm for 15 min at 4ºC. The clear supernatant after centrifugation was used to measure the enzymatic activities. The activities of superoxide dismutase (SOD; EC 1.15.1.1), ascorbate peroxidase (APX; EC 1.11.1.11), catalase (CAT; EC 1.11.1.6) and glutathione reductase (GR; EC 1.6.4.2) were measured following the methods of [184], [185], [186] and [187] respectively as described previously [188].

The SOD mediated photochemical inhibition of nitro blue tetrazolium (NBT) in to formazone, lay the foundation of SOD activity measurement. The assay mixture for SOD activity measurement consists of 50 mM phosphate buffer (pH 7.8), 0.1 mM EDTA, 23 mM Methionine, 75 µM NBT, 2 µM riboflavin with relevant aliquot of enzyme extract. Both dark and light blanks were also considered in the reaction corresponding to samples showing minimum and maximum reduction of NBT respectively. After adding all the reaction components, reaction was initiated with the exposure to intense light for 15 min. After 15 min reaction was terminated by switching off the light and placing the tubes in the dark. The resultant mixture was analyzed for the quantification of formazone formation by measuring absorbance at 560 nm. One unit of SOD activity correspond to protein concentration needed to inhibit 50% of the introductory NBT reduction (light blank) under light.

The activity of CAT was quantified by measuring the rate of reduction of H_2O_2. The reaction mixture for CAT contained 50 mM phosphate buffer (pH 7.0) with 20 mM H_2O_2 and appropriate aliquot of enzyme. Decrease in absorbance, correlating with that of H_2O_2 break down was measured as rate kinetic at 240 nm (Molar extinction coefficient 43.6 M cm^{-1}).

The activity of APX was measured by measuring the rate of oxidation of the ascorbate in reaction mixture which comprised of, 50 mM phosphate buffer (pH 7.0), 0.1 mM EDTA, 0.1 mM H_2O_2, 0.5 mM sodium-ascorbate along with suitable aliquot of enzyme extract. The activity of the APX was calculated using (Molar extinction coefficient 2.8 mM cm^{-1}).

The activity of GR was assayed, on the basis of GSH mediated reduction of DTNB [5,5'-dithiobis-(2-nitrobenzoic acid)]. The reaction mixture used in the assay comprised of 100 mM potassium phosphate buffer (pH 7.5), 0.5 mM EDTA, 5mM GSSG, 0.75 mM DTNB, 0.5 mM

NADPH, and suitable enzyme aliquot. The increase in O.D at 412 was monitored upto 5 min under rate kinetic mode. The molar extinction coefficient (13.6 X 10^3 M cm^{-1}) was used to calculate the activity of GR.

2.4. Measurement of total antioxidant capacity

The total antioxidant capacity of the plant leaf samples was analyzed by oxygen radical absorbance capacity (ORAC) assay. The principle of this assay relies the ROS quenching ability of the soluble antioxidants present in the plant's extract as described [189]. Liquid nitrogen grounded leaf tissue (50 mg) was extracted with 1 mL of 50% ice cold acetone. After centrifugation the resultant supernatant was used for the ORAC assay. A black fluorescent microtiter plate was used in the study. A systemic addition of 150 µL of 0.08 µM fluorescein, followed by addition of 25 µL of samples extract with different dilutions (10, 20, 40 and 80-fold) was carried out in microtiter plate in a standard format [189]. Known concentrations of the Trolox (6.25 – 50 µM) were used as standard along with phosphate buffer as blank. Sample's dilutions, standard (Trolox) and blank all get prepared in 75 mM phosphate buffer (pH 7.0). After incubating the microtiter plant at 37°C for 10 min, 25 µL 2,2'-Azobis(2-amidinopropane) dihydrochloride (AAPH) was added and immediately subjected for rate kinetics measurement upto 1h, with 5 min intervals and intermittent shaking before taking subsequent reading, at 37°C. A multi-detection plate reader (Biotek, Synergy HT), was used to run a fluorescence kinetics read with an excitation /emission wavelengths of 485/530 nm. The net area under curve (AUC), depicted the total antioxidant capacity and normalized to fresh weight of the samples.

2.5. Estimation of Na^+ and K^+ in leaf samples

The harvested leaf tissues were allowed to dry in a hot air oven at 70°C, in expectation to achieve a constant weight. Around 200 mg of the dried leaf tissue were acid digested with Conc HNO_3 at dry heat block (DBK Instruments) at 140°C. The digested samples were resolubilized in 1.5 mL nanopure MQ-water and taken to 2 mL of the centrifuge tube, after centrifugation at 15000 X g at 20 min. The supernatant was taken carefully and filtered through 0.45 µM filter and subjected to atomic absorption spectroscopy with 1:10 dilutions. The resultant concentrations were normalized to the initial dry weight of the samples and represented as % DW.

2.6. Estimation of the Malondialdehyde (MDA) content

The MDA content in the leaf samples was quantified following the protocol [190]. Briefly liquid nitrogen grounded tissue leaf tissues (200 mg) were extracted with 1.2 mL 80% ethanol. After centrifugation, 400 µL of the aliquots from each tube were dispensed in 2 individual set, containing 400 µL blank (-TBA) and test solution (+TBA) respectively as follows

- Blank (TBA solution accommodating 20.0% (w/v) trichloroacetic acid (TCA) + 0.01% butylated hydroxytoluene)
- Test (TBA solution accommodating 20 % TCA + 0.65% TBA)

After mixing, the tubes were incubated in a boiling water bath for 20 min, followed by cooling and centrifugation at 5000 x g for 5 min. Absorbance were recorded using spectrophotometer (Shimadzu UV 1800) at 532 nm, 600 nm and 440 nm, and. The MDA content can be calculated as

$A = [(Abs\ 440_{Test}) - (Abs600_{Test}) - (Abs\ 532_{Blank}) - (Abs600_{\ Blank})]$

$B = [(Abs\ 532_{Test} - Abs600_{Test})\ 0.0571]$

MDA equivalent (nmol mL^{-1}) = (A-B/157000) 10^6

Finally, the MDA equivalent was normalized to the fresh weight of the samples and represented as nmol g^{-1} FW.

2.7. Histochemical staining for thiols

The specific reactivity of iodoacetamide (IAN; sigma I1149)) towards reduced thiol (-SH) group was used to assay the redox status in plant's root under different treatment conditions. The histochemical staining with IAN was able to label the free and protein bound thiol in root tissue. In brief, hydroponically grown 14 d old rice seedlings were given a 24 h pretreatment with 7.5 µM TU and 1 µM H_2O_2 before imposing further treatments under control and NaCl-conditions (control, TU, H_2O_2, NaCl, NH and NT) for 24 h. After 24 h, intact seedlings were immersed in solution containing 10 µM of IAN in respective treatment media for 10 min followed by thorough washing for 5 min. Root of individual seedlings was imaged in ten biological replicates under fluorescence microscope (Olympus-IX73) using FITC filter with an exposure time of 1s. Fluorescence intensity of IAN was analyzed using Image J software (version 1.53d; https://image j.nih.gov).

2.8. Detection of protein carbonylation status

For estimating the protein carbonyl status, roots were harvested followed by total protein extraction using ice cold extraction buffer **(**50 mM potassium phosphate pH 7.5, containing 1 % protease inhibitor cocktail (Sigma; P 9599). The homogenate was centrifuged at 15000 x g for 30 min and supernatant containing soluble proteins were collected and subjected to protein quantification and protein carbonyl (PC) quantification. An equal protein concentration (80 µg) from different treatment conditions were derivatized to 2,4-dinitrophenylhydrazone (DNP)

before resolving on SDS PAGE (12 %), as per kit protocol. Western blotting with anti-2, 4-dinitrophenylhydrazone antibody was used to analyze the status of protein carbonylation among different treatments using Millipore S7150 kit following the kit protocol. Preparation of protein sample and Western blotting was done using 1:150 dilution of the anti-DNP antibody. The detection of dinitrophenylhydrazone was carried out by using HRP labeled anti DNP secondary antibody (1:300). The chemiluminescent detection was performed using enhanced chemiluminescence (ECL, Bio-Rad) as substrate with G: BOX Chemi XRQ system (Syngene).

2.9. Identification of differential proteins using iTRAQ approach

Leaves were harvested and pulverized in liquid nitrogen. The dried powder around 500 mg was homogenized in 2mL of ice-cold extraction buffer (50 mM potassium phosphate pH 7.5, containing 1 % protease inhibitor cocktail. After centrifugation at 15000 x g for 30 min, the supernatants containing soluble proteins were collected. Absolute quantification of the protein concentration in homogenates was carried out using Bradford method [191].

Proteins intended for iTRAQ (isobaric tag for relative and absolute quantification) analysis were precipitated with equal volume of chilled acetone containing 20% TCA. The whole mixture was incubated overnight at -20°C with an afterward centrifugation at 5,000 x g for 30 min at 4°C. The precipitated protein pellets were repeatedly washed with chilled acetone (5 times). Each wash step involved the addition of 2 mL acetone to the pellet, followed by 10 min centrifugation at 5,000 x g at 4°C. Finally, the protein pellets were air-dried for a short duration (5 min) and re-dissolved in a buffer containing 7 M urea, 2 M thiourea, 40 mM DTT, and 4 % CHAPS. The protein was concentrated using 3kDa milipore filter along with 15 times volumes exchange with 50 mM TEAB (triethylammonium bicarbonate) buffer. After centrifugation, the

supernatant endured a reductive alkylation reaction using 25 mM DTT and 55 mM IAA. A protein equivalent (100 µg) was digested with trypsin [10: 1 as protein: trypsin (w/w)] for overnight at 37°C. After the digestions, samples were dried under vacuum concentrator and resolubilized with 0.5 M TEAB- buffer. The labeling of the digested peptides was achieved using iTRAQ 8-plex kits (AB Sciex, USA) according to the manufacturer's protocol. Two individual sets of 8-plex iTRAQ experiments were carried out with leaf protein of different treatments. For iTRAQ labeling, 113, 114, 115, 116, 117, 118, 119 and 121 Da tags were fixed up in 70 µl of isopropanol. The different iTRAQ tags were tagged to different tryptic digested samples (100 µg) with 2 h incubation at room temperature. After 2 h, the labeling reaction was attenuated with the addition of 50 µl LC–MS grade water. All 6 samples from individual sets were pooled, vacuum dried and, resolubilized in 8 mM ammonium formate buffer (pH 3). The reconstituted labeled peptides pool was further fractionated with the help of ICAT Cartridge under escalating concentration of ammonium formate buffer (pH 3) ranging from 35 -, 75-, 100 -, 125 -, 150 -, 250 -, 350 - and 500 mM. The peptides fractions were again vacuum dried and reconstituted in 0.1% formic acid before subjecting it to LCMS-MS based analysis with Eksigent nano-LC system coupled to 5600 TTOF (Sciex). The various parameters involved in the study were followed as described under [192]. The results containing mass spectra (MS) and MS/MS spectra scan was computed in the form of ".wiff" files. The original files (.wiff) from individual treatments were put forward for protein identification with the assistance of Protein Pilot™ software (v. 4.5) against the *O. sativa* Swiss Prot database applying paragon search method. The search parameters were specified as: trypsin being digestion enzyme allowing two missed cleavages, cysteine residue modification with IAA, N-termini of peptides along with lysine side

chains modification under iTRAQ 8-Plex labelling, bias correction was adapted, and global protein false discovery rate (FDR) was fixed to 1%.

2.10. Metabolite analysis using GC-MS

The harvested leaf samples from various treatments were snap chilled with liquid nitrogen and stored at -80ºC for further analysis. The samples were extracted as per [193]. In brief, 250 mg of liquid nitrogen grounded leaves were extracted with 1.4 mL of ice-cold methanol with internal standard spiking (100 µL of ribitol 1 mg mL^{-1} solution). The extracted homogenates were mixed vigorously and incubated at 70ºC for 15 min, followed by adding 1 mL of MQ water and 750 µL of HPLC grade chloroform. Following 15 min centrifugation at 22,000 x g, upper aqueous layer was taken in a fresh tube and subjected to vacuum drying. The derivatization of vacuum dried samples was caried out by adding 40 µL of methoxyamine hydrochloride for 2 h at 37ºC, followed by reacting and incubating the content with 60 µL of N, O-Bis(trimethylsilyl)trifluoroacetamide (BSTFA) for another 30 min at 37ºC. A defined sample volume (2 µL) of was injected into GC column fitted in GCMS-QP2010 (Shimadzu, Kyoto, Japan) system having an AOC-5000 auto-sampler. The transfer line and ion source were adjusted to 300ºC and 250ºC respectively. Helium was used as carrier gas with a flow rate of 1 mL min^{-1}.

The temperature program was calibrated as, 1 min isothermal heating at 70ºC, followed by ramping of the oven temperature upto 76ºC with 1ºC min^{-1} rate-kinetics. Further the temperature was increased upto 310ºC with a ramping rate of 6ºC min^{-1} and stabilized for 5 min at 310ºC. A scan range of 7-700 m/z at arate of eight scans s^{-1} was used for recording the mass spectra. Identification of the compounds was based on the mass fragmentation pattern and relative

retention time using NIST 2014library. Two points normalization was carried out before absolute quantification of the identified metabolites. The individual metabolites were corrected to relative retention ratio (area under peak), with internal standard ribitol and finally normalized with initial fresh weight of plant tissue.

2.11. Quantification of regulatory enzymes of TCA cycle

About 300 mg fresh leaf samples were homogenized with 1.5 mL of extraction buffer containing 100 mM Tris–HCl buffer (pH 8.0), 1 mM EDTA, 3 mM $MgCl_2$, 1 mM DTT and 1 mM PMSF. After centrifuging the homogenates at 22000 X g for 10 min at 4°C the resultant supernatant was dialyzed against extraction buffer at 4°C for 4 h. The dialyzed extracts were finally used for the quantification of various enzymes involved in TCA.

The activity of malate dehydrogenase (MDH) was calculated by measuring the rate of NADH consumption in the presence of oxaloacetic acid (OAA) as per [194]. In short, 50 µL of the extract was added in the reaction mix containing 50 mM Tris–HCl (pH 7.8), 0.5 mM EDTA, 2 mM $MgCl_2$, and 2 mM OAA. The reaction was initiated by adding 0.2 mM NADH and rate kinetics of the decrease in absorbance at 340 nm was observed. A respective enzyme blank for each sample was also calculated for final MDH specific enzymatic activity. Enzyme activity was expressed as unit mg^{-1} protein corresponding to nmol NADH oxidized mg^{-1} protein s^{-1}.

The aminating activity of glutatmate dehydrogenase (GDH) was assayed as per [195]. A 50 µL of the supernatant was added in the reaction mix containing 75 mM Tris–HCl buffer (pH 8.0), 1 mM $MgCl_2$, 20 mM α-ketoglutarate and 150 mM $(NH_4)_2SO_4$. The reaction was initiated by adding 0.2 mM NADH, followed by measuring the rate of NADH oxidation at 340 nm. A respective enzyme blank for each sample was also calculated for final GDH specific enzymatic

activity. Enzyme activity was expressed as unit mg^{-1} protein corresponding to nmol NADH oxidized mg^{-1} protein s^{-1}.

The quantification of glutamate decarboxylase (GAD) activity was on the basis of quantification of resultant product of glutamate decarboxylation i.e., γ-amino butyric acid (GABA). The specific estimation of GABA by GABase enzyme is coupled with $NADP^+$ reduction and can be linked with GAD activity and assayed as described [196]. About 25 µL of extract was treated with assay buffer containing 150 mM potassium phosphate (pH 6), 0.1 mM pyridoxal-5-phosphate and 20 mM L-glutamate in a final volume of 200 µL. A blank assay for every individual sample without glutamate was also incorporated for the correction of nonspecific absorbance. After incubating the reaction at 30°C for 60 min, the reaction was terminated by boiling for 10 min. After cooling to room temperature, the content was centrifuged and subjected to GABA estimation by GABase assay. In the GABase assay 20 µL of the end product of reaction one was reacted with 75 mM potassium pyrophosphate (pH 8.6), 1.5 mM $NADP^+$, 3 mM 2-mercaptoethanol, 5 mM α-ketoglutarate and 0.02 units of GABase (source *Pseudomonas fluorescens*) in a total volume of 200 µL. The rate kinetics for $NADP^+$ reduction was monitored as increase in absorbance at 340 nm. A standard curve with known amount of amount of GABA was constructed for the calculation of GABA content. Finally, the Enzyme activity was expressed as unit mg^{-1} protein.

2.12. Histochemical staining for superoxide radical

In vivo detection of superoxide radicals in leaf tissue using nitroblue tetrazolium (NBT) histochemical staining was carried out following the protocol [197] with some modifications. Superoxide radical mediated NBT reduction in tissue resulted in the formation of blue colored

formazone which can be subsequently visualized and quantified. Briefly, 4 cm leaf segment from the young leaves were excised and dipped in 0.1 % NBT solution (50 mM phosphate buffer, pH 7.4). Further, the NBT solution tubes containing leaf segments were subjected to vacuum infiltration (400 mm Hg) with 3 on/off cycles of 1 min each. Further, the vacuum infiltrated leaf segments were kept overnight at room temperature in the same solution. On the following day, removal of chlorophyll of the leaf segments was carried out with 80% alcohol. Finally, the leaf segments were scanned and analyzed for NBT stain intensity using image J software (version 1.53d; https://image j.nih.gov).

2.13. Quantification of AsA/DHA ratio

The concentration of ascorbate (AsA) and dehydroascorbate (DHA) contents were estimated using α-α′-bipyridyl-based colorimetric method [198]. Ascorbate quantification by this method is derived from ascorbate mediated reduction of ferric ions to ferrous ions, which have complex forming ability with α-α′-bipyridyl having absorbance maxima at 525 nm. Briefly 50 mg of the liquid nitrogen ground leaf tissue powder was extracted with 1 mL of 6% TCA. Two subsets, corresponding to total ascorbate quantification (AsA_{Total}) and reduced ascorbate (AsA_{red}) quatifiaction for individual samples were taken with following compositions; AsA_{Total} (200 µL extract+ 100 µL DTT (10 mM) + 100 µL NEM (0.5%) and AsA_{Red} (200 µL extract+ 200 µL D.w).

The specific absorbance at 525 nm was measured after adding and incubating (37°C for 1 h) the above subsets with 1.5 mL of the detection reagent (α -α′-bipyridyl, $FeCl_3$ in highly acidic medium). The amount of the oxidized Ascorbate (AsA_{oxi}) was quantified by subtracting the AsA_{Total} - AsA_{red} and the results were exhibited as ASA/DHA ratio.

2.14. RNA isolation, cDNA preparation and real-time expression analysis

All the materials used in the preparation of RNA (microcentrifuge tubes, pipette tips, and glassware) were treated with DEPC to remove RNase contamination. The total RNA from the leaf tissue was extracted using TRI-reagent (Sigma T-9494), as per manufacturer's protocol. The isolated RNA was checked for quality assurance by taking 260/280 and 260/230 ratio (>2), along with observing the band intensity of rRNA (28/18 s) under denaturing gel electrophoresis. Further, about 2 µg RNA equivalent was used for the synthesis of cDNA employing Superscript III RT (18080-093; Invitrogen) following the manufacturer's protocol. Rotor-Gene 6600 was used for the analysis of Real-time PCR. A web-based Quant-prime tool.33 was used to design all the primers for real-time PCR analysis by integrating the information of exon–intron junction and amplicon size upto 150 bp. Further, sequence analysis of RT-PCR amplicons was carried out to ascertain the specificity of all primers. The primers used in expression analysis are listed in Table. 2.2.

Table-2.2: Details of the primers used for gene-specific real-time PCR

Gene details	Primer sequences
Trehalose–phosphate phosphatase (*TPP*; LOC_Os02g44235)	For- TGCTGAAAAGGTTACCAAGTCC
	Rev- TGCGACCAGTTTCCAATCCT
Late embryogenic abundant protein group-3 (*LEA3*; LOC_Os04g52110)	For- CCATGCTGCTCGGTGGC
	Rev- GTACGACGGCCTCGGATGAT
Phosphatidylinositol-4-phosphate 5-kinase (*PIPK*; LOC_Os04g59540)	For- GCAATCTGGAACGACACAGC
	Rev- TCCACTCCCACCAGTAACGA

Translocator protein (*TSPO*; LOC_Os05g05930)	For- GAGCCGGGATCCGAGGAA
	Rev- TAGAACGAGGCGGCCATCAG
Early nodulin 20 (*EN20*; LOC_Os06g46740)	For- TCGCCGTCGGTTTCACCTA
	Rev- GTTCGCCCCATCGGTCC
Potassium transporter (*HAK21*; LOC_Os03g37930)	For- CTCACTGGGACGAACAGGAT
	Rev- CCCAATGCCGTGCTCAAAAG
Dehydrin (*DHD*; LOC_Os11g26760)	For- GCAGATGATGGGGAACACCG
	Rev- TCCATGAAGCCCTTCTTCTCG
Late embryogenic abundant protein group-1 (*LEA1*; LOC_Os03g20680)	For- AGGCGACCAAGAACAAGCTG
	Rev- TTGAACTCCGTCGCCTTCTG
Tubulin (*TUB*; LOC_Os01g59150.1)	For- TTTGTGTTCGGGCAATCTGGTG
	Rev-AGTGGCATACTTGGAATCCTTGC

For real time expression analysis, 1:5 diluted cDNA templates (2.5 µL), 10 µM forward and reverse primer (1.5 µL each), 4.5 µL of PCR grade water (Sigma W 1754) and 10 µL of SYBR green PCR reaction mix (Sigma; S-4320) were combined in a final reaction volume of 20 µL. The relative expression of target/reference genes for each treatment and respective control was used for the calculation of Ct value (cycle threshold), followed by fold change calculation (log2 expression fold) using REST-384 version 2 software. The relative expression of Tubulin (*TUB*) was used as reference gene expression for all calculations. The PCR protocols used for the expression analysis were specified as: initial denaturation 95°C for 15 min; 40 repeated cycles (94°C for 20 s, 55°C for 30 s, and 72°C for 30 s) followed by 72°C for 10 min. Finally, a

threshold cutoff of ± 1.2-fold change was applied to detect significant change in genes expressions.

2.15. Quantification of parameters associated with plant growth and yield

A physical measurement with the help of meter scale was employed for the estimation of various plant growth parameters particularly plant height, flag leaf length, leaf width and panicle length. Further, the quantification of panicles number per plant as well as 1000 seed weight were also achieved manually. Chlorophyll Meter SPAD-502 plus-konica Minolta was used for the quantification of leaf chlorophyll content and represented as SPAD value. The final SPAD value was calculated after taking average of five independent different points value in the same leaf.

2.16. Evaluation of stomatal conductance and PS-II stability

The parameters related to gaseous exchange were quantified using Gas Analyzer, GFS-3000 (Walz, Germany). After gaining the insight of plant response with a light curve, 1000 μmol m^{-2} s^{-1} photon flux was optimized as the most suitable photosynthetic photon flux density (PPFD) for the study. Various parameters related to measurement of photosynthetic efficiency were represented here as; chamber temperature (25°C), cuvette air flow 750 mL min^{-1}, Relative humidity (60%) and atmospheric CO_2 concentration (400 ppm CO_2). All the parameters were analyzed in young flag leaf after 5d of 3rd foliar spray. A simultaneous measurement of stomatal conductance, transpiration and net photosynthetic rate was carried out with GFS-300 under above specified conditions. The ratio between net photosynthesis and transpiration was used for the calculation of water use efficiency (WUE). Various chlorophyll fluorescence parameters, defying the stability of PS-II photosystem were also recorded with GFS -3000 systems as per [199]. For the quantification of maximum quantum efficiency of

photosystem-II (F_v/ F_m), chlorophyll fluorescence from 20 min dark adapted leaf was recorded, suggesting the back ground signal or minimum fluorescence (F_o) under the conditions where most of the PSII reaction center were open for electronic transitions. Similarly, the chlorophyll fluorescence of dark-adapted leaf after saturating light impulse was also measured, denoting the maximum chlorophyll fluorescence from closed PSII center (F_m). The quantification of maximum quantum efficiency of PSII (F_v/ F_m) was based on the relative fluorescence strength from the open and close PS-II centers represented as minimum (F_o) and maximum fluorescence (F_m) respectively and can be calculated as [F_v /F_m = (F_m − F_o)/F_m]. Similarly, the quantification of non-photochemical quenching (NPQ) involves the maximum fluorescence signal from a dark (F_m) and light adapted leaf (F'_m) and can be computed as [NPQ = F_m/F'_m – 1] [199]. The initial rise in the chlorophyll fluorescence following shifting from dark to light conditions was subsequently quenched and finally attain a steady state fluorescence (F_s) due to increased competition between photochemical and non-photochemical events. Steady state chlorophyll fluorescence (F_s) has an important role in the quantification of quantum yield of photosystem-II (PS-II yield) and electron transfer rate (ETR).

2.17. Spatial quantification of sucrose and starch

Hot ethanolic extraction (80%) was carried out in lyophilized samples (10 mg) of different plants parts involving young leaf (YL), old leaf (OL) and developing inflorescence (DI), with subsequent centrifugation at 15,000 x g for 15 min at room temperature. The quantification of sucrose and starch were carried out in the supernatant and pellet respectively using commercially available kits for sucrose- (SCA-20; Sigma) and starch- (STA-20; Sigma Aldrich) quantification, respectively according to the manufacturer's protocol.

2.18. Measurement of the activities of source-sink metabolic homeostasis related enzymes

Liquid nitrogen ground samples (~300 mg), from different plants parts i.e., young leaf (YL), old leaf (OL) and developing inflorescence (DI) were extracted using ice cold buffer [(containing 100 mM chilled MOPS (50 mM; pH 7.5), EDTA (1 mM), $MgCl_2$ (15 mM), PMSF (2 mM) and PVP (2%; w/v)]. After 15 min centrifugation at 12,000 x g for 15 min at 4°C, the resultant supernatant was separated and used for the analysis of FBPase, SPS, and Susy activities following the methods of [200, 201].

The activity of SPS was measured by adding 35 µL of the supernatant with 35 µL of a reaction buffer containing 100 mM MOPS NaOH (pH 7.5), 4 mM fructose-6-phosphate, 20 mM glucose 6-phosphate, 5 mM $MgCl_2$, 1 mM EDTA and 3 mM UDPG. An individual set devoid of UDPG served as enzyme blank for the reaction. Both the sets were incubated for 60 min in water bath at 37°C. After the completion of incubation period, the reaction was terminated by adding 70 µL of 30% KOH followed by 10 min heating in a boiling water bath. After cooling the tube contents, sucrose was quantified with the help of freshly made anthrone reagent (comprised of 150 mg of anthrone, 76 mL of H_2SO_4 and30 mL of distilled water). Finally, 1 mL of anthrone reagent was added to 140 µL of reaction mixture, followed by 20 min incubation at 37°C. After 20 min absorbance was recorded at 650 nm using spectrophotometer. The amount of sucrose produced can be estimated by calculating Δ OD (test OD - blank OD), and used for the analysis of specific activity (µM min^{-1} mg^{-1} protein) of enzyme.

Similarly, the activity of the sucrose synthase (SuSy) was measured by adding 35 µL of enzyme extract in 35 µl of reaction mix containing 50 mM MOPS NaOH (pH 7.5), 15 mM $MgCl_2$, 25 mM UDP-glucose (UDPG) and 25 mM fructose. Individual reaction(s) without

UDPG considered as blank for the reaction. The assay method SuSy is very much similar to SPS. The only difference is use of fructose in place of Fructose 6-phosphate and reduction in incubation time from 60 min to 30 min. The resultant sucrose formation was quantified using anthrone reagent and expressed as specific activity (μM min^{-1} mg^{-1} protein).

For the activity measurement of FBPase, the liquid nitrogen crushed leaf samples were extracted in extraction buffer comprising 100 mM Tris HCl (pH 8), 1 mM EDTA, 16mM $MgCl_2$, 20 mM DTT, 2% PVP, 0.05% triton X-100, 2 mM PMSF. The homogenates were subjected to 20 min centrifugation (12,000 x g) at 4°C and resultant supernatant was used for measuring enzymatic activity.

The FBPase activity was measured by coupling FBPase mediated F6P production, with $NADP^+$ reduction with the help of enzymes (phosphoglucose isomerase and glucose-6-phosphate dehydrogenase). The reaction was started by mixing 0.3 μM $NADP^+$ in a reaction mixture comprised of 50 mM Tris HCl (pH 8), 0.6 μM fructose 1, 6 bis-phosphate, 0.6 units of glucose 6-phosphate dehydrogenase,1.2 units of phosphoglucose isomerase and relevant aliquot of enzyme. The spectrophotometric analysis involving rate kinetics of the increase in absorbance at 340 nm was used to calculate the specific activity (molar extinction coefficient 6.3 x103 M^{-1} cm^{-1}).

Additionally, the spectrophotometrically quantification of the activities of two major classes of soluble invertases [Neutral invertase (NI) and acid soluble invertase (AI)] in the plant samples was carried out following the method [200]. The AI activity was estimated in a reaction mix containing 100 mM sodium acetate buffer (pH 4.5), 60 mM sucrose and suitable aliquot of enzyme. Similarly, quantification of the NI activity was done in a reaction mix (1 mL) comprised of 100 mM sodium acetate buffer (pH 7.5), 60 mM sucrose and suitable aliquot of enzyme.

Blank reactions (control) comprised of all reaction component except sucrose were maintained for individual sample. After incubating the reaction mixtures at 37°C for 20 minutes, the reaction was terminated by 10 min boiling in boiling water bath. Further, the content was cool to room temperature and the resultant hexose sugar produced in the reaction mixtures were quantified using Nelson's arseno-molybdate reagent containing 50 mM disodium hydrogen arsenate and 40 mM ammonium molybdate in 0.9 M H_2SO_4. The absorbance was recorded at 620 nm and specific activity (μM glucose produced min^{-1} mg^{-1} protein) was calculated using glucose standard curve. The protein content in the sample was estimated as per the Bradford method.

2.19. Statistical analysis

The experiments were performed under randomized block design with three biological replicates. The validity and variability of the entire datasets were confirmed by One-way analysis of variance (ANOVA), Further Duncan's multiple range test (DMRT) was carried out to define the level of significance between treatments. The outcome of the DMRT was annotated as different letters indicating significantly different values (DMRT, $p \leq 0.05$). The data sets of the source leaf and developing sink were also subjected to Principal component analysis (PCA) using Origin 2016 (Origin Lab, Northampton, MA, USA), and maximum variance in the datasets was explained with first two components (PC1 and PC2).

For proteomics study, differentially expressed proteins showing p-value of ≤0.05, were taken into consideration. Further the ratio of average expression between treatment and control was defined as fold changes, which subsequently changed to log2-value for relative expression analysis. The student's t-test, was used to compare the statistical significance in the protein's expression levels in between different treatments. A ±1.2-fold change was fixed as threshold

corresponding to significant change in abundance with p-value < 0.05. Further, the fold change data was normalized using both row- and column-wise for clustering analysis and MeV software was used to construct heatmap (http://mev.tm4.org/).

Similarly, significant change in metabolites profile in between control and treatment groups was tested using student's t-test on MetaboAnalyst 3.0 software [202]. MetaboAnalyst 3.0 was used in constructing heatmap, PCA loading plot, and correlation matrix [202]. To identify the key metabolites associated with each treatment condition, principal component analysis was performed using Origin (v. 2018). The PCA scores were derived for each metabolite using following formula: Final PCA score of metabolite 'A' = [(PC1 coefficient of metabolite 'A' X PC1 score of treatment 'A') + (PC2 coefficient of metabolite 'A' X PC2 score of treatment 'A')].

Chapter 3
Results and Discussion

Section I: Studies on ameliorative potential of thiourea and H_2O_2 treatments under salinity stress in rice

3.1. Introduction

The maintenance of cellular redox homeostasis plays a critical role for sustained plant growth and survival under stress conditions. Various antioxidant responses (enzymatic/non-enzymatic) contribute towards scavenging of the ROS. Plant's perception towards any exogenous chemicals, perturbs the cellular redox status in a positive or negative manner, depending on the nature and dose of stimulus [47]. The efficient activation of antioxidant machinery, in turn regulates the downstream signaling towards stress amelioration. This led to the hypothesis, that exogenous application of any chemical which can positively modulate the redox homeostasis in plants may enhance the stress tolerance potential for subsequent stress exposure. The present study has appraised extensively applied redox modulators like H_2O_2 and TU for alleviating salt stress in rice. Although, earlier studies have well established the application of TU (Table 1.3) and H_2O_2 (Table 1.4) for mitigating various abiotic stress and increasing yield potential at field level, no comparative analysis for a mechanistic view was reported yet. Taking into account of their contrasting chemical nature TU (a ROS scavenger) and H_2O_2 (a biological ROS), were expected to show an opposite effect on the cellular redox state, which is described as the ratio of reduced to oxidized form of major redox couples in various subcellular compartments.

In order to demonstrate the ameliorative potential of TU and H_2O_2 towards salinity tolerance, the time dependent kinetics for antioxidant enzyme and ion accumulation was performed in seedlings subjected to NaCl stress with/without TU and H_2O_2 treatments. Based on

our data, the importance of the efficient activation of nonenzymatic and enzymatic antioxidant system, in regulating the ROS mediated damage and K^+ retention was highlighted.

3.1.1. Results

3.1.1.1. Optimization of TU, H_2O_2 and NaCl doses for hydroponics study

The selection of working concentration of the NaCl was carried out using post-germination phenotyping at seedling stage with increasing NaCl concentrations (ranging from 50-100 mM). Finally, based on the reduction in biomass 50mM NaCl was selected as IC-50 dose, at which upto 48.15% reduction in biomass was observed as compared to control (Fig. 3.1.1).

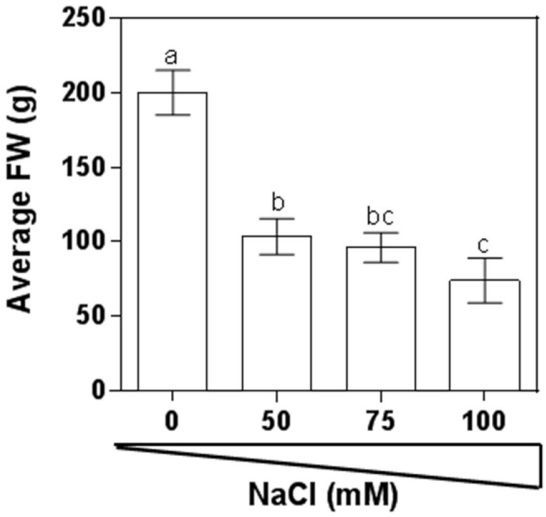

Fig. 3.1.1: Dose-dependent post-germination phenotyping of rice seedlings under NaCl treatment. The rice seedlings were grown hydroponically for 14 days under control conditions and then subjected to variable doses of NaCl such as 0 (control), 50, 75 and 100 mM. After 7 days of treatments, average fresh weight was quantified from 30 seedlings. The data represent mean ± S.E and different letters indicate the significantly changed values (DMRT, $p \leq 0.05$).

Similar dose-dependent study was also carried out with H_2O_2 and TU (ranging from 1-100 µM). The optimum working doses for H_2O_2 (1.0 µM) and TU (7.5 µM) were selected in accordance with gain in seedling biomass (Fig. 3.1.2). The optimized doses for NaCl (50 mM), H_2O_2 (1.0 µM) and TU (7.5 µM) were remained fixed for all the medium supplementation studies.

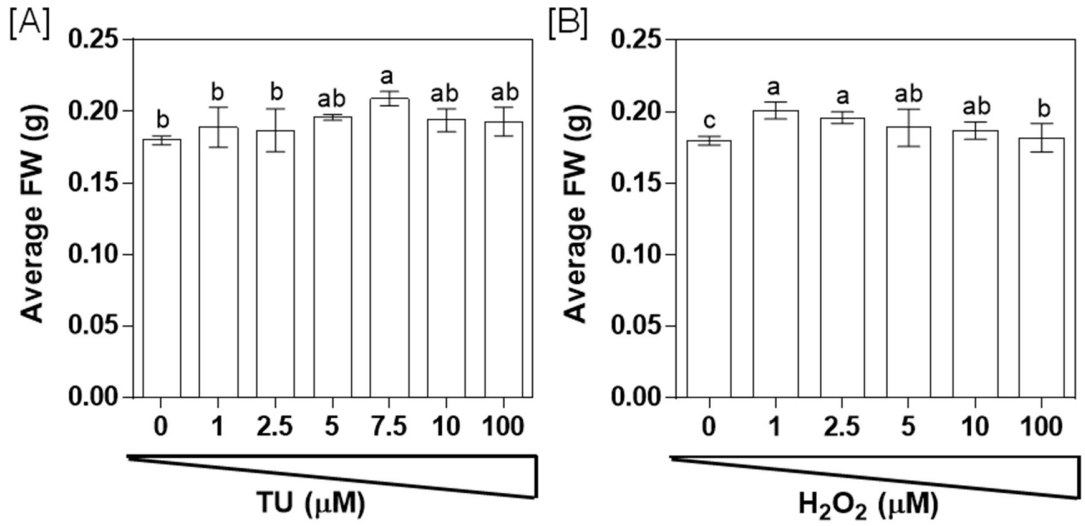

Fig. 3.1.2: Dose-dependent post-germination phenotyping of rice seedlings under TU and H_2O_2 treatments. The rice seedlings were grown hydroponically for 14 days under control conditions and then subjected to variable doses of thiourea (A) or H_2O_2 (B). After 7 day of treatments, average fresh weight was quantified from 30 seedlings. The data represent mean ± S.E and different letters indicate the significantly changed values (DMRT, $p \leq 0.05$).

3.1.1.2. Demonstration of ameliorative potential of TU and H_2O_2 under NaCl stress

A considerable growth penalty like delicate stem and senescent leaves was observed in the NaCl-treated seedlings (Fig. 3.1.3). Further, as compared to control about 14.75 and 16.36% respective decrease in root and shoot lengths (Fig. 3.1.4 A-B) along with 35.03% decrease in the fresh biomass was observed (Fig. 3.1.4 C) in NaCl-treated seedlings. On the other hand, a

significant growth recovery was observed under NH and NT treatments respectively, in terms of shoot length (13.11 and 16.96%; Fig. 3.1.4 A), root length (17.46 and 21.75%; Fig. 3.1.4 B), and biomass (22.55 and 20.59%; Fig. 3.1.4 C) relative to NaCl-treated seedlings. Similarly, upto 62.80% increase in the total antioxidant capacity was reported in NaCl-treated seedlings as compared to those under control conditions. The total antioxidant capacity was further upregulated under NH (37.7%) and NT (31.05%) treatments relative to NaCl treatment (Fig. 3.1.4 D). Although as compared to control upto 45.56% increase was observed in the antioxidant capacity under TU treated seedlings, it remained unchanged under H_2O_2-alone treatment,

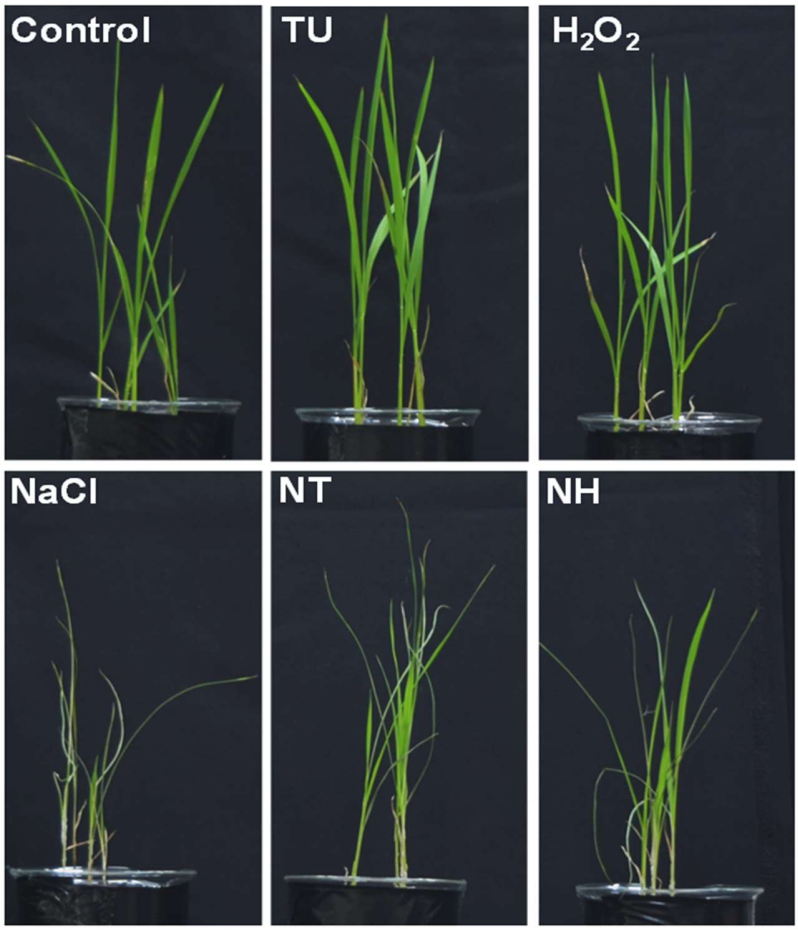

Fig. 3.1.3: Post-germination phenotyping of rice seedlings under different treatments. The differential phenotype was observed after 7 days of treatments supplementation under salt stress.

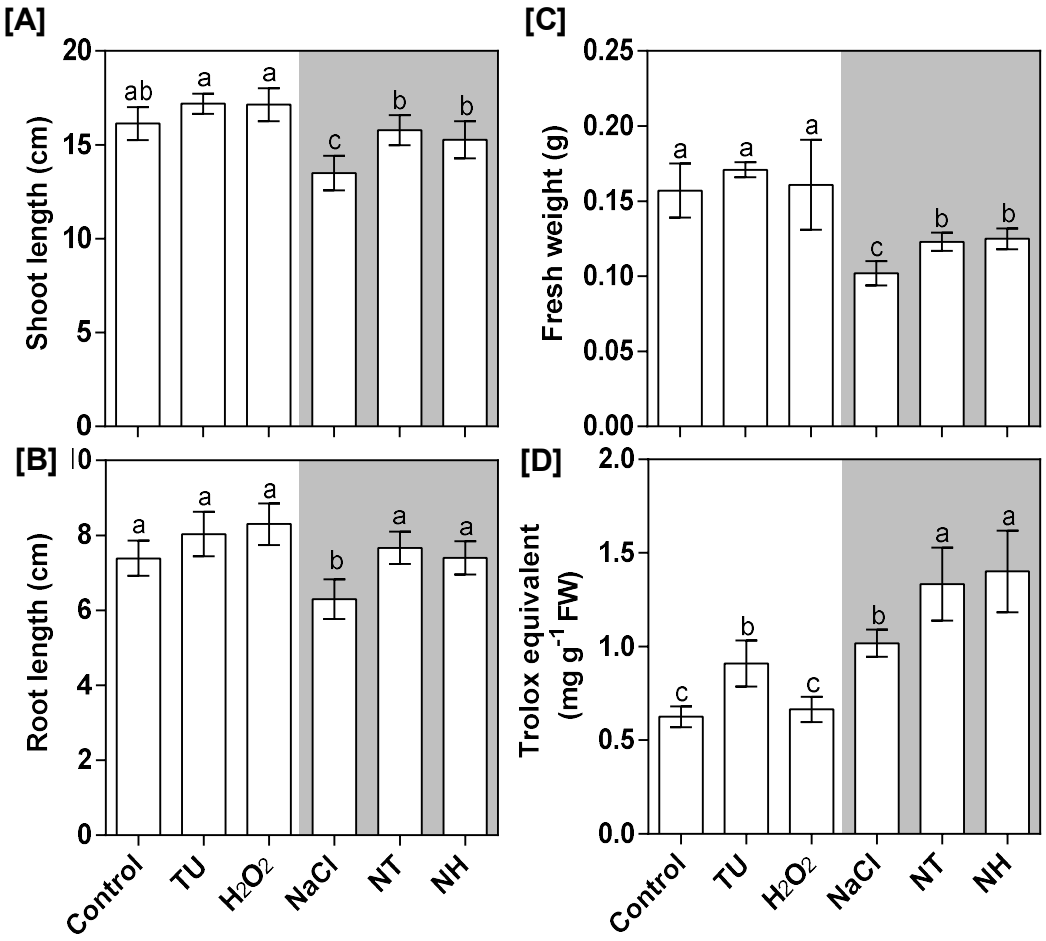

Fig. 3.1.4: Quantification of growth parameters and antioxidant capacity in rice seedlings under different treatments. All the values are mean of triplicates ± SD. Different letters indicate significantly different values (DMRT, $p \leq 0.05$).

3.1.1.3. Estimation of MDA as an indicator of oxidative damage

The stable product of lipid peroxidation i.e., malondialdehyde (MDA) was quantified biochemically in leaf tissues under various treatments after 5 d of the NaCl stress. Although no significant change was observed in the MDA equivalent in TU and H_2O_2 treatments, a sharp increase upto 260% corresponding to corresponding to 18.2 nmol MDA g^{-1} FW was observed

compared to control condition (Fig. 3.1.5). Further, the increase in MDA content was restricted to only 11.2 and 10.8 nmol MDA g^{-1} FW under NH and NT treatments respectively corresponding to 38.46 and 40.66% less MDA accumulation as compared to NaCl alone.

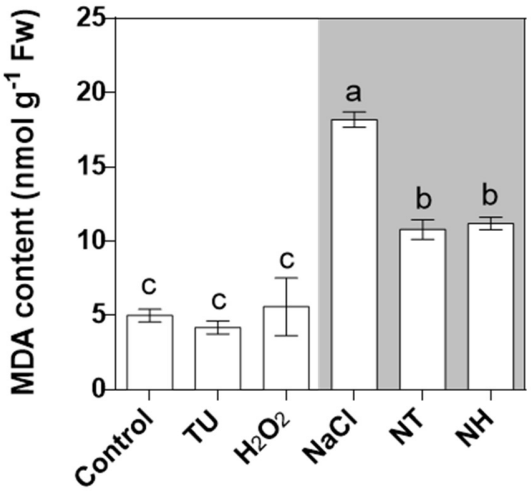

Fig. 3.1.5: Quantification of lipid peroxidation as MDA equivalent. All the values are mean of triplicates ± SD. Different letters indicate significantly different values (DMRT, $p \leq 0.05$).

3.1.1.4. The temporal regulation of antioxidant enzyme activities in rice seedlings

The time dependent regulation of antioxidant enzyme activities under various treatment conditions were analyzed in leaf tissue. In the interest of understanding the overall pattern of enzymatic activities, the median value of the data distribution from all four time-points (1, 6, 24 and 48 h) was computed and compared across analyzed treatments (Fig. 3.1.6; Table 3.1.1). In general, the activities of SOD, CAT and GR were improved by 31.15, 86.33 and 30.49%, respectively under NaCl treatment relative to control (Fig. 3.1.6A-C). The activities of SOD and GR were found to be further increased by (35.19 and 10.6%) and (32.92 and 9.25%) under NH and NT treatments respectively. On the contrary, about 22.72% decrease in the CAT activity was also observed in NT treated seedings relative to NaCl treatment (Fig. 3.1.6 B). Although, in general the activities of SOD, CAT and GR remined upregulated under TU and H_2O_2 alone

treatments as compared to control, relative high activities were observed under H_2O_2 supplementation (Fig. 3.1.6A-C, Table 3.1.1). Additionally, the median distribution of the APX over the analyzed time points clearly remained unchanged among various treatments (Fig. 3.1.6D). However, the differential regulation of APX activity was observed at 48h time point, showing about 29% decrease under NaCl-treated leaves relative to control. On the other hand, for the same time point upto 22.55 and 81.28% increase in NH and NT respectively as compared to NaCl treatment (Table 3.1.1). No such change in APX activity at 48h was noticed under H_2O_2 and under TU alone treatments (Table 3.1.1).

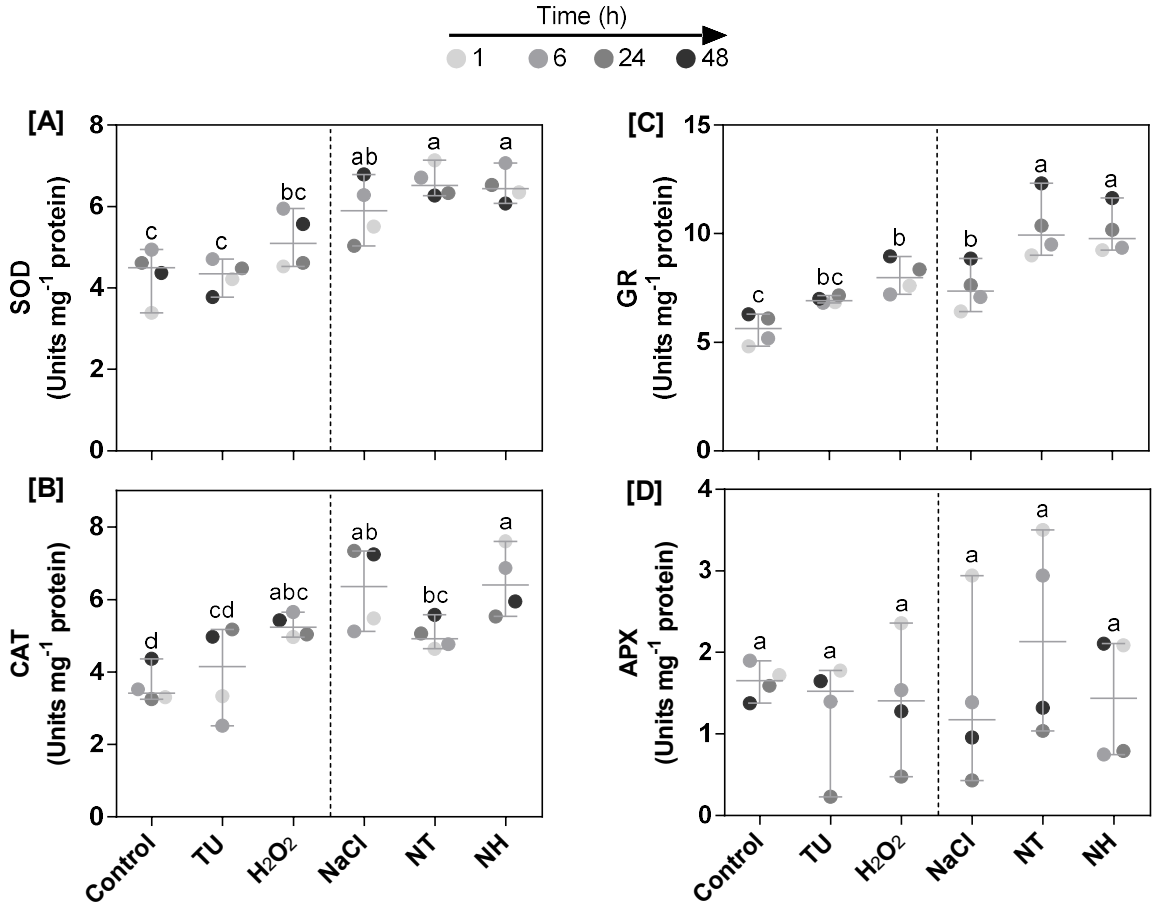

Fig. 3.1.6: The temporal regulation of antioxidant enzyme activities in rice seedlings. The data was represented in the form of median value with range was computed using individual data

from all four time-points (1, 6, 24 and 48 h). Different letters indicate significantly different values (DMRT, $p \leq 0.05$).

Table-3.1.1: Temporal kinetics of various antioxidant enzymes

Treatments	1 h	6 h	24 h	48 h
A. SOD (Units mg^{-1} protein)				
Control	3.39^{e} (± 0.15)	4.94^{b} (± 0.55)	4.62^{b} (± 0.52)	4.37^{c} (± 0.15)
TU	4.22^{d} (± 0.09)	4.71^{b} (± 0.17)	4.48^{b} (± 0.66)	3.78^{c} (± 0.45)
H_2O_2	4.53^{d} (± 0.05)	5.95^{ab} (± 0.10)	4.62^{b} (± 0.38)	5.57^{b} (± 0.15)
NaCl	5.51^{c} (± 0.69)	6.28^{a} (± 0.46)	5.04^{b} (± 0.36)	6.79^{a} (± 0.62)
NT	7.14^{a} (± 0.47)	6.71^{a} (± 0.46)	6.33^{a} (± 0.70)	6.27^{ab} (± 0.47)
NH	6.35^{b} (± 0.36)	7.07^{a} (± 1.50)	6.53^{a} (± 0.82)	6.08^{ab} (± 0.70)
B. CAT (Units mg^{-1} protein)				
Control	3.30^{c} (± 0.40)	3.52^{c} (± 0.27)	3.25^{c} (± 0.30)	4.36^{c} (± 0.70)
TU	3.33^{c} (± 0.51)	2.52^{d} (± 0.99)	5.17^{b} (± 0.90)	4.97^{bc} (± 1.00)
H_2O_2	4.96^{b} (± 0.70)	5.65^{b} (± 0.50)	5.04^{b} (± 0.30)	5.43^{bc} (± 0.90)
NaCl	5.48^{b} (± 0.78)	5.12^{b} (± 0.18)	7.34^{a} (± 0.41)	7.24^{a} (± 0.44)
NT	4.64^{b} (± 0.25)	4.77^{b} (± (0.56)	5.06^{b} (± 0.63)	5.58^{bc} (± 0.49)
NH	7.60^{a} (± 0.37)	6.87^{a} (± 0.21)	5.53^{b} (± 0.73)	5.94^{b} (± 0.48)
C. GR (Units mg^{-1} protein)				
Control	4.82^{d} (±0.45)	5.18^{c} (±0.33)	6.09^{c} (±0.80)	6.29^{c} (±0.58)
TU	6.84^{c} (±0.39)	6.82^{b} (±0.82)	7.16^{bc} (±0.04)	7.00^{c} (±0.64)
H_2O_2	7.61^{b} (±0.66)	7.20^{b} (±0.57)	8.35^{b} (±0.51)	8.96^{b} (±0.20)
NaCl	6.42^{c} (±0.21)	7.08^{b} (±0.39)	7.63^{b} (±0.84)	8.86^{b} (±0.72)
NT	9.00^{a} (±0.45)	9.51^{a} (±0.48)	10.37^{a} (±0.68)	12.32^{a} (±0.56)
NH	9.24^{a} (±0.01)	9.36^{a} (±0.41)	10.19^{a} (±1.39)	11.64^{a} (±1.28)
D. APX (Units mg^{-1} protein)				
Control	1.72^{e} (±0.01)	1.9^{b} (±0.05)	1.59^{a} (±0.07)	1.38^{bc} (±0.26)
TU	1.78^{e} (±0.01)	1.4^{c} (±0.05)	0.23^{c} (±0.21)	1.65^{b} (±0.21)
H_2O_2	2.36^{c} (±0.23)	1.54^{c} (±0.06)	0.48^{bc} (±0.35)	1.28^{bc} (±0.30)
NaCl	2.94^{b} (±0.10)	1.39^{c} (±0.19)	0.43^{bc} (±0.09)	0.96^{c} (±0.09)
NT	3.5^{a} (±0.16)	2.94^{a} (±0.16)	1.04^{ab} (±0.59)	1.32^{bc} (±0.16)
NH	2.09^{d} (±0.34)	0.75^{d} (±0.34)	0.79^{bc} (±0.42)	2.11^{a} (±0.24)

3.1.1.5. Temporal regulation of ion accumulation (Na^+ and K^+) in rice leaves

Akin to antioxidant enzymatic activities, the ion accumulation pattern was also analyzed considering the median distribution along all the 4 individual data points (1, 6, 24 and 48 h). No significant change in the overall Na^+ accumulation pattern was observed across different analyzed treatments (Fig. 3.1.7 A). On the contrary, TU and H_2O_2 mediated improved K^+ retention was observed under control (TU and H_2O_2 alone) as well as NaCl treatment (NT and NH) relative to control and NaCl treatment respectively (Fig. 3.1.7 B). A sharp decline in K^+ accumulation corresponding to about 59.22% was observed at 48 h, under NaCl relative to control. Alternatively, about 105.47 and 147.32% increase in K^+ accumulation was observed under NH and NT treatments, respectively at the same time point (48 h), compared to NaCl treatment. Likewise, the improved K+ retention was also observed at 48 h for H_2O_2 and TU alone treatments showing a respective increase of about 33.42, 38.58% relative to control (Fig. 3.1.7, Table 3.l.2).

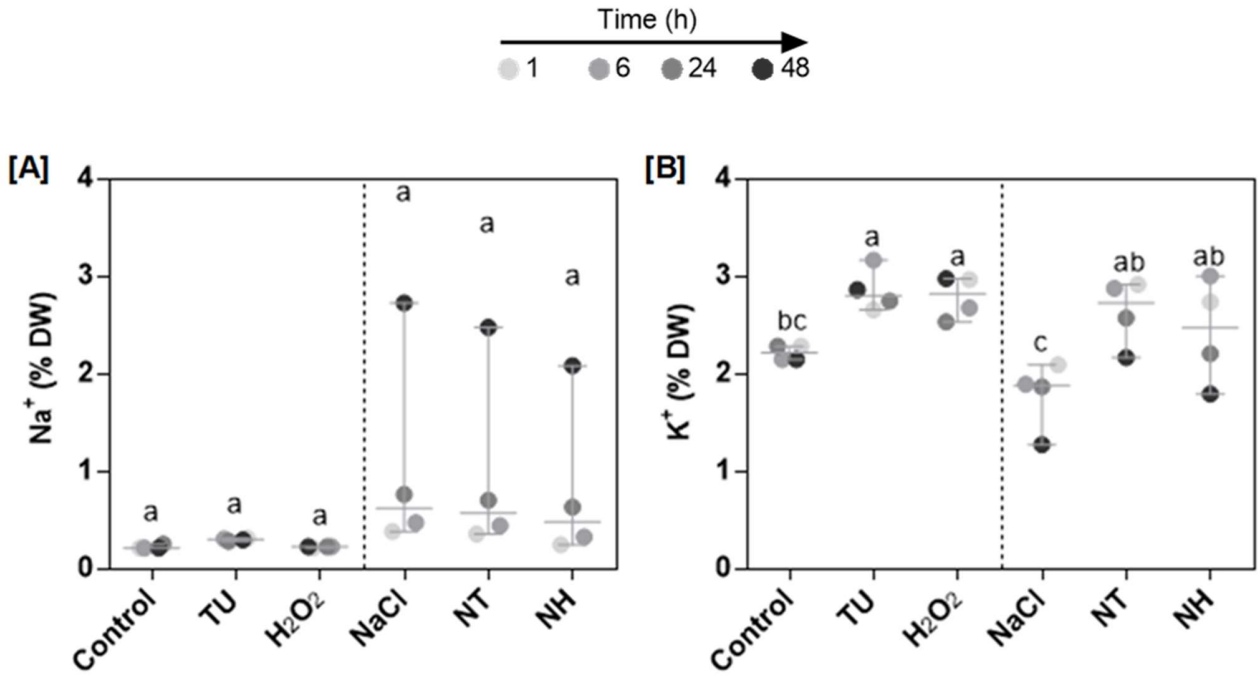

Fig. 3.1.7: Time dependent accumulation of Na^+, K^+ and Na^+/K^+ ratio in the leaf of rice

seedling subjected to different treatments. All the values are mean of triplicates ± SD. Different letters indicate significantly different values (DMRT, $p \leq 0.05$).

Table-3.1.2: Temporal accumulation of Na^+ and K^+ in leaf tissue

	1 h	6 h	24 h	48 h
A. Na^+ content (% DW)				
Control	0.220^{c} (± 0.01)	0.215^{d} (± 0.01)	0.260^{de} (± 0.02)	0.220^{d} (± 0.01)
TU	0.324^{b} (± 0.03)	0.308^{c} (± 0.03)	0.286^{d} (± 0.02)	0.296^{d} (± 0.02)
H_2O_2	0.223^{c} (± 0.02)	0.225^{d} (± 0.02)	0.233^{e} (± 0.02)	0.226^{d} (± 0.01)
NaCl	0.388^{a} (± 0.01)	0.482^{a} (± 0.01)	0.773^{a} (± 0.02)	2.730^{a} (± 0.04)
NT	0.355^{a} (± 0.03)	0.446^{b} (± 0.01)	0.705^{b} (± 0.01)	2.477^{b} (± 0.08)
NH	0.251^{c} (± 0.02)	0.325^{c} (± 0.01)	0.639^{c} (± 0.03)	2.086^{c} (± 0.05)
B. K^+ content (% DW)				
Control	2.287^{bc} (± 0.24)	2.146^{b} (± 0.18)	2.290^{b} (± 0.30)	2.151^{b} (± 0.14)
TU	2.660^{abc} (± 0.50)	3.166^{a} (± 0.31)	2.750^{a} (± 0.26)	2.870^{a} (± 0.23)
H_2O_2	2.973^{a} (± 0.34)	2.683^{a} (± 0.25)	2.543^{ab} (± 0.18)	2.981^{a} (± 0.51)
NaCl	2.104^{c} (± 0.15)	1.903^{b} (± 0.05)	1.271^{c} (± 0.06)	0.877^{c} (± 0.04)
NT	2.917^{a} (± 0.22)	2.883^{a} (± 0.21)	2.581^{ab} (± 0.19)	2.169^{b} (± 0.18)
NH	2.742^{ab} (± 0.31)	3.010^{a} (± 0.52)	2.212^{bc} (± 0.21)	1.802^{b} (± 0.09)

3.1.2 Discussion

Irrespective of their contrasting redox modulatory chemistry, *in vivo* supplementation of both H_2O_2 as well as TU enhanced the redox competence and invigorate plant growth under NaCl stress conditions (Fig. 3.1.1). The negative effect of salinity was observed over root length, shoot length and biomass of the seedlings. The result of the study demonstrated more prominent effect over root length rather than shoot length. Root being the first organ of the plant system that is in direct contact with the salinity responded more quickly and vigorously [203]. Salinity inhibits the root growth by repressing the cell division and meristematic region elongation and thereby limiting primary root length [204]. Further root meristematic region was reported to be

regulated by auxin levels and its redistribution [205]. Salinity induced ROS in root suppresses the auxin biosynthesis resulted in inhibition of root growth [206]. Thiourea, as a ROS scavenger may decrease the ROS load in the root system thereby protecting the auxin signaling. On the other hand, H_2O_2 supplementation may regulate the synthesis and redistribution of auxin via polar auxin transport, to bring about changes in root system architecture. Plants were reported to respond to varied concentration of H_2O_2 by establishing very dense root system with profuse lateral roots and smaller primary root [207]. The toxic effect of salt stress, reported to be associated with increased accumulation of lipid peroxidation products which in turn destabilize the plasma membrane integrity and functionality (refer section 1.4). The relative increase in the MDA content under salt stress was reported to be used as an indicator for assessing salt-tolerant cultivars in alfalfa [208]. Moreover, a significant negative correlation in between MDA and leaf relative water content along with photosynthesis was reported in cotton genotypes, justifying its regulatory role in plant growth and survival [209]. In the present study, reduced accumulation of MDA was observed under NH and NT treatments relative to NaCl alone. The decrease in lipid peroxidation under NT and NH treatments can be attributed to improved ROS and ionic homeostasis.

The unbalanced nutrient and toxic ion accumulation in shoot are responsible for the salinity mediated inhibitory effects on biomass accumulation. The salinity mediated increase in ROS induces the activation of enzymatic and non-enzymatic antioxidant machinery to offset the oxidative stress [210]. The soluble non enzymatic antioxidant system which involves ascorbate, glutathione, polyphenols etc. provides buffering capacity to cytoplasmic and intracellular matrix to scavenge the ROS [45]. Oxygen radical scavenging assay is a representative for the total non-enzymatic antioxidant pool (antioxidant capacity). Results of the present study indicated up-

regulation of the antioxidant capacity under NT and NH treatments. The increase in the antioxidant capacitance can be directly related to stress tolerance under salinity. Further, the improved antioxidant enzymatic system was also found to play an important role for imparting tolerance towards various abiotic stresses including salinity [211].

Since the ROS induced perturbance in the cellular redox homeostasis, is the decisive factor for growth penalty like decrease in biomass and shorter root and shoot length under salt stress, therefore the ameliorative potential of H_2O_2 and TU could largely be attributed to preserve this redox homeostasis. The existence of such overlapping responses, suggested the generation of reducing redox intracellular milieu with H_2O_2 supplementation. This is validated by H_2O_2 mediated increased activation of various antioxidant enzymes like SOD, CAT and GR under both control and NaCl stress conditions (Fig. 3.1.5A-C). The ability of H_2O_2 to trigger the plant's antioxidant defense has also been demonstrated in various crops like soybean [212] rice [213] and wheat [214]. unlike H_2O_2, the enzymatic antioxidants were sparsely activated in TU-treated control plants, thereby facilitating the activation of alternate branch of antioxidant defense (non-enzymatic antioxidants) to maintain reducing redox environment. Earlier study also demonstrated the activation of non-enzymatic antioxidants system under TU treatment in *B. juncea* [215]. Additionally, the improved activity of CAT [216], APX [217] and GR [218] was found to mediate their protective effect under salt stress. Here the results revealed that most of the antioxidant enzymes which were upregulated under H_2O_2 supplementation alone, might help the plant system to encounter the subsequent salt stress in a better way. The results were consistent with the previous reports which demonstrated the H_2O_2 mediated stress tolerance was coupled with efficient activation of antioxidant enzyme and limiting the endogenous ROS

accumulation [172, 173]. Activation of antioxidant machinery in turn helps in protecting the structural integrity and functionality of cellular organelles under abiotic stress.

Further the catalase activity has shown its maximum activity for the initial phase of the salt imposition (upto 6 h), then after improved APX activity takes over the charge of fine-tuning the H_2O_2 level and associated signaling (Fig 3.1.6, Table 3.1.2). The pretreatment mediated increased endogenous H_2O_2 activated the catalase and downstream signaling pathway which responded very aggressively towards the subsequent NaCl exposure in the initial phase resulting in activation of defense related genes. The activated defense system in turn was able to detoxify the ROS load with activation of APX. The increased activity of APX maintains the ascorbate pool towards reducing end and thereby facilitates the ROS detoxification [179]. On the other hand, the activity of GR and APX was up-regulated under NT showing that thiourea maintains the cellular redox homeostasis. Besides improved redox balance, increased K^+ retention was found to mediate its protective function under NH- and NT- treatments showing superior plant growth and survival relative to NaCl treatment (Fig. 3.1.1).

A positive correlation between high-level K^+ retention and salinity tolerance has been manifested in crops like barley and rice [219]. Potassium (K^+) acts as a cofactor for various enzymes regulating metabolic status and protein translation of plants [220]. Further K^+ homeostasis also plays a crucial role in regulating the membrane potential, turgor and cytoplasmic pH change [221]. The NaCl-triggered K^+-leakage is strongly linked with ROS generation and subsequent stimulation of K^+-efflux channels involving guard cell outward rectifying K^+ channel (GORK) and stelar K^+ outward rectifier (SKOR) [222].

Thus, the medium supplementation of TU and H_2O_2 increase the activities of antioxidant enzymes along with higher K^+ retention capability which conclusively appeared as improved plant growth and survival under the NaCl stress conditions.

Section II: To study the molecular mechanisms of TU and H_2O_2 mediated salinity tolerance

3.2. Introduction

The increased production of ROS under stress conditions oxidizes various biomolecules including lipids, proteins and DNA [45]. Out of the various byproducts of ROS mediated damages, lipid peroxidations and protein carbonylations are the most toxic to plants. The lipid peroxidation and protein carbonylation are thus stable indicators of the ROS mediated damage and can be correlated well with that of loss of structural integrity and functionality of bio membranes [51]. Both lipid peroxidation and protein carbonylation can be quantified as function of time for the damage estimation to lipids and proteins [48, 49]. Apart from the LPO and PC formation, alternation in the expression pattern of various stress responsive genes is an immediate response in plants. The activation of stress responsive genes, downstream to various signaling mediators helped the plants to overcome the undesirable effect of salt stress [39]. Most of the salt stress responsive genes belong to *LEA* group of protein, chaperones, K^+ channel protein and transmembrane proteins. The delicate balance in between the ROS generation and their neutralization depicts the ultimate fate of plant system for stress tolerance or death [45, 47]. The study of differential proteome under various treatments including TU and H_2O_2 with or without NaCl highlighted the critical protein machinery associated with their ameliorative potential. Activation of antioxidant enzymatic systems, protection of chloroplast and mitochondria function along with active involvement of thioredoxin (Trx) and glutaredoxin (Grx) system were found to be key regulators for imparting salinity tolerance.

Redox regulation plays an important role in various plant metabolic activities which includes carbon anabolism in chloroplast and carbon catabolism in mitochondria [100, 110]. The negative effect of salt stress mediated decrease in carbon assimilation and increase in

ATP requirement may alter the flux of the metabolites in pathways indispensable for plant's survival under stress conditions [40, 100]. In general activation of some specific shunts like GABA shunt, malate valve was activated under stress condition in order to facilitate the carbon flow in the tricarboxylic acid **(**TCA) cycle and energy supply to mitochondria [119, 120, 121].

3.2.1. Results

3.2.1.1. Status of early salt responsive genes under various treatments

Based on the published transcriptome of rice seedlings [223], top eight salt stress responsive genes were chosen for their expression analysis in leaf tissue under studied treatment conditions. The outcome of the study reflected an upregulated expression of most of the salt responsive genes under TU and H_2O_2 supplementations, in both control as well as NaCl stress conditions (Fig. 3.2.1). The most noticeable impact was seen in *LEA1* (late-embryogenic abundant 1), *HAK21* (high-affinity K^+ transporter), dehydrin and *TSPO* (translocator protein), whose expression were improved by 475, 279.42, 113.41 and 162.78% under TU, and 625, 285.92, 94.72 and 362.58% under H_2O_2-treatment relative to control. Likewise, as compared to NaCl the relative expression of these genes was found to be further upregulated corresponding to of *HAK21* (201.42; NH and 166.75%; NT), *LEA1* (350%; NH and 1450%; NT), dehydrin (59.54%; NH and 48.85%; NT) and *TSPO* (39.97%; NH and 84.89%; NT) (Fig. 3.2.1 A–E). On the other hand, the expression profile of other analyzed genes *PIPK*, *TPP,* and *EN20* were primarily upregulated under H_2O_2 and TU alone treatments relative to control. No significant change in the expression profile of *PIPK*, *TPP* while upto 285.06% increase in *EN20* was observed under NT treatment relative to NaCl treatment. Similarly, the expression of *TPP* and *PIPK* were found to be downregulated by upto 34.08 and 39.39% respectively in NH-treated leaves, while about 144.67% upregulation in *EN20* expression relative to NaCl treatment (Fig. 3.2.1 F–H).

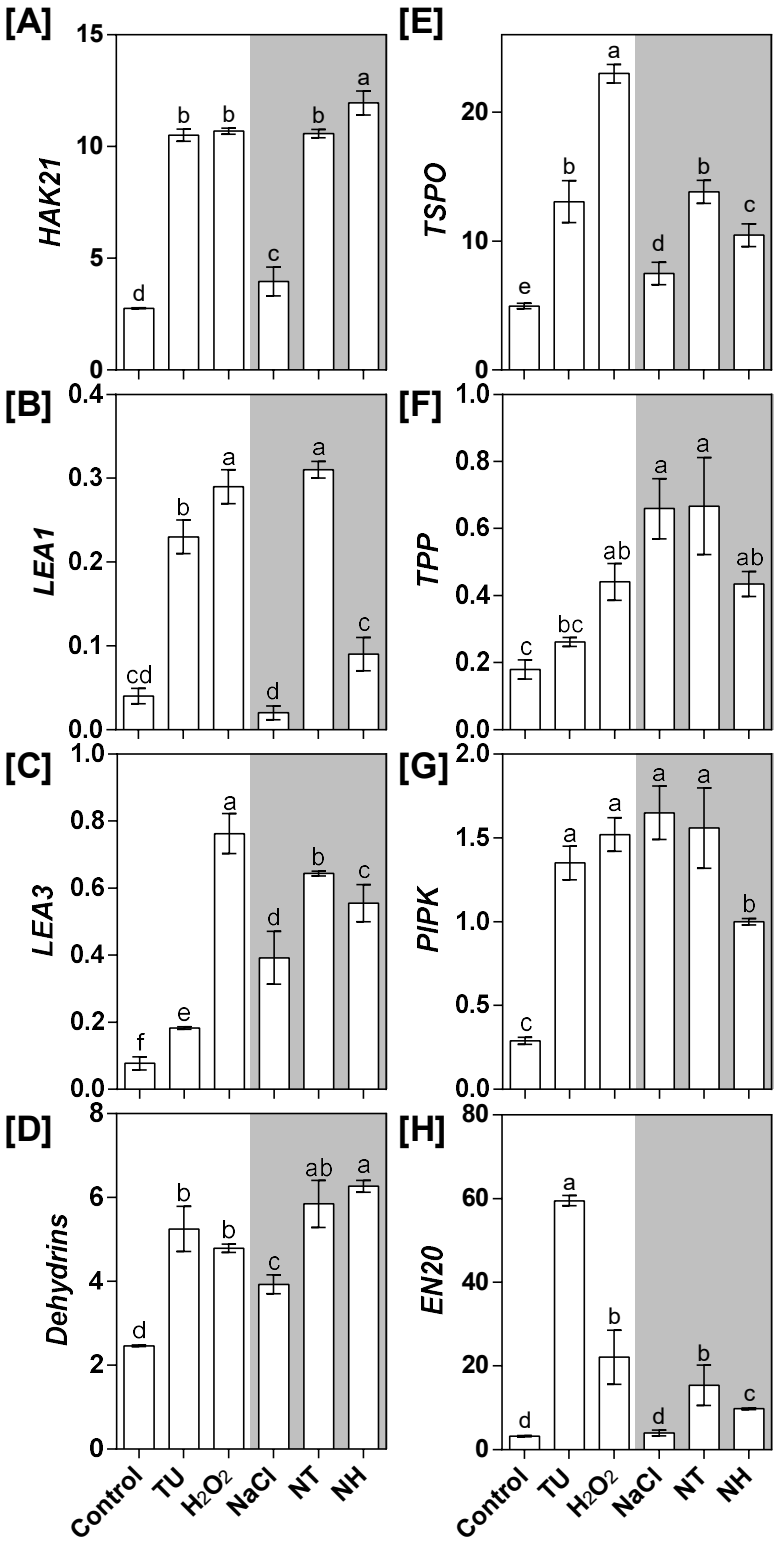

Fig. 3.2.1: Real time expression analysis of salt stress responsive genes. The relative expression of various salt responsive gene was analysed in the leaf tissue after 6 h of

treatment. The various genes included for the study were high-affinity K^+ transporter (*HAK21*; A), late embryogenic abundant protein-1 and 3 (*LEA1*; B and *LEA3*; C), dehydrins (D), translocator protein (*TSPO*; E), trehalose-phosphate phosphatase (*TPP*; E), phosphatidylinositol-4-phosphate 5 kinase (*PIPK*; F) and early nodulin-20 (*EN20*; H). All the values are mean of triplicates ± SD and are normalized using *tubulin* as constitutive gene. Different letters indicate significantly different values (DMRT, $p \leq 0.05$).

3.2.1.2. Detection of protein carbonyls

Since, both TU and H_2O_2 showed tolerance towards salt stress, the level of protein carbonylation (PC) as an oxidative stress marker was analyzed among different treatment conditions. An antibody based immunodetection with anti-2,4-dinitrophenylhydrazone, showed a general increase in the PC content under NaCl treatment relative to control conditions. On the contrary, relatively lower levels of PC were observed under NH and NT treatments, compared to seedlings under NaCl stress conditions (Fig. 3.2.2). Under non-stresses conditions, PC levels remained unchanged under H_2O_2; however, got reduced in TU treated plants.

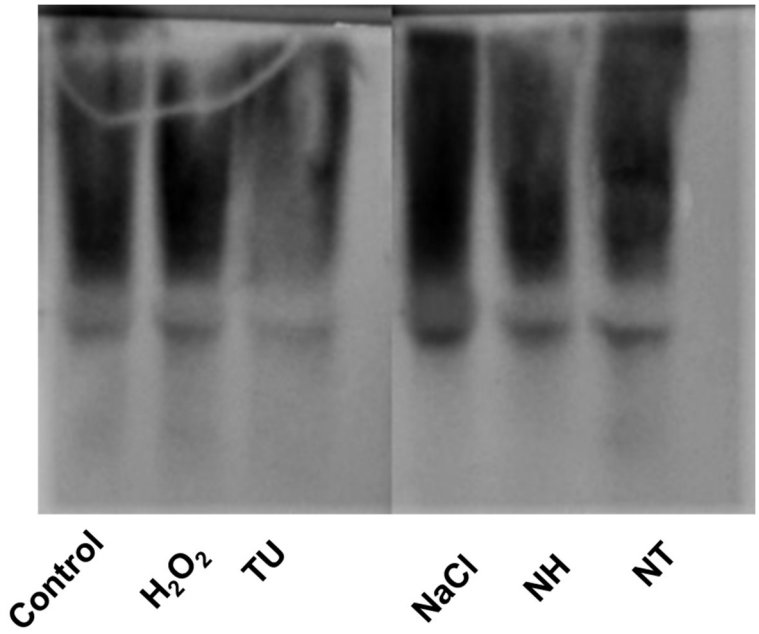

Fig. 3.2.2: Detection of protein carbonyls under different treatments

3.2.1.3. Quantification of redox status in root tissue under different treatments

The iodoacetamide (IAN) based histochemical staining was carried out to estimate the overall redox status in roots. The IAN fluorescence intensity was significantly increased by 84 and 47.5 % under TU and H_2O_2 supplementation, respectively compared to those of control (Fig. 3.2.3). In contrast, under NaCl stress, IAN fluorescence intensity was reduced, indicating oxidative redox status. Under NT and NH treated roots, IAN fluorescence intensity was increased by 160.6 and 177.7%, respectively, relative to NaCl treatment (Fig 3.2.3).

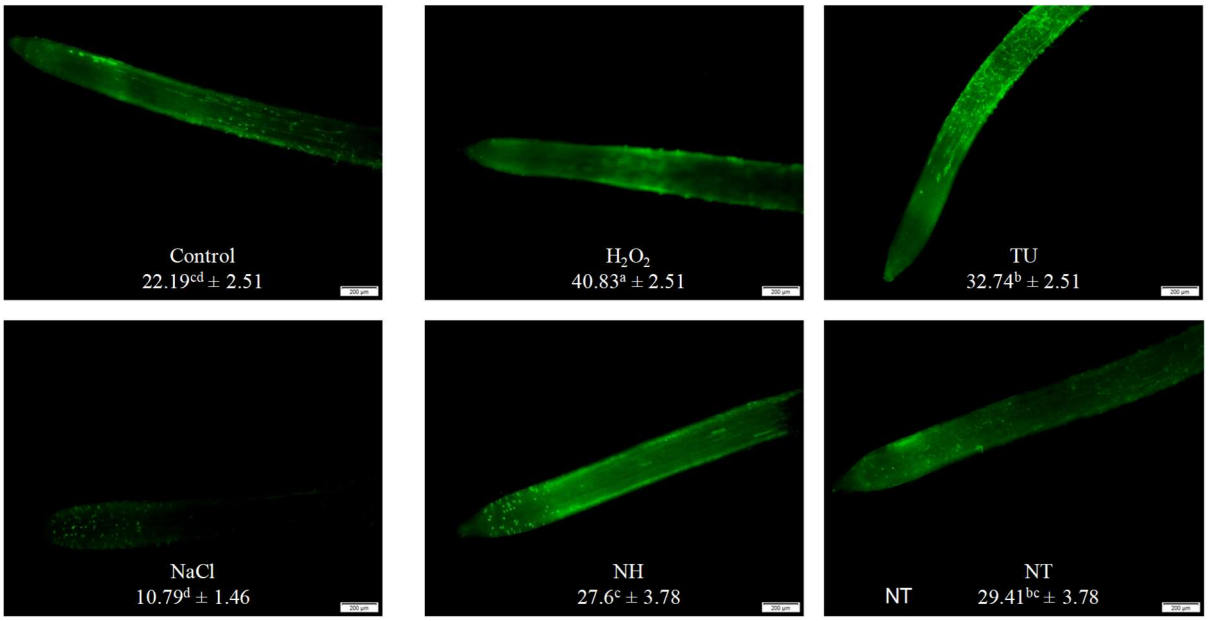

Fig. 3.2.3: Status of reduced thiols in roots of rice seedlings under various treatments. Iodoacetamide stain intensity was quantified using image J software and represented as mean ± S.D of 10 individual biological replicates. Different letters indicate significantly different values (DMRT, $p \leq 0.05$).

3.2.1.4 Identification of differentially expressed proteins (DEPs) using iTRAQ approach

To understand the molecular basis of TU and H_2O_2 mediated protection, proteomic analysis was carried an iTRAQ-based approach. A total of 425 DEPs were identified across different treatments by applying $p \leq 0.05$ as statistical cut-off limit. A fold change cut-off 1.2

was also applied to identify the top-ranked DEPs. Initially, venn analysis was performed to identify the overlapping and specific DEPs under different treatments.

A total of seven major clusters of DEPs were identified (Fig. 3.2.4, Table 3.2.1). First five clusters represent specific DEPs under NaCl (54; Cluster-1), NT (18; Cluster-2), NH (27; Cluster-3), TU (17; Cluster-4) and H_2O_2 (12; Cluster-5) treatments. Cluster-6 included 41 DEPs which were common among all the treatments; while, cluster-7 contained 48 DEPs which were shared between NaCl, NT and NH treatments. In addition, heat-map based hierarchical clustering was performed to understand the expression pattern of ASD (Fig. 3.2.5) and NRD (Fig. 3.2.6) clusters.

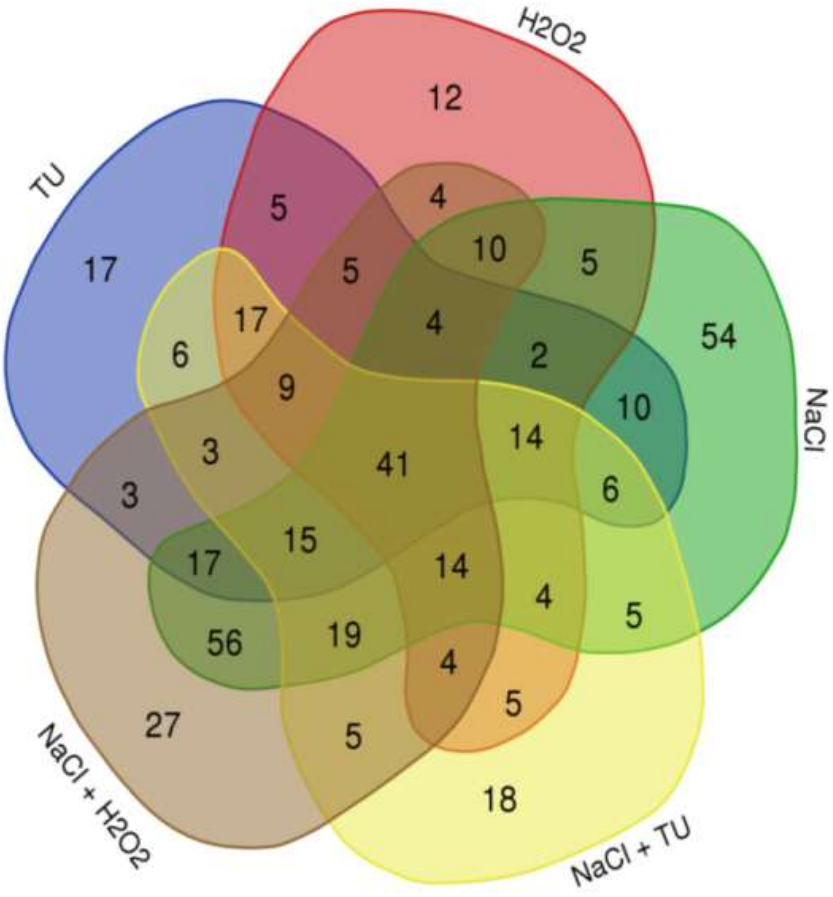

Fig. 3.2.4: Venn diagram showing differentially expressed proteins under various treatments.

Table-3.2.1: Cluster-wise presentation of differentially expressed proteins

Clusters	DEPs under treatments	Number of DEPs	Abbreviations
Cluster 1	NaCl specific DEPs	54	NSD
Cluster 2	NaCl responsive TU dependent DEPs	18	NTD
Cluster 3	NaCl responsive H2O2 dependent DEPs	27	NHD
Cluster 4	TU specific DEPs	17	TSD
Cluster 5	H_2O_2 specific DEPs	12	HSD
Cluster 6	All treatment specific DEPs	41	ASD
Cluster 7	NaCl responsive and redox modulated DEPs	14+15+19	NRD

Four independent groups were identified in ASD clusters (Fig. 3.2.5), of which the group-3 DEPs were mainly related to photosynthesis and carbon assimilation, such as, glutamate dehydrogenase, glyceraldehyde-3-phosphate dehydrogenase, phosphoglucomutase and inorganic pyrophosphatase. The expression levels of group-3 ASD were downregulated under NaCl treated shoot; while, partial restoration in expression was observed under both NT and NH treatment. The expression pattern was also differential under NT and NH treatment (Fig. 3.2.5). For instance, the inorganic pyrophosphatase level was downturned under NaCl treatment as compared to control. On the contrary, upto 1.61- and 1.21-fold increase in inorganic pyrophosphatase level was detected under NH and NT treatments

respectively. Similarly, the level of ATP synthase was increased significantly by 2.06-fold in NT; while, under NH treatment, it was found comparable to those of NaCl alone treatment. Most of the group1, 2 and 4 ASDs were found to be upregulated under NaCl treatment (Fig. 3.2.5). These were comprised of components related to defense (superoxide dismutase and late-embryogenic abundant protein) and protein folding (peptidyl-prolyl cis-trans isomerase). In TU and H_2O_2 alone treatments, group-3 ASDs (related to growth) were found to be up-regulated while, most of the group-1 and 3 ASDs (related to defense) remained downregulated (Fig. 3.2.5). The group-2 ASDs were found to be up- and down-regulated under TU and H_2O_2 alone treatments, respectively. The group-2 ASDs included chloroplastic proteins such plastocyanin domain containing protein [-1.67 (TU) and 1.38 (H_2O_2)] and oxygen-evolving enhancer protein [1.55 (TU) and 1.23 (H_2O_2)] (Fig. 3.2.5).

The expression pattern of NRD clusters was also analysed using the heat-map based clustering approach. This yielded a total of three distinct groups (Fig 3.2.6). Most of the group-2 NRDs were related to photosynthesis and carbon assimilation and their expression pattern overlap with those of group-3 ASDs (downregulated under NaCl and partially restored in NT and NH treatments). In contrast, group-1 and 3 NRDs were found up-regulated under NaCl treatment; while, contrasting expression pattern was observed under TU and H_2O_2 alone treatments (Fig. 3.2.6). Most of the group-1 NRDs like sucrose synthase 2 [2.02-fold (NT) and 1.41-fold (NH] and glucose-1-phosphate adenylyltransferase [2.06-fold (NT) and 0.94-fold (NH)] were up- and down-regulated under NT and NH treatment, respectively; while vice versa pattern was seen for group-3 NRDs like thioredoxin [1.39-fold (NT) and 3.49 (NH)] and glutaredoxin [1.64-fold (NT) and 4.06-fold (NH)] (Fig. 3.2.6).

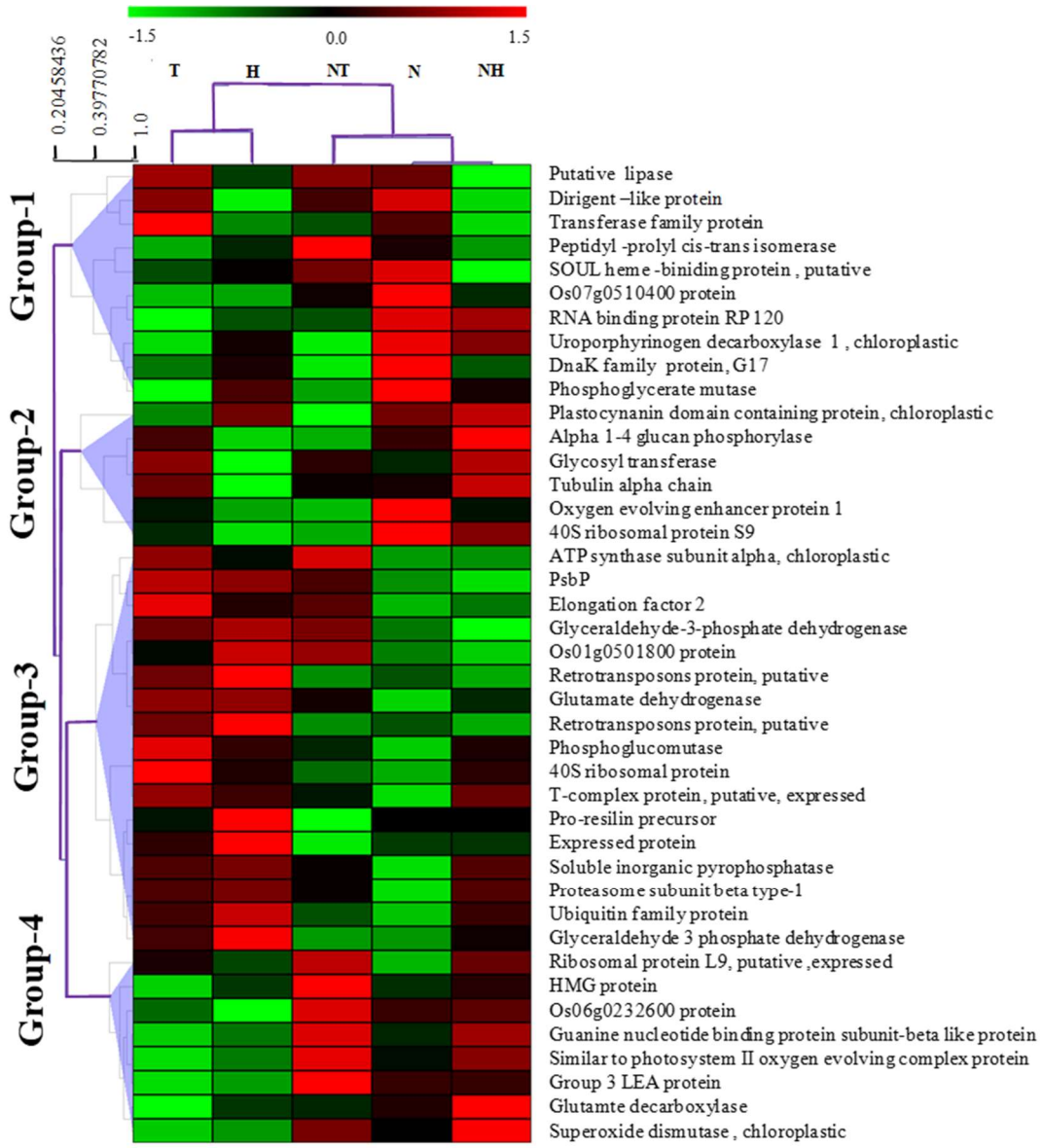

Fig. 3.2.5: Heat-map based clustering of All treatment specific DEPs (ASDs) in rice. Individual replicates are separated using hierarchical clustering, with the dendrogram scaled to represent the distance between each branch. Normalized signal intensities (log2 transformed and row adjustment) are visualized as a color spectrum and the scale from least abundant to highest ranges is from −1.5 to 1.5. Green color indicates low and red color indicates high abundance of detected proteins.

In addition, the treatment-specific DEPs (Table 3.2.2) highlighted the defense activation and metabolic slow-down under NaCl stress; while partial restoration was

observed under NT and NT treatment. Besides, photosynthesis was found to be boosted under TU and H_2O_2 alone treatments.

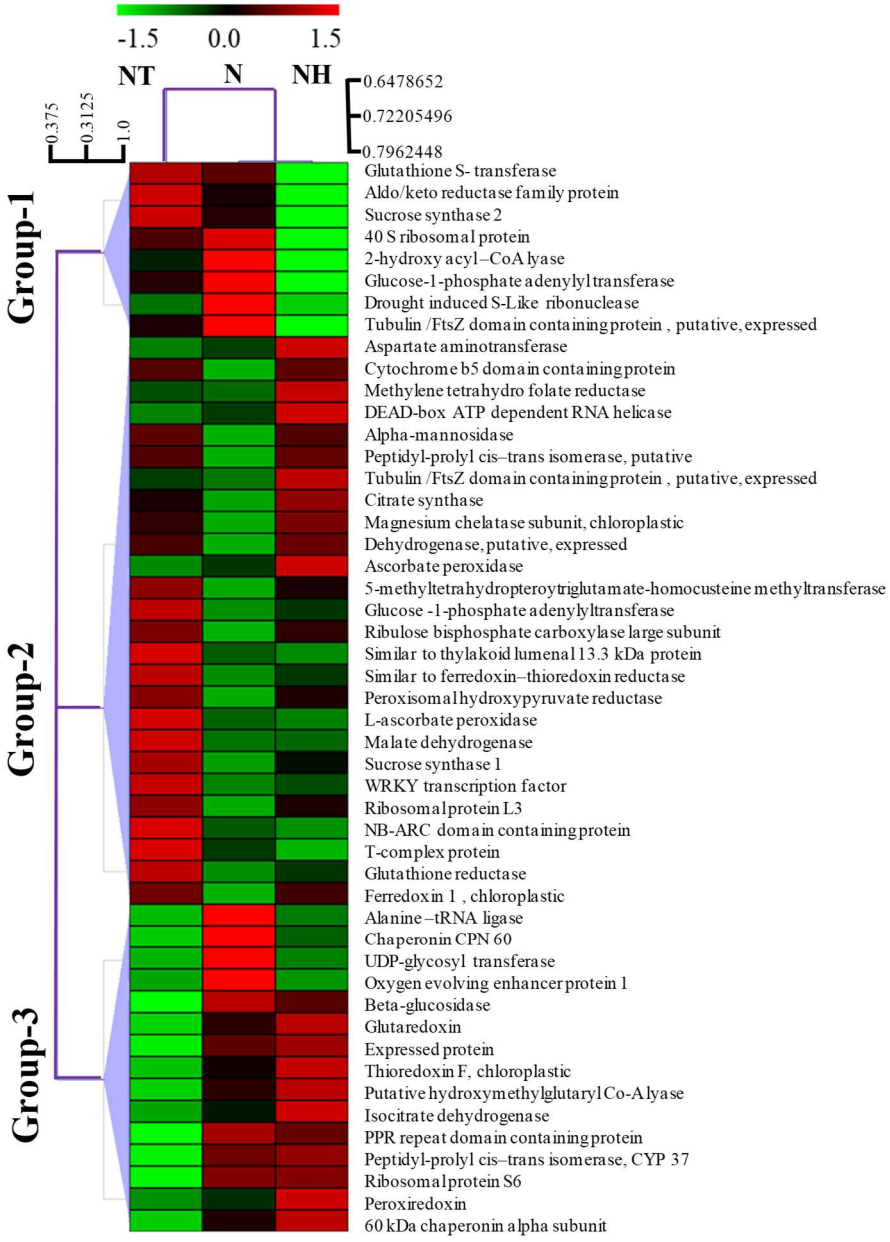

Fig. 3.2.6: Heat-map based clustering of NaCl responsive and redox modulated DEPs (NRDs) in rice. Individual replicates are separated using hierarchical clustering, with the dendrogram scaled to represent the distance between each branch. Normalized signal intensities (log2 transformed and row adjustment) are visualized as a color spectrum and the scale from least abundant to highest ranges is from −1.5 to 1.5. Green color indicates low and red color indicates high abundance of detected proteins.

Table-3.2.2: List of treatment-specific DEPs.

Locus id	FC (Log_2)	Annotation	% coverage	Peptide
NaCl-specific DEPs (NaCl Vs. Control)				
LOC_Os02g54060.1	2.44	Germin-like protein 3-3	37.46	13
LOC_Os01g10850.1	2.42	Peroxidase	33.64	9
LOC_Os07g02330.1	2.10	Probable protein phosphatase 2C	49.58	22
LOC_Os01g55730.1	2.02	AGAP003732-PA, putative, expressed	37.65	11
LOC_Os09g30414.1	1.87	Aspartic proteinase nepenthesin-2 precursor	21.65	8
LOC_Os01g01400.1	1.80	Ribonuclease	86.05	12
LOC_Os01g51300.1	1.62	WD domain, G-beta repeat domain containing protein	71.61	31
LOC_Os06g02380.1	1.58	Chloroplast chaperonin 60,	70.09	24
LOC_Os09g07350.1	1.51	Fasciclin-like arabinogalactan protein 8	19.14	5
LOC_Os11g02440.1	1.50	Chalcone-flavonone isomerase family protein	52.36	15
LOC_Os03g27230	1.49	Phospho-2-dehydro-3-deoxyheptonate aldolase	29.85	9
LOC_Os08g42040.1	1.46	Lipid transfer protein	45.18	42
LOC_Os06g44260.1	1.45	GDP-mannose 3,5-epimerase	23.06	6
LOC_Os06g45820.1	1.41	FtsH protease	51.08	12
LOC_Os09g37240.1	1.41	Similar to glutathione transferase16	36.51	7
LOC_Os03g09910.1	1.38	Probable LL-diaminopimelate aminotransferase,	22.63	11
LOC_Os10g42280.1	1.38	Cyclase/Dehydrase family protein	21.59	6

LOC_Os09g04790.1	1.36	Fibrillin	26.18	5
LOC_Os01g37020.1	1.33	Carboxyl-terminal peptidase	41.08	7
LOC_Os07g46990.1	1.32	Superoxide dismutase [Cu-Zn]	46.71	15
LOC_Os08g03520.2	1.22	Cold shock domain protein	45.63	9
LOC_Os02g55140.1	-1.21	Leucine aminopeptidase 2, chloroplastic	26.42	12
LOC_Os05g33100.1	-1.22	Putative endo-1,31,4-beta-D-glucanase	22.08	5
LOC_Os01g68710.3	-1.22	Peptidyl-prolyl cis-trans isomerase, FKBP-type	38.51	12
LOC_Os10g41410	-1.28	Nucleoside diphosphate kinase	85.43	51
LOC_Os02g43830.2	-1.28	3-isopropylmalate dehydratase small subunit	37.42	6
LOC_Os06g45120.1	-1.30	ATP synthase	80.32	55
LOC_Os12g36880	-1.30	Pathogen resistance protein PBZ	32.16	6
LOC_Os02g08380.1	-1.32	Uncharacterised protein family	45.22	8
LOC_Os07g41820.1	-1.34	Stress responsive A/B Barrel domain containing protein	19.28	10
LOC_Os07g32880.1	-1.41	ATP synthase gamma chain	46.5	17
LOC_Os02g10640.1	-1.45	26S protease regulatory subunit 4 homolog	24.96	11
LOC_Os03g19510	-1.45	ATP-dependent Clp protease proteolytic subunit	29.8	8
LOC_Os05g32820.1	-1.49	Peptide-N4-asparagine amidase A	21.05	6
LOC_Os01g13700.1	-1.54	DNA-binding protein	30.21	31
LOC_Os01g36710.1	-1.58	Putative glycosyl hydrolase	32.12	9
LOC_Os02g42960.1	-1.59	Thylakoid lumenal protein,	82.16	46

LOC_Os01g07910.1	-1.61	NADH-cytochrome b5 reductase (CYB5R)	72.56	45
LOC_Os05g22970.1	-1.63	Lactoyl-glutathione lyase	38.1	4
LOC_Os02g44320.1	-1.66	LTP family protein precursor	26.14	6
LOC_Os07g43810.1	-1.70	RNA recognition motif containing protein	28.61	9
LOC_Os01g45274.1	-1.75	Carbonic anhydrase	59.56	92
LOC_Os06g29180.1	-1.77	Formate dehydrogenase, mitochondrial	28.99	7
LOC_Os01g65410.1	-1.82	Serine hydroxymethyltransferase	54.22	43
LOC_Os07g11110.1	-1.97	Similar to mRNA-binding protein	42.46	9
LOC_Os07g04160.1	-2.14	Peptidyl-prolyl cis-trans isomerase	31.28	12
LOC_Os02g32814.1	-2.22	Copper chaperone homolog CCH	29.89	13
LOC_Os02g47020.1	-2.22	Phosphoribulokinase	68.24	59
LOC_Os01g70020.1	-2.29	DEK C terminal domain containing protein,	28.19	6
LOC_Os04g53740.1	-2.36	Thioredoxin-like protein	65.18	33
LOC_Os09g39780.2	-2.47	Peptidyl-prolyl cis-trans isomerase	46.88	33
LOC_Os05g41640.1	-2.62	Phosphoglycerate kinase	57.23	95
LOC_Os02g40830.1	-2.84	Succinyl-CoA ligase (SCoAL)	30.57	9
NT-specific DEPs (NT Vs. Control)				
LOC_Os04g44830.1	1.66	Thioredoxin 1	31.11	15
LOC_Os01g71230.1	1.60	NAC transcription factor	58.92	32
LOC_Os03g36670	1.59	Retrotransposon protein, putative, Ty3-gypsy subclass	20.16	4

LOC_Os01g11810.1	1.55	Alpha-galactosidase	37.09	7
LOC_Os01g74650.1	1.50	Cysteine synthase	30.16	21
LOC_Os02g35900.2	1.49	Thioredoxin	60.12	31
LOC_Os01g09370.1	1.45	Similar to Ankyrin-like protein	37.28	17
LOC_Os12g39860.2	1.34	Adenine phosphoribosyltransferase 1,	50.23	22
LOC_Os03g03990.1	1.34	Chloroplast signal recognition particle 43 KD protein,	33.57	11
LOC_Os12g12580.1	1.33	Chaperone protein ClpC2, chloroplastic	49.18	30
LOC_Os02g51470.1	1.33	ATP synthase F1, delta subunit	63.13	25
LOC_Os02g34810.1	1.29	L-ascorbate peroxodase 1 chloroplastic	62.18	38
LOC_Os09g38030.1	1.22	UDP-GLUCOSE PYROPHOSPHORYLASE 1	58.29	32
LOC_Os01g26970.2	1.21	Conserved hypothetical protein	72.16	45
LOC_Os03g10240.2	-1.22	DUF677 domain containing protein	20.16	6
LOC_Os06g35050.1	-1.33	Arogenate dehydrogenase 1	21.26	9
LOC_Os10g06130.4	-1.57	RNA recognition motif containing protein, expressed	11.65	2
LOC_Os07g38300.2	-1.73	Ribosome-recycling factor	20.68	13
NH-specific DEPs (NH Vs. Control)				
LOC_Os08g04450.2	1.90	Similar to DAG protein,	38.15	12
LOC_Os09g37060.1	1.77	Protein phosphatase 2A, regulatory B subunit	48.35	12
LOC_Os03g03910	1.68	Catalase	42.68	20
LOC_Os01g68770.1	1.65	Similar to Selenium binding protein	32.81	6

LOC_Os02g14440.2	1.55	Peroxidase	33.64	9
LOC_Os06g20320.1	1.38	Peptidyl-prolyl cis-trans isomerase, FKBP-type	48.1	15
LOC_Os07g25430.1	1.34	Putative Photosystem I reaction center subunit IV	44.3	13
LOC_Os03g08280	1.32	Proteasome subunit alpha type	25.11	3
LOC_Os06g05880.1	-1.30	Profilin	32.06	6
LOC_Os02g47140.2	-1.58	L11 domain containing ribosomal protein	28.65	11
LOC_Os01g44250.1	-1.58	CBS domain containing protein	24.88	4
LOC_Os02g22260.2	-1.74	Homolog of the Arabidopsis FNRL protein, Fruit protein	21.18	6
TU-specific DEPs (T Vs. Control)				
LOC_Os02g01030.1	1.98	Tetratricopeptide repeat domain containing protein	68.47	17
LOC_Os03g05360.1	1.59	UDP-glucose 6-dehydrogenase 3	33.33	12
LOC_Os01g13690.2	1.58	Branched-chain amino acid aminotransferase-like	13.25	3
LOC_Os07g28400.1	1.42	CDGSH iron-sulfur domain containing protein (NEET)	72.16	34
LOC_Os03g56670.1	1.41	Photosystem I center protein	71.46	38
LOC_Os03g24220	1.37	Villin-3, putative, expressed	31.06	7
LOC_Os02g41630.2	1.34	Phenylalanine ammonia-lyase	31.23	11
LOC_Os03g63410.1	1.30	Elongation factor Tu	55.89	15
LOC_Os12g09790.1	1.30	Similar to Cyt-P450 monooxygenase.	82.16	55
LOC_Os04g58710.1	1.30	AMP-binding domain containing protein	10.62	2
LOC_Os06g07932.1	1.28	Flavonol synthase/flavanone 3-hydroxylase	37.81	22

LOC_Os11g05050.1	1.24	Stem-specific protein TSJT1	25.86	8
LOC_Os02g07260.1	-1.22	Phosphoglycerate kinase	50.5	20
LOC_Os07g06450.1	-1.24	Similar to RNA binding protein	30.42	6
LOC_Os03g04110.1	-1.30	Chitin elicitor-binding protein	15.73	7
LOC_Os09g26730.1	-1.66	Chaperonin	54.29	17
LOC_Os05g01110.1	-1.69	Similar to 50S ribosomal protein L28, chloroplast	25.86	5
H_2O_2-specific DEPs (H_2O_2Vs. Control)				
LOC_Os11g09280.1	2.31	Protein disulfide-isomerase	38.31	14
LOC_Os09g10760.1	2.11	Similar to Plastid-specific 30S ribosomal protein	34.74	17
LOC_Os01g01280.1	1.63	Thylakoid lumen protein	60.89	32
LOC_Os02g56130.1	1.59	Proliferating cell nuclear antigen (PCNA)	55.24	31
LOC_Os12g38910	1.59	Calmodulin-binding, plant family protein	57.05	16
LOC_Os12g42090.1	1.46	Similar to 37 kDa inner envelope membrane protein	68.21	38
LOC_Os04g42000.1	-1.36	6,7-dimethyl-8-ribityllumazine synthase	23.51	9
LOC_Os04g26910.1	-1.48	Probable aldo-keto reductase	17.66	4
LOC_Os05g41870.1	-1.57	Glycine-rich cell wall protein	20.19	7
LOC_Os06g39344.3	-1.66	HAD-superfamily hydrolase	28.55	5
LOC_Os03g31170	-1.95	Inosine-uridine preferring nucleoside hydrolase	32.58	6
LOC_Os04g40530.1	-2.25	Methyltransferase domain containing protein	52.14	17

3.2.1.5. Metabolite profiling under various treatments

GC-MS based metabolomics analysis was also performed to understand the metabolomics basis of TU and H_2O_2 mediated amelioration of NaCl stress conditions. PCA indicated that individual replicates under different treatments were clustered together. In addition, a clear separation of NaCl, NT and NH treatments was observed (Fig. 3.2.7), supporting the phenotypic ameliorating effect observed at seedling- (Fig. 3.1.3) and mature plant (Fig. 3.3.1) stages.

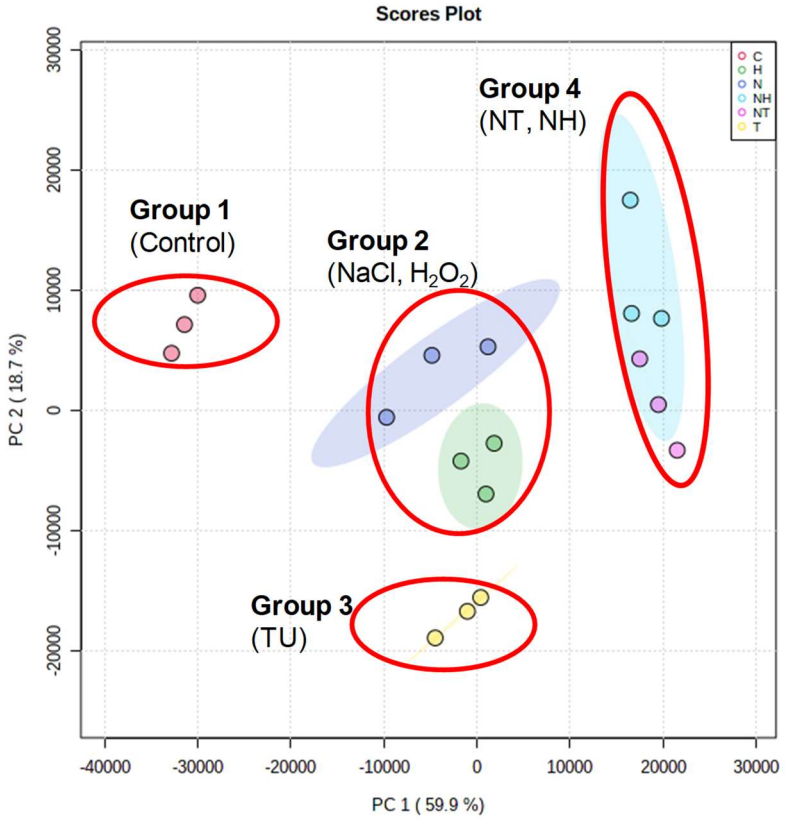

Fig. 3.2.7: PCA analysis of metabolic profiles of leaf tissue to understand treatment-variable interaction. The principal component analysis (PCA) was performed to identify the treatment specific metabolic variables. The biplots were generated using all the quantified metabolites. The lines originating from central point of biplots indicate positive or negative correlations of different variables; where their closeness indicates correlation strength with particular treatment.

A total of 61 non-redundant metabolites [sugars (20), sugar alcohols (16), amino acid (5), TCA cycle intermediates (7) and signalling intermediates (7)] were identified and successfully annotated across different treatments. The differential quantification of various metabolites under different treatments was represented as heat map (Fig. 3.2.8).

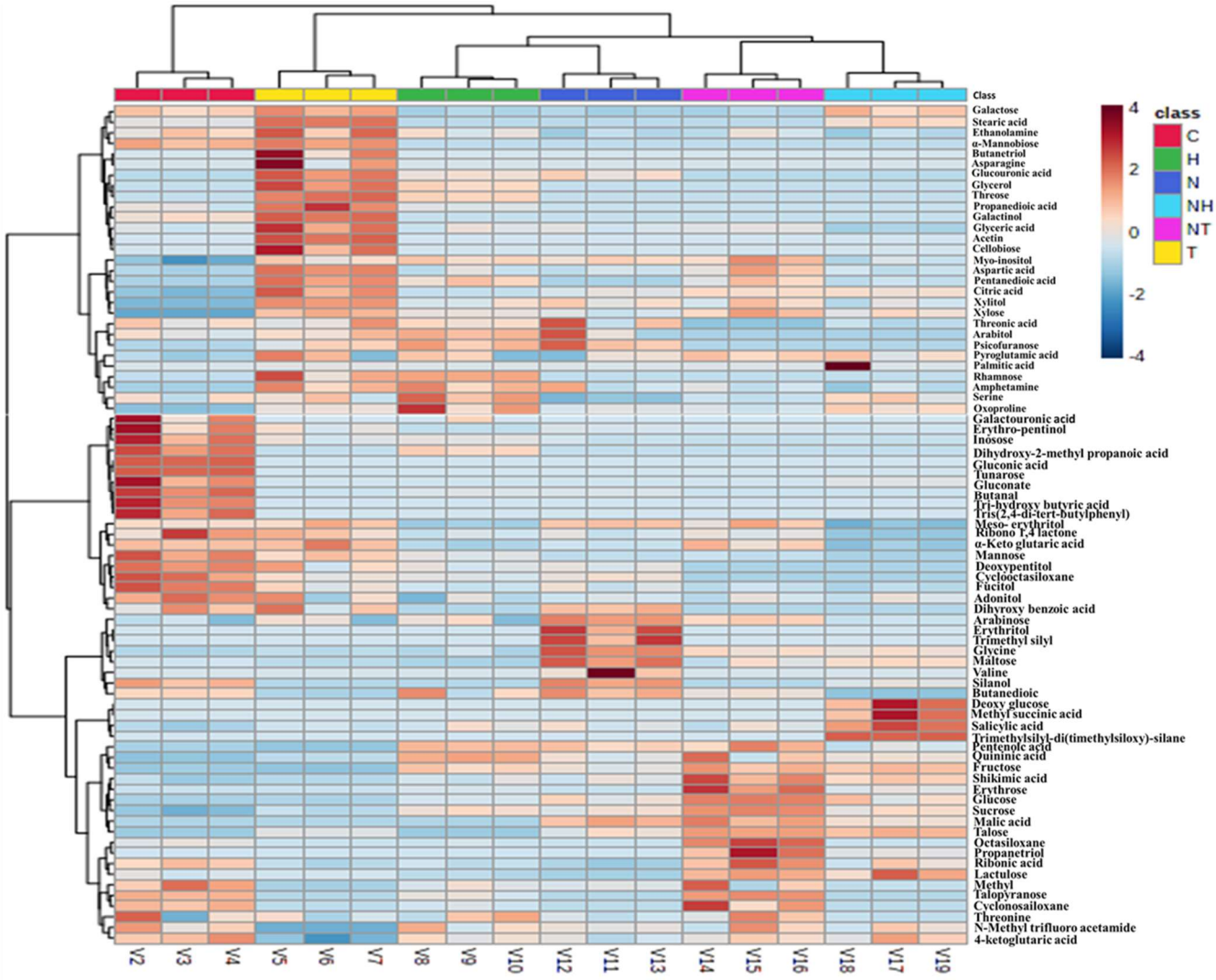

Fig. 3.2.8: Heat map for the differential metabolites under different treatments.

Individual replicates are separated using hierarchical clustering, with the dendrogram scaled to represent the distance between each branch. Normalized signal intensities (log2 transformed and row adjustment) are visualized as a color spectrum and the scale from least abundant to highest ranges is from −4.0 to 4.0. Blue color indicates low and red color indicates high levels of the detected metabolites.

In order to identify the key metabolites that governed the phenotypic alterations across different treatments, top-five and bottom-five metabolites were selected on the basis of high and low PCA score, respectively. If the metabolite function is found unexplored, the next ranked metabolite was selected (Appendix Table) for the top-hit metabolite across all the treatments.

There was a differential response for organic acids, for example increase in maleic acid (MA; 21.5-fold) and Citric acid (1.6-fold) along with decrease in 2-ketoglutarate (α -KG; 0.6-fold) under NaCl stress as compared to control (Table 3.2.3). Further, an improved organic acid content was observed corresponding to 1.14, 1.42 and 1.23-fold increased accumulation for MA, α-KG and citric acid respectively under NT treatment as compared to NaCl treatment. On the contrary, under NH treatment a relative increased and decreased accumulation of citric acid (1.3-fold) MA content (0.56- fold) was observed as compared to NaCl treatment (Table 3.2.3). Although no change in proliferating cell nuclear antigen content was observed with TU and H_2O_2 treatment under control conditions, a large increase under NaCl treatment (11.15-fold) was observed. A significant decline in Gly content was observed under NH (0.42-fold) and NT (0.48-fold) treatments compared to that NaCl alone treatment. Similarly, aspartatic acid (Asp) content was increased under NaCl treatment (1.23-fold) as compared to that of control. A further reinforcement in the Asp level corresponding to 1.65-fold under NT was also observed as compared to NaCl stress (Table 3.2.3). No such increase in Asp content was observed under NH compared to those of NaCl treatment. The large increase in Asp content was also observed under TU (2.70-fold) and H_2O_2 (1.28-fold) alone treatments.

Table-3.2.3: Top-ranked metabolites identified on the basis of PCA score. All the values are mean±SD of three biological replicates. Different letters indicate significantly different values (DMRT, $p \leq 0.05$).

Metabolite	Control	TU	H_2O_2	NaCl	NaCl + TU	NaCl + H_2O_2
Control						
Citric acid	$165.1^{d} \pm 22.3$	$551.4^{a} \pm 25.12$	$197.0^{c} \pm 97.9$	$266.8^{c} \pm 23.6$	$328.3^{b} \pm 11.7$	$351.0^{b} \pm 12.8$
L-Aspartic acid	$440.0^{c} \pm 21.0$	$1190.2^{a} \pm 103.2$	$562.9^{b} \pm 57.7$	$541.5^{b} \pm 54.2$	$892.8^{a} \pm 38.1$	$533.4^{b} \pm 205.6$
Sucrose	$16186.9^{d} \pm 2991.9$	$25276.0^{c} \pm 2251.6$	$38889.6^{b} \pm 2761.1$	$38360.6^{b} \pm 6335.2$	$56717.9^{a} \pm 295.3$	$39255.2^{b} \pm 1212.0$
Xylose	0	$106.3^{a} \pm 2.12$	$77.5^{b} \pm 7.32$	$63.8^{b} \pm 8.11$	$109.5^{a} \pm 11.69$	$83.1^{b} \pm 18.01$
Myo-Inositol	$464.1^{c} \pm 327.6$	$1976.1^{ab} \pm 176.4$	$2081.4^{a} \pm 263.4$	$1991.3^{ab} \pm 163.9$	$2403.4^{a} \pm 225.7$	$1291.6^{b} \pm 463.9$
Salycylic acid	$55.3^{c} \pm 9.7$	$76.7^{c} \pm 18.4$	$96.6^{bc} \pm 66.9$	$92.3^{b} \pm 19.1$	$88.1^{b} \pm 26.5$	$196.1^{a} \pm 21.5$
Glycine	$56.1^{c} \pm 22.3$	$83.5^{c} \pm 65.4$	$79.9^{c} \pm 14.2$	$625.6^{a} \pm 90.7$	$302.2^{b} \pm 37.2$	$265.6^{b} \pm 35.8$
Oxoproline	$282.5^{d} \pm 12.4$	$1066.7^{c} \pm 169.5$	$1839.4^{a} \pm 22.4$	$905.3^{c} \pm 62.6$	$814.2^{c} \pm 123.9$	$1272.0^{b} \pm 87.1$
Quinic acid	$38.9^{d} \pm 14.8$	$377.4^{c} \pm 8.4$	$1509.6^{a} \pm 15.2$	$732.1^{b} \pm 174.1$	$1217.1^{ab} \pm 733.2$	$834.0^{b} \pm 38.7$
Gluconic acid	$109.9^{a} \pm 11.2$	0	0	0	0	0
Serine	$1189.3^{ab} \pm 701.7$	$1265.2^{ab} \pm 534.6$	$1910.1^{ab} \pm 529.7$	$480.7^{c} \pm 119.6$	$1353.9^{b} \pm 30.08$	$1887.5^{a} \pm 355.9$
TU						
D-Fructose	$2259.1^{c} \pm 200.0$	$1776.5^{d} \pm 23.50$	$6757.5^{ab} \pm 578.25$	$5034.9^{b} \pm 524.95$	$8139.8^{a} \pm 1083.5$	$7427.5^{a} \pm 411.8$
Maleic acid	$122.2^{c} \pm 6.6$	$174.9^{c} \pm 24.7$	$102.9^{c} \pm 361.0$	$2657.9^{a} \pm 357.6$	$3046.5^{a} \pm 57.4$	$1495.1^{b} \pm 570.9$
2-Ketoglutaric acid	$413.1^{a} \pm 5.5$	$446.3^{a} \pm 14.2$	$236.5^{cd} \pm 57.1$	$273.5^{c} \pm 5.4$	$389.3^{b} \pm 16.8$	$201.6^{d} \pm 47.7$

Maltose	254.1^{d} ± 25.1	129.9^{e} ± 2.5	54.1f ± 9.3	1140.3^{a} ± 162.2	347.0^{c} ± 36.8	562.7b ± 195.9
L- Glycine,	56.1^{c} ± 22.3	83.5^{c} ± 65.4	79.9^{c} ± 14.2	625.6^{a} ± 90.7	302.2^{b} ± 37.2	265.6^{b} ± 35.8
D-Glucose,	191.7^{e} ± 3.7	271.1^{d}±20.0	839.8c ±45.4	1386.8^{b} ±413.6	3094.4^{a} ±594.2	1577.3^{b} ± 29.3
Shikmic acid	202.3^{d} ±82.9	247.8^{d} ± 66.2	363.7^{c} ± 3.8	399.5^{b} ± 76.7	902.3^{a} ± 54.7	609.4^{ab} ± 291.9
Myo -inositol	464.1^{c} ± 327.6	1976.1^{ab} ± 176.4	2081.4^{a} ± 263.4	1991.3^{ab} ± 163.9	2403.4^{a} ± 225.7	1291.6^{b} ± 463.9
L-Aspartic acid	440.0^{c} ± 21.0	1190.2^{a} ±103.2	562.9 ^{b} ±57.7	541.5^{b} ±54.2	892.8^{a} ±38.1	533.4^{b} ±205.6
Citric acid	65.1^{d} ± 22.3	551.4^{a} ± 25.12	197.0^{c} ± 97.9	266.8^{c} ± 23.6	328.3^{b} ± 11.7	351.0^{b} ± 12.8
Sucrose	16186.9^{d} ± 2991.9	25276.0^{c} ± 2251.6	38889.6^{b} ± 2761.1	38360.6^{b} ± 6335.2	56717.9^{a} ± 295.3	39255.2^{b} ± 1212.0
H_2O_2						
Myo-Inositol	464.1^{c} ± 327.6	1976.1^{ab} ± 176.4	2081.4^{a} ± 263.4	1991.3^{ab} ± 163.9	2403.4^{a} ± 225.7	1291.6 ^{b} ± 463.9
Xylose	0	106.3^{a} ± 2.12	77.5^{b} ± 7.32	63.8^{b} ± 8.11	109.5^{a} ± 11.69	83.1^{b} ± 18.01
Maleic acid	122.2^{c} ± 6.6	102.9^{c} ± 361.0	174.9^{c} ± 24.7	2657.9^{a} ± 357.6	1495.1^{b} ± 570.9	3046.5^{a} ± 57.4
Sucrose,	16186.9^{d} ± 2991.9	25276.0^{c} ± 2251.6	38889.6^{b} ± 2761.1	38360.6^{b} ± 6335.2	56717.9^{a} ± 295.3	39255.2^{b} ± 1212.0
L-Aspartic acid	440.0^{c} ± 21.0	1190.2^{a} ± 103.2	562.9^{b} ± 57.7	541.5^{b} ± 54.2	892.8^{a} ± 38.1	533.4^{b} ± 205.6
Quinic acid	38.9^{d} ± 14.8	377.4^{c} ± 8.4	1509.6^{a} ± 15.2	732.1^{b} ± 174.1	1217.1^{ab} ± 733.2	834.0^{b} ± 38.7
D-Fructose	2259.1^{c} ± 200.0	1776.5^{d} ± 23.50	6757.5^{ab} ± 578.25	5034.9^{b} ± 524.95	8139.8^{a} ± 1083.5	7427.5^{a} ± 411.8
L-Oxoproline	282.5^{d} ± 12.4	1066.7^{c} ± 169.5	1839.4^{a} ± 22.4	905.3^{c} ± 62.6	814.2^{c} ± 123.9	1272.0^{b} ± 87.1
D-Glucose	191.7^{e} ± 3.7	271.1^{d} ± 20.0	839.8^{c} ± 45.4	1386.8^{b} ± 413.6	3094.4^{a} ± 594.2	1577.3^{b} ± 29.3
Shikimic acid	202.3^{d} ± 82.9	247.8^{d} ± 66.2	363.7^{c} ± 3.8	399.5^{b} ± 76.7	902.3^{a} ± 54.7	609.4^{ab} ± 291.9
NaCl						
D-Fructose,	2259.1^{c} ± 200.0	1776.5^{d} ± 23.50	6757.5^{ab} ± 578.25	5034.9^{b} ± 524.95	8139.8^{a} ± 1083.5	7427.5^{a} ± 411.8

Shikimic acid	$202.3^{d} \pm 82.9$	$247.8^{d} \pm 66.2$	$363.7^{c} \pm 3.8$	$399.5^{b} \pm 76.7$	$902.3^{a} \pm 54.7$	$609.4^{ab} \pm 291.9$
L-Aspartic acid	$440.0^{c} \pm 21.0$	$1190.2^{a} \pm 103.2$	$562.9^{b} \pm 57.7$	$541.5^{b} \pm 54.2$	$892.8^{a} \pm 38.1$	$533.4^{b} \pm 205.6$
Quininic acid	$38.9^{d} \pm 14.8$	$377.4^{c} \pm 8.4$	$1509.6^{a} \pm 15.2$	$732.1^{b} \pm 174.1$	$1217.1^{ab} \pm 733.2$	$834.0^{b} \pm 38.7$
Maleic acid	$122.2^{c} \pm 6.6$	$102.9^{c} \pm 361.0$	$174.9^{c} \pm 24.7$	$2657.9^{a} \pm 357.6$	$1495.1^{b} \pm 570.9$	$3046.5^{a} \pm 57.4$
Sucrose	$16186.9^{d} \pm 2991.9$	$25276.0^{c} \pm 2251.6$	$38889.6^{b} \pm 2761.1$	$38360.6^{b} \pm 6335.2$	$56717.9^{a} \pm 295.3$	$39255.2^{b} \pm 1212.0$
Salicylic acid	$55.3^{c} \pm 9.7$	$76.7^{c} \pm 18.4$	$96.6^{bc} \pm 66.9$	$92.3^{b} \pm 19.1$	$88.1^{b} \pm 26.5$	$196.1^{a} \pm 21.5$
Maltose	$254.1^{\mathbf{d}} \pm 25.1$	$129.9^{\mathbf{e}} \pm 2.5$	$54.1^{f} \pm 9.3$	$1140.3^{\mathbf{a}} \pm 162.2$	$347.0^{\mathbf{c}} \pm 36.8$	$562.7^{b} \pm 195.9$
Myo-Inositol	$464.1^{c} \pm 327.6$	$1976.1^{ab} \pm 176.4$	$2081.4^{a} \pm 263.4$	$1991.3^{ab} \pm 163.9$	$2403.4^{a} \pm 225.7$	$1291.6^{b} \pm 463.9$
D-Glucose	$191.7^{\mathbf{e}} \pm 3.7$	$271.1^{\mathbf{d}} \pm 20.0$	$839.8^{c} \pm 45.4$	$1386.8^{\mathbf{b}} \pm 413.6$	$3094.4^{a} \pm 594.2$	$1577.3^{\mathbf{b}} \pm 29.3$
NaCl + TU						
D-Fructose	$2259.1^{c} \pm 200.0$	$1776.5^{d} \pm 23.50$	$6757.5^{ab} \pm 578.25$	$5034.9^{b} \pm 524.95$	$8139.8^{a} \pm 1083.5$	$7427.5^{a} \pm 411.8$
Maleic acid	$122.2^{c} \pm 6.6$	$102.9^{c} \pm 361.0$	$174.9^{c} \pm 24.7$	$2657.9^{a} \pm 357.6$	$1495.1^{b} \pm 570.9$	$3046.5^{a} \pm 57.4$
Pentenoic acid	$121.9^{b} \pm 11.7$	$104.7^{b} \pm 25.2$	$140.2^{ab} \pm 67.8$	$119.0^{b} \pm 3.5$	$119.08^{b} \pm 13.4$	$184.25^{a} \pm 14.57$
Quininic acid	$38.9^{d} \pm 14.8$	$377.4^{c} \pm 8.4$	$1509.6^{a} \pm 15.2$	$732.1^{b} \pm 174.1$	$1217.1^{ab} \pm 733.2$	$834.0^{b} \pm 38.7$
L- Glycine	$56.1^{c} \pm 22.3$	$83.5^{c} \pm 65.4$	$79.9^{c} \pm 14.2$	$625.6^{a} \pm 90.7$	$302.2^{b} \pm 37.2$	$265.6^{b} \pm 35.8$
Maltose	$254.1^{\mathbf{d}} \pm 25.1$	$129.9^{\mathbf{e}} \pm 2.5$	$54.1^{f} \pm 9.3$	$1140.3^{\mathbf{a}} \pm 162.2$	$347.0^{\mathbf{c}} \pm 36.8$	$562.7^{b} \pm 195.9$
Sucrose	$16186.9^{d} \pm 2991.9$	$25276.0^{c} \pm 2251.6$	$38889.6^{b} \pm 2761.1$	$38360.6^{b} \pm 6335.2$	$56717.9^{a} \pm 295.3$	$39255.2^{b} \pm 1212.0$
2-Ketoglutaric	$413.1^{a} \pm 5.5$	$446.3^{a} \pm 14.2$	$236.5^{cd} \pm 57.1$	$273.5^{c} \pm 5.4$	$389.3^{b} \pm 16.8$	$201.6^{d} \pm 47.7$
L-Aspartic acid	$440.0^{c} \pm 21.0$	$1190.2^{a} \pm 103.2$	$562.9^{b} \pm 57.7$	$541.5^{b} \pm 54.2$	$892.8^{a} \pm 38.1$	$533.4^{b} \pm 205.6$
Salycylic acid	$55.3^{c} \pm 9.7$	$76.7^{c} \pm 18.4$	$96.6^{bc} \pm 66.9$	$92.3^{b} \pm 19.1$	$88.1^{b} \pm 26.5$	$196.1^{a} \pm 21.5$
$NaCl+H_2O_2$						

Maleic acid	122.2^{c} ± 6.6	102.9^{c} ± 361.0	174.9^{c} ± 24.7	2657.9^{a} ± 357.6	1495.1^{b} ± 570.9	3046.5^{a} ± 57.4
D-Fructose,	2259.1^{c} ± 200.0	1776.5^{d} ± 23.50	6757.5^{ab} ± 578.25	5034.9^{b} ± 524.95	8139.8^{a} ± 1083.5	7427.5^{a} ± 411.8
Pentenoic acid	121.9^{b} ± 11.7	104.7^{b} ± 25.2	140.2^{ab} ± 67.8	119.0^{b} ± 3.5	119.08^{b} ± 13.4	184.25 ^{a} ± 14.57
Quininic acid	38.9^{d} ± 14.8	377.4^{c} ± 8.4	1509.6^{a} ± 15.2	732.1^{b} ± 174.1	1217.1^{ab} ± 733.2	834.0 ^{b} ± 38.7
D-Glucose	191.7$^{\mathbf{e}}$ ± 3.7	271.1$^{\mathbf{d}}$ ± 20.0	839.8^{c} ± 45.4	1386.8$^{\mathbf{b}}$ ± 413.6	3094.4^{a} ± 594.2	1577.3$^{\mathbf{b}}$ ± 29.3
Shikimic acid	202.3^{d} ± 82.9	247.8^{d} ± 66.2	363.7^{c} ± 3.8	399.5^{b} ±76.7	902.3^{a} ± 54.7	609.4^{ab} ± 291.9
L- Glycine	56.1^{c} ± 22.3	83.5^{c} ± 65.4	79.9^{c} ± 14.2	625.6^{a} ± 90.7	302.2^{b} ± 37.2	265.6^{b} ± 35.8
Sucrose	16186.9^{d} ± 2991.9	25276.0^{c} ± 2251.6	38889.6^{b} ± 2761.1	38360.6^{b} ± 6335.2	56717.9^{a} ± 295.3	39255.2^{b} ± 1212.0
L-Aspartic acid	440.0^{c} ± 2.0	1190.2^{a} ± 103.2	562.9 ^{b} ± 57.7	541.5^{b} ± 54.2	892.8^{a} ± 38.1	533.4 ^{b} ± 205.6
Maltose	254.1$^{\mathbf{d}}$ ± 25.1	129.9$^{\mathbf{e}}$ ± 2.5	54.1^{f} ± 9.3	1140.3$^{\mathbf{a}}$ ± 162.2	347.0$^{\mathbf{c}}$ ± 36.8	562.7^{b} ± 195.9
Myo-Inositol	464.1^{c} ± 327.6	1976.1^{ab} ± 176.4	2081.4^{a} ± 263.4	1991.3^{ab} ± 163.9	2403.4^{a} ± 225.7	1291.6 ^{b} ± 463.9
L- Serine	1189.3^{ab} ± 701.7	1265.2^{ab} ± 534.6	1910.1^{ab} ± 529.7	480.7^{c} ± 119.6	1353.9 ^{b} ± 30.08	1887.5^{a} ± 355.9

The carbohydrates metabolism related metabolites were also detected under different treatments. For instance, sucrose content was increased under TU and H_2O_2 by 1.56- and 2.4-fold, respectively relative to control. Under NaCl stress, sucrose content was increased by 2.36-fold relative to control; while, under NT treatment, it was further improved by 1.47-fold compared to NaCl stress (Table 3.2.3). Additionally, maltose content was significantly increased under NaCl by 4.48-fold relative to control conditions. This increase was limited to 0.49- and 0.30- fold under NH and NT treatments, respectively in comparison to NaCl stress. The alteration in glucose content was also observed under NaCl (7.23-fold), NT (16.13-fold) and NH (8.22-fold) treatments relative to control (Table 3.2.3).

The differential quantification of various signalling related metabolites showed increased accumulation of SA content under H_2O_2 (1.74-fold) and NH (3.54-fold) treatments as compared to control (Table 3.2.3). SA content remained unchanged under TU and NT treatments. Besides, shikimic acid content was significantly increased by 2.25-fold under NT compared to those of NaCl stress. The myo-inositol (MI) content was found differentially accumulated under TU (4.25-fold) and H_2O_2 (4.48-fold) treatments, relative to control (Table 3.2.3). Under NaCl stress, MI content was promoted to 4.29-fold relative to control. In contrast, it was slightly decreased by 0.64-fold under NH; while, no change in MI content was observed under NT as compared to NaCl treatment.

3.2.1.6. Quantification of TCA cycle related enzymes under TU and H_2O_2 treatments

The key TCA cycle enzymes like malate dehydrogenase (MDH), glutamate dehydrogenase (GDH) and glutamate decarboxylase (GAD) were quantified in under various treatments. The result revealed nearly alike MDH activity under H_2O_2 as well as NH treatments. Alternatively, MDH activity was increased under TU (44.4%) and NT (102.01%) treatments compared to control (Fig. 3.2.9 A). Although, GDH and GAD activity was

significantly increased under NaCl (90.0 and 37.7%) and H_2O_2 (52.6 and 34.6%), minimal change in GDH activity was observed along with 22.9% increase in GAD activity under TU treatment relative to control (Fig. 3.2.9 B, C). Upon H_2O_2 supplementation, both GDH and GAD activities were further increased by 34.2 and 24.6%, respectively relative to NaCl stress (Fig. 3.2.9 B, C).

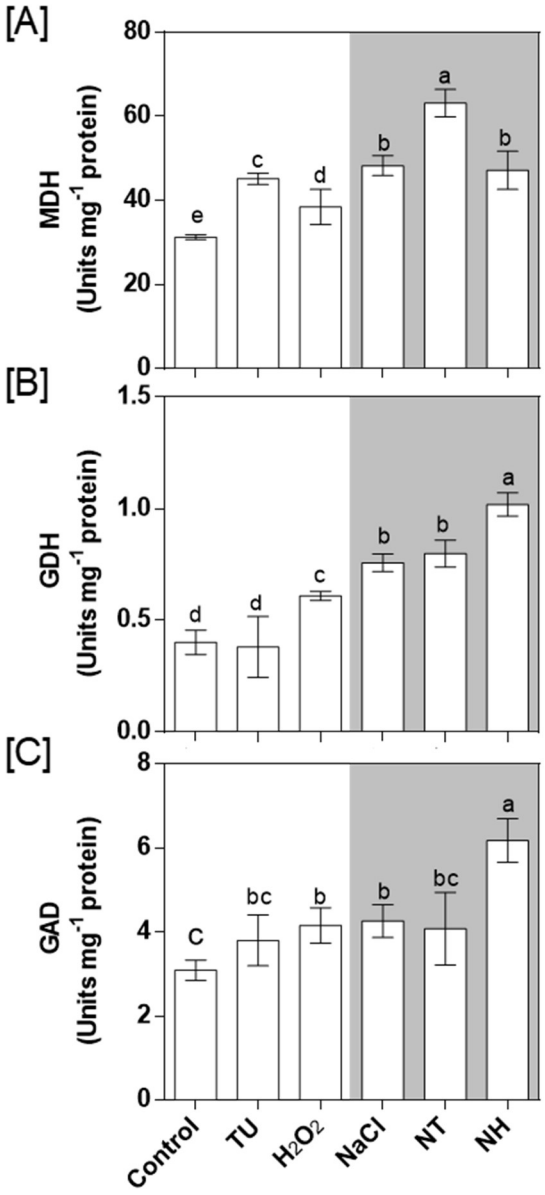

Fig. 3.2.9: Quantification of enzymatic activity of TCA cycle enzymes under various treatments. [A] malate dehydrogenase (MDH), [B] glutamate dehydrogenase (GDH) and [C]

glutamate decarboxylase (GAD) activity. All the values are mean of triplicates ± SD. Different letters indicate significantly different values (DMRT, $p \leq 0.05$).

3.2.2. Discussion

The activation of stress-responsive genes and better retention of K^+ ions, prompted us to investigate the effect of TU and H_2O_2, at the protein/metabolic level. Based on various biochemical and proteomic studies, PBRs mediated positive regulation of various redox regulatory proteins and enzymes involved in carbon assimilation was established as one of the mechanisms for stress tolerance [8]. Additionally, improved assimilation of N, C and S under PBRs application along with increased synthesis of free amino acids, phenolics, carbohydrates and proteins were also reported to enhance plant resilience towards stresses [224].

Initially, the levels of PC and oxidative status were quantified in roots and the results highlighted the establishment of reducing redox status under both NT and NH treated roots. The genetic approach of over-expressing detoxifying enzyme aldo-keto reducarbonylectase-1 (*AKR1*) in tobacco and rice was reported to improve tolerance towards glucose, NaCl and methyle-viologen induced oxidative stress [225]. In contrast, knocking down/out of genes involved in carbonyl scavenging resulted in sensitive phenotypes towards stresses [226]. The heat-map based clustering analysis of DEPs clearly indicated the decreased abundance of various proteins under NaCl treatment, which were involved in the maintenance of photosynthesis and cellular energetics (Fig 3.2.5 and Fig. 3.2.6). On the other hand, PsbP level was restored, which was co-related with improved PSII function and better stress tolerance observed under NT and NH treatments. Earlier studies also reported the regulatory role of PSbP in recovery of PS II under heat [227] and salt stress [228]. Further, the reductant supply in chloroplastic ETC is mediated by light dependent photooxidation of water molecule

by OEC proteins. The salinity responsiveness of OEC can be co-related with that of differential PS II activity towards salinity amelioration [110] (Fig 3.2.5).

Salt stress also perturbed the mitochondrial respiration limiting the ATP and reductant supply with increased ROS production. Plants try to cope the stress by various approaches which includes; (1) avoiding the over-reduction of mitochondrial ETC particularly with the mediation of alternate oxidase (2) modification of the TCA cycle intermediates (3) maintain efficient ATP synthesis [100]. The increased expression of ATP synthetase subunit under NT and NH treatment (ASD) can be correlated with that of improved ATP supply for sustain the plant growth under stress conditions. Glutamate dehydrogenase (GDH), as a linker between carbon and nitrogen metabolism differentially regulated under salt stress (ASD) showing increased ammonia assimilation under salt stress [229]. Further overexpression of GDH was reported to altered the metabolic profile and improve the plant vigour under salt stress [230]. The increased expression of pyrophosphatase (PPA) under TU, H_2O_2, NH and NT (ASD) treatments were also linked to adaptive acclimation of salt stressed plants by maintaining the osmotic and ionic balance and improving the photosynthetic efficiency. The earlier report with *OsPPA* loss of function mutant was also validated the potential importance of PPA towards stress amelioration [231]. FTR mediated electron transfer from ferredoxin to thioredoxin in photosynthetic active tissue play an important role in redox regulation. Upto 4 –fold decrease in FTR abundance under NaCl stress (Fig 3.2.6), suggesting the compromised ROS scavenging through Trx-Prx system [232]. This was also supported by reduced level of thiol-accumulation in roots. In contrast, the peroxiredoxins (Prx), glutaredoxins (Grx) and thioredoxin (Trx) levels were up-regulated, particularly under NH treatments (Fig. 3.2.6), which justify their higher anti-oxidant capacitance.

Further the negative effects of salt stress over carbon metabolism were evident by the decreased abundance of carbonic anhydrase (CA), NADH-cytochrome b5 reductase

(CYB5R), rubisco large subunit, succinyl COA ligase (SCoAL) and isocitrate dehydrogenase (ICDH) (Table 3.2.2; NSD). The salinity stress mediated reduction in proteins like rubisco and CA was also reported earlier in rice [233]. Leaf CA is an important enzyme that facilitated the CO_2 diffusion at rubisco's active site. The downregulated abundance of CA under salt stress can be attributed to feedback inhibition through CO_2mediated decreased stomatal conductance [234]. Results of the study are consistent with previous reports where increased abundance of rubisco and CA has been demonstrated in salt tolerance rice variety (pokali) compared to sensitive one (IR-64) [233]. Sucrose synthase (SuSy) and glucose-1 P adenyle transferase plays a crucial role by sucrose breakdown for ensuring energy, and remobilization as transient starch. An increase expression of the Susy was reported to be an adaptive response under salt stress by remobilization of the carbon resource in tomato [235]. The increased abundance of Susy and glucose 1 p adenylate transferase under NT suggested a possible role of early sugar remobilization for salinity tolerance. On the contrary, no such increase was observed under NH treatments, suggesting the involvement of other protective pathways at early stages of stress.

Along the same line, the increased expression of CYB5R has been reported to protect the membrane lipid from destabilisation by supplying the reductants to membrane bound desaturase and may be regarded as one of the important steps required for salinity tolerance [236]. The increased expression of CYB5R was also observed here under TU and H_2O_2 supplementation while a decreased expression under NaCl stress can be correlated well with that of ROS mediated membrane destabilisation. Similarly, the important role of elongation factor-TU (EF-TU) in maintaining the PSII stability was reported and linked the photoinhibition with EF-TU oxidation [237]. The inactivation of EF-TU is mediated via oxidation of regulatory cysteine residue, Cys82, to sulfenic acid resulting in formation of intermolecular disulfide bond [237]. In the present study, the TU supplementation was found

to reduce the oxidative deactivation of EF-TU, as indicated by the 1.3-fold increased abundance of EF-TU protein under TU treatment (Table. 3.2.2; TSD). These changes together help in maintaining the chloroplastic protein synthesis and photosynthetic efficiency under NaCl stress conditions.

The differential expression of protein like cysteine synthase, glutathione associated and thioredoxin under NT treatment (NTD) highlighted the involvement of S-cycle under thiourea treatment. The increased expression of these proteins was proved helpful in salinity tolerance. Cysteine plays an important role in mediating primary metabolism, protein synthesis and the formation low molecular weight defense compounds [238]. The result of this study revealed that TU treatment modulated the expression of protein containing S-like cysteine synthetase, thioredoxin under NT and CDGSH domain containing protein (also termed as NEET protein). NEET proteins are localised in the stroma of the chloroplast and involved in the synthesis of heme-proteins and reported to be associated with decreasing the ROS load [239].

The specific activation of proliferating cell nuclear antigen (PCNA) under H_2O_2 treatment (Table 3.2.2; HSD) in control condition may be linked with that of improved mitotic index and plant growth under the treatment. The PCNA was reported to be an important counter part of thioredoxin interactome and modulates the redox buffering capacity of the cell by improving reduced glutathione content [240]. Similarly, the increased expression of protein disulfide-isomerase under H_2O_2 treatment reflects activation of mild stress responses which helped the plants in adapting the subsequent stress imposition in a better way. The protective effect of PDI was also reported in *Arabidopsis* for various abiotic stresses including drought, salt and H_2O_2 [241].

The increased expression of catalase and peroxidase under NH treatment (NHD) corroborated with other study where exogenous H_2O_2 increased the activity of catalase and

other peroxidases in maize [242] and *Panax ginseng* [243] under salt stress. The H_2O_2 mediated increased expression of selenium binding protein (SBP) along with inhibition with GSH supplementation was also reported in Arabidopsis [244] suggesting the potential antioxidant behaviour of SBP where GSH level were compromised. Similarly, the increased expression of Serine-Threonine Protein Phosphatase like Protein phosphatase 2A (PP2A) under NH treatment can be correlated with that of improved plant growth under salt stress and in consistent with previous report [245]. The exogenous ROS level was also reported to modulate the PP2A expression and related downstream signalling [246]. Although no information is available for the DAG protein, however it is associated with chloroplast development in manually curated database of rice proteins. Significant increase in organic acids like Citric acid, and MA under TU and H_2O_2 supplementation under control conditions reflected a better flux of metabolites from cytoplasm to mitochondrial TCA cycle. The increased inflow can be subsequently linked to increased production of ATP, NADH and $FADH_2$ which eventually lead to better growth and vigour [247].

Although the ratio of Gly/Ser has been shown to be an indicator of photorespiration, the level of Gly is mainly changed under stress conditions [248]. The metabolomics data revealed an increased accumulation of Gly under NaCl, which indicated increased photorespiration. Under non-stressful conditions, photorespiration lowers the quantum yield of photosynthesis which can be considered as a wasteful process, but under stressful condition, photorespiration is shown to be helpful in protecting regenerating RUBP and dissipating excess energy for sustaining Calvin cycle. Earlier reports have also linked curtailing of the photorespiration as an adaptive feature for improving the crop yield [249].

Salicylic acid (SA), as a signalling mediator was reported to improved tolerance at early stage of osmotic stress in *A. Sativa* by regulating stomatal conductance, photorespiration and antioxidant defense [250]. The active involvement of SA in regulating

K^+ loss via a GORK channel is associated with improved salinity tolerance in *A. thaliana* [251]. Increase in SA content under H_2O_2 and NH treatments suggested the involvement of SA mediated signalling mechanism for salinity stress amelioration. The TU supplementation also induced an increase in shikimic acid content indicating the protective role of secondary metabolites (phenolics) biosynthesis for salinity amelioration. The increased accumulation of phenolics was reported to be associated with salinity tolerance behaviour in rice by maintaining the ROS homeostasis [91] Further TU mediated increased expression in the genes involved in phenolics biosynthesis was also reported [252].

Similarly, the increase in MI content under TU, H_2O_2 and NT treatments justified the improved growth under control and salt conditions. Various transgenic studies using myo-inositol 1 phosphate synthase (MIPS) gene have shown that this gene ensures resistance to various abiotic stresses including osmotic and salt stress in crop plants [253]. The possible role of MIP and MIPS as a positive modulator of plant defense under salt stress was evident by the study where constitutive overexpression of MIPS gene liked with increased expression of stress responsive marker genes including *RD 29 A, RD 29 B, P5CS, KIN1 and COR 47* in *Arabidopsis* [254]. Metabolite profile related to sugars revealed an increased synthesis of sucrose under TU and H_2O_2 supplementation under both control and stress conditions. The increase in sucrose synthesis can be correlated to photosynthetic efficiency of the leaf as sucrose is the most stable and most preferred metabolite for translocation. The increased sucrose content particularly under stress treatment also suggested its role as an osmotic adjustment. Further the coordinated activation of sucrose biosynthesis enzymes was also reported in *Brassica* under TU treatment under field conditions [131] enhancing the yield potential. We also observed the similar co-ordinated activation of sucrose synthesis in the pot studies, suggesting improvement in yield and stress tolerance.

Environmental stress also modulates the leaf starch metabolism with increased maltose content during the day under photorespiratory conditions [255]. The stress mediated growth and yield impairment in plants can be considered as due to impaired sucrose synthesis in leaf and increased remobilisation of transient starch for sustain growth. Remobilisation of starch provides energy and carbon source under photoinhibitory condition [256]. The increased starch degradation [257] or repression of starch biosynthesis [258] under stress conditions both can be led to increase in maltose content. Although some studies correlated the increased degradation of sucrose as an adaptive mechanism for stress tolerance [256], the result of present study showed the salinity mediate increase in maltose content is an inhibitory effect over photosynthesis and plant growth. On the contrary, relatively high glucose content particularly under NT treatment may be correlated with improved carbon and nitrogen metabolism by regulating ROS homeostasis [259]. The result was consistent with previous reports, where improved nitrogen reductase activity under TU treatment was corelated with improved photosynthesis and yield [260]. The relative increase in the α-KG under H_2O_2 supplementation may also be linked with increased ROS scavenging capacity [261]. Further increased α-KG may also channelize the carbon flux towards glutamine synthesis under coordinated action of glutamate dehydrogenase (GDH) and glutamine synthetase thereby regulating glutathione level. Additionally, the increase in GDH and glutamate decarboxylase (GAD) under H_2O_2 supplementation revealed the involvement of GABA shunt, in maintaining the plant growth under stress condition. The mild oxidative stress mediated increase in GABA shunt activity was also reported earlier [262] along with positive regulatory role of GABA for maintaining the photosynthetic efficiency and imparting stress tolerance towards various abiotic stresses [263]. Similarly, the relative importance of increased malate content for stress amelioration is also consistent with previous reports where TU treatment led to increase in MA content [131]. The result of the

study suggested a possible involvement of malate valve under TU supplementation. The malate valve facilitates the transfer of reducing equivalent in the form of metabolites (MA, OAA) in-between mitochondria and chloroplast and thereby increased sustainability towards maintaining photosynthesis and respiration at the cost of low ROS production, particularly under stress conditions. The overexpression of cytosolic MDH was reported to improve tolerance towards salt and cold stress by improving the redox homeostasis [194].

Thus, TU and H_2O_2 response was studied at multiple-organization levels including gene, protein and metabolites. The over-lapping and specific components were identified under both control and NaCl stress conditions.

Section III: Studies on photosynthetic efficiency, source-sink relationship and grain yield under TU and H_2O_2 treatment conditions

3.3. Introduction

The osmotic and ionic components of salt stress make their significant contribution towards increasing the yield gap by inhibiting photosynthesis in source leaf (stomatal conductance/ metabolic inhibition), decreasing sucrose translocation and reducing the number/activity of the sink tissues [129]. Further, the salinity mediated decrease in chlorophyll and carotenoids, altered the stability of the photosystems, thereby posing a great risk for increased ROS production in chloroplast [264]. The long-term exposure under salt stress is mostly associated with toxic sodium accumulation in plants cell. The plants under salt stress cope up the adverse conditions at the cost of increased mitochondrial respiration to supply ATP for osmolytes synthesis or Na^+ sequestration [100]. The impaired electron flow in photosynthesis, along with increased mitochondrial respiration promotes ROS production and thereby shifts the ROS homeostasis towards oxidative stress. Additionally, various enzymes of the carbon metabolism were shown to be regulated by ROS status or K^+/Na^+ ratio.

The present section is basically focused towards analysing the potential of TU and H_2O_2 for minimising the yield gap under realistic field conditions. Towards this, the study was carried out on fully mature plants under stress conditions. The comparative analysis of antioxidant machinery, ionic homeostasis, photosynthesis, source sink relationship along with final yield was carried out in the current section. The yield of any crop reflects a coordinated action of sucrose synthesis in the source leaves, its transport from site of synthesis to developing sink organs and, finally the utilised/stored form in the sinks. The metabolic flux of carbon from source to sink- tissues has been reported to be negatively affected under salt stress, resulting in yield gap [1, 265]. Moreover, most the enzymes involved in the source-

sink metabolic homeostasis were reported to be under redox regulation. Thus, understanding the source sink equilibrium under PBRs of contrasting chemistry like TU (reducing) and H_2O_2 (oxidising) under field conditions is of prime interest for revealing the molecular components of TU and H_2O_2 mediated yield enhancement. The data will also be helpful for deciphering the integrative function of various enzymes regulating the sucrose biosynthesis and metabolic homeostasis in different plant tissues like young leaf (YL), old leaf (OL) and developing inflorescence (DI) under salt stress. The principal component analysis was also carried out to figure out treatment specific variables, which helped in establishing the TU and H_2O_2 mediated protective effects over yield under salt stress.

3.3.1. Results

3.3.1.1. Enhanced plant growth and yield characteristics under foliar application of TU and H_2O_2

The phenotypic difference in plant growth (Fig. 3.3.1) and associated yield parameters (Fig. 3.3.2) under different treatment conditions highlighted an improved plant vigor together with enhanced seed setting can be presented as a morphological evidence of TU and H_2O_2 mediated ameliorative effect under salt stress. A significant decrease in the harvest index (35%) (Fig. 3.3.2 A), yield per plant (38%) (Fig. 3.3.2 B) and 1000 seed weight (20%) (Fig 3.3.2 C) was observed under NaCl treatment compared to control. At the same time, TU and H_2O_2 foliar application prompted a protective effect on 1000 seed weight and yield per plant, which were improved by ~30-34% and ~25-27% (Fig. 3.3.2) under NT and NH treatments, respectively relative to NaCl treatment. Additionally, compared to WS control various parameters of the yield were also significantly improved under TU and H2O2 alone treatments. The yield per plant, 1000 seed weight and harvest index harvest index, 1000 seeds weight and yield per plant were improved by about 17.16, 11.08 and 13.19% under TU and 12.53, 12.71 and 15.87% under H_2O_2 alone, as compared to WS control (Fig. 3.3.2).

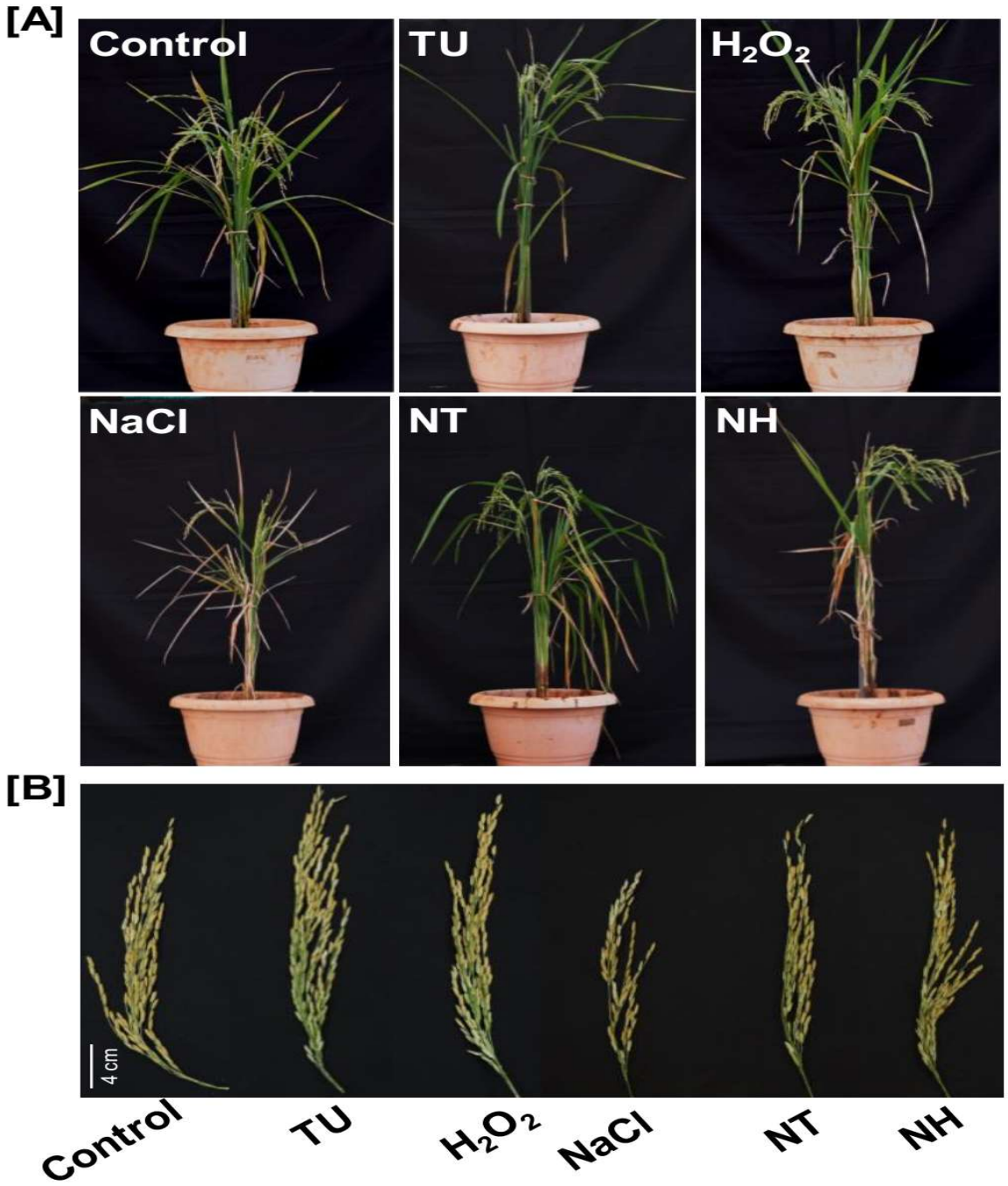

Fig. 3.3.1: Differential phenotype at pot level showing the ameliorative potential of the TU and H_2O_2 treatments under NaCl stress, at plant growth (A) and yield (B).

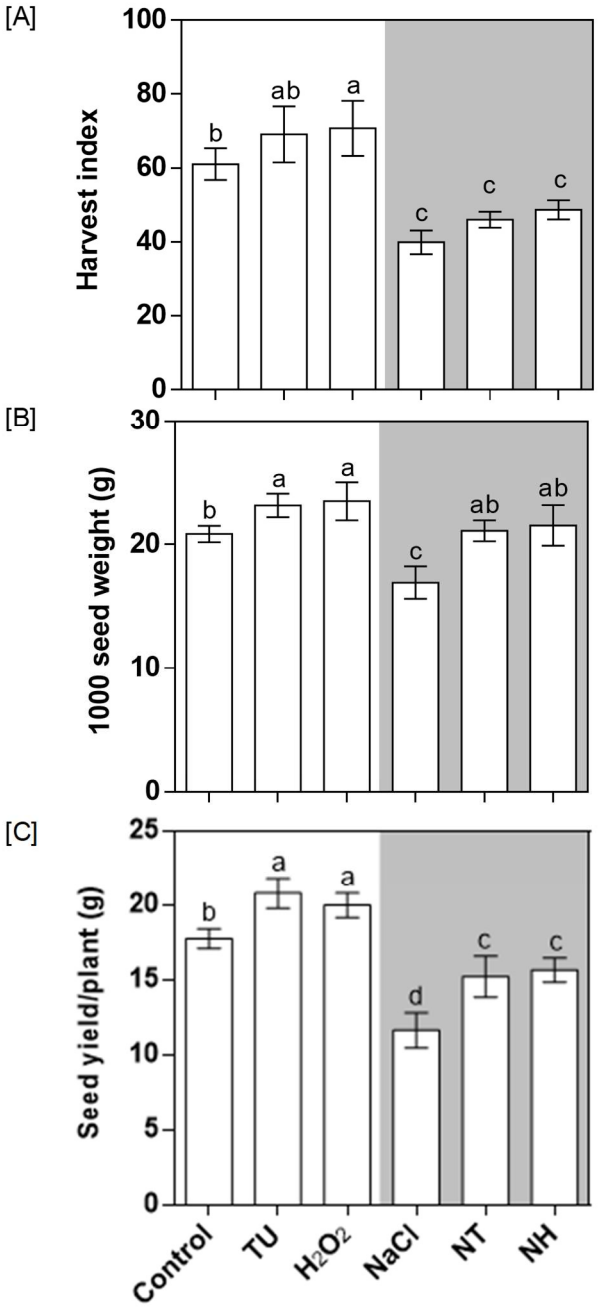

Fig. 3.3.2: Effect of foliar-applied TU and H_2O_2 treatments on yield attributes such as harvest index (A), seed yield per plant (B) and 1000 seed weight (C). All values represent mean of 10 plants ± S.E. Different letters indicate significantly different values (DMRT, $p \leq 0.05$).

Quantitative estimation of various plant growth parameters showed a decrease in number of panicles (18%), panicle length (15%), plant length (11%), flag leaf length (12%) and chlorophyll content (16%) under NaCl treatment relative to control condition (Table 3.3.1). As compared to NaCl, an improved panicle number, panicle length and leaf width corresponding to (24.39, 13.46 and 13.33%) respective increase under NT and (24.39, 10.10 and 6.67%) respective increase under NH treatments were observed (Table 3.3.1). Further, H_2O_2 foliar spray improved both the characteristics of source leaf like leaf length (19%) and leaf width (12%) as well as of sink tissue by increasing the number of tillers (18%) and productive panicles (13%). On the other hand, upto 12% increase in leaf chlorophyll content and 13% increase in tillering and productive panicle formation were observed under TU treatment.

Table-3.3.1: Quantification of various growth parameters under different treatment conditions. The values represent mean of ten biological replicate ± SE. Different letter indicates significantly different values (DMRT, $p \leq 0.05$).

Treatment	Plant height (cm)	Leaf length (cm)	Leaf width (cm)	Panicle Length (cm)	Panicle number	Chlorophll (AU unit)
WS	107.7^{b} (± 0.6)	33.2^{c} (± 1.8)	1.6^{b} (± 0.08)	24.5^{a} (± 0.6)	5.0^{c} (± 0.2)	40.4^{b}
TU	110.7^{a} (± 1.2)	35.8^{b} (± 1.6)	1.7^{b} (± 0.06)	24.7^{a} (± 0.4)	5.7^{a} (± 0.4)	45.1^{a} (±1.1)
H_2O_2	110.6^{a} (± 1.2)	39.3^{a} (± 1.4)	1.8^{a} (± 0.04)	24.9^{a} (± 0.5)	5.6^{ab} (± 0.4)	40.4^{b}
NaCl	95.9^{e} (± 0.5)	29.0^{d} (± 1.0)	1.5^{c}(± 0.04)	20.8^{c} (± 0.6)	4.1^{d} (± 0.3)	33.8^{c}
NT	104.8^{c} (± 1.2)	32.6^{c} (± 1.4)	1.7^{b} (± 0.05)	23.6^{b} (± 0.5)	5.1^{bc} (± 0.3)	40.7^{b}
NH	102.1^{d} (± 0.5)	31.8^{c} (± 0.6)	1.6^{b} (± 0.04)	22.9^{b} (± 0.2)	5.1^{bc} (± 0.2)	39.0^{b} (±1.5)

3.3.1.2. Change in ionic and redox equilibrium under TU and H_2O_2 foliar spray

The histochemical staining was done to ascertain the load of ROS, particularly superoxide in the young leaf. The result of the histochemical staining clearly had shown a

decrease and increased basal level of $O_2^{\bullet-}$ in the young leaf under TU and H_2O_2 foliar spray respectively. Further the intense blue color in NaCl stressed leaf reflected the extent of ROS load, which showed recovery under NT and NH treatments (Fig.3.3.3 A).

The differential effect of the treatments was also ascertained by analyzing the cellular redox status in the form of AsA_{red}/AsA_{Oxi} (AsA/DHA) and activity of GR which actively participates in maintenance. In general, a 28.5% increase in the GR activity under NaCl which was further intensified up to 64 % and 99% respectively for NT and NH treatments relative to control condition (Fig. 3.3.3 B).

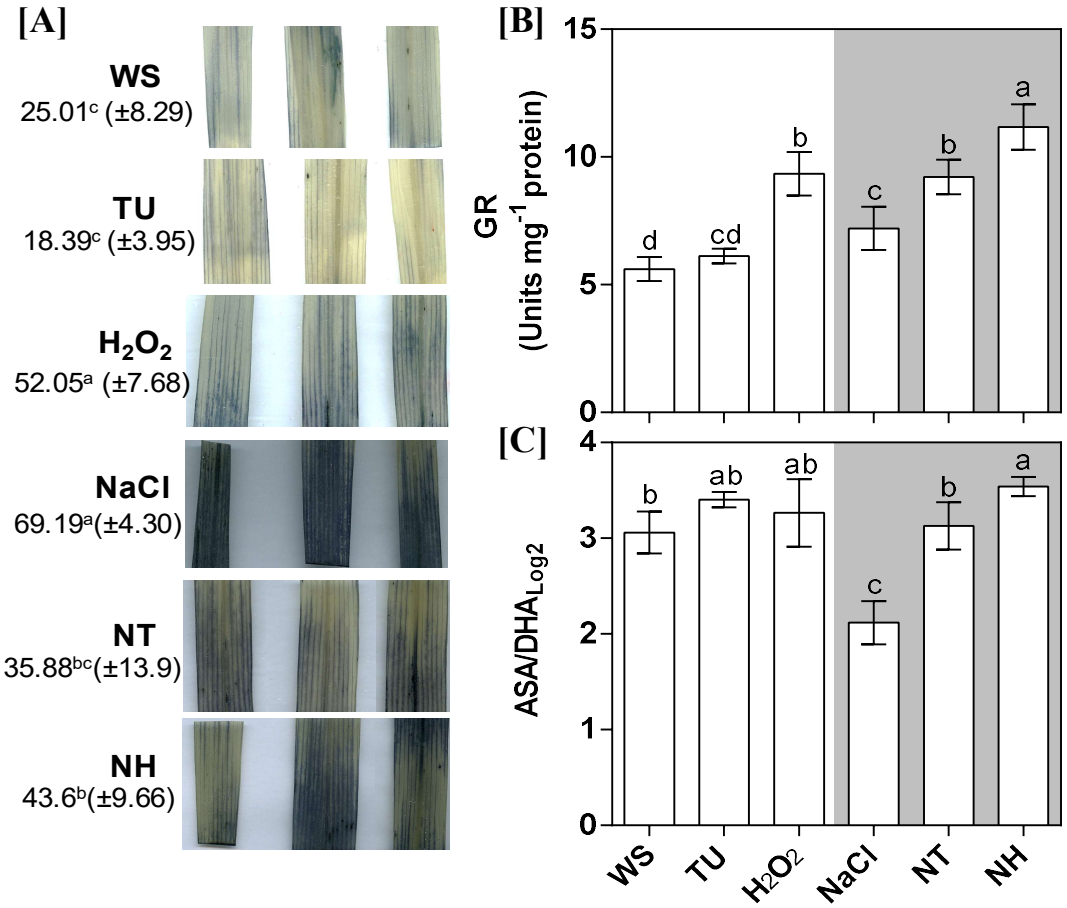

Fig. 3.3.3: Measurement of the redox status in terms of the superoxide level, GR activity and AsA/DHA ratio. Estimation of various parameters like (A) glutathione reductase (GR) activity (B) ascorbate/dehydroascorbate (AsA/DHA) ratio and (C) NBT stain intensity was

quantified using image J software (version 1.53d; https://image j.nih.gov) and represented as average arbitrary units (± S.D.). All the values are mean of triplicates ± SD. Different letters indicate significantly different values (DMRT, $p \leq 0.05$).

Similarly, the effect of salinity was also evident in AsA/DHA (red/oxi) ratio, as 30.7% decrease in this ratio was observed under NaCl treatment (Fig 3.3.3 C). On the contrary the negative effect of salinity over AsA (red/oxi) ratio was nullified under both the treatments; with no significant change in ratio under NH treatment while 13% increase under NT treatment was registered relative to control. In summary, an improved sustenance of GR activity and reduced ascorbate pool was observed, corresponding to 27.94 and 47.6% increase under NT and 55 and 67% increase under NH treatments (NH), relative to NaCl treatment. Although, no such upregulation in the activity of GR and AsA/DHA ratio (Fig. 3.3.3 B, C) was observed under TU alone treatment, the activity of GR under H_2O_2 alone treatment was found to be increased upto 66.6% compared to WS control.

The spatial ion accumulations were also analyzed in various plant parts involved in maintaining source sink equipoise under studied treatment conditions. The differential ion accumulation was quantified in the young leaf (YL), Old leaf (OL) and developing inflorescence (DI) tissue. In general, the highest loading of the Na^+ was observed in the OL while Na^+ accumulation in the sink tissue was maintained at the lower level. The Na^+ content of the YL and DI was observed to be increased upto 403.8 and 70.21% respectively under NaCl treatment (Table 3.3.2). On the other hand, a relative low accumulation of Na^+ was observed in NH-treated plants, for all the analyzed plant tissue which includes YL, OL and DI corresponding to 38.57, 21.48 and 50%, respectively as compared to NaCl- treated plants. The same trend for maintaining the low Na^+ in YL, and DI was also observed for NT-treated plants with the exception of Na^+ content in OL which intensified by 15.97% relative to plants subjected to NaCl-stress. Additionally, no significant change was observed in Na^+

accumulation pattern under TU treatment as compared to WS-control. On the contrary, a relative low accumulation (34.18%) of Na^+ in the YL along with up to 45.91% increased accumulation in OL was observed under H_2O_2 alone treatments compared to those of WS control.

Table-3.3.2: Spatial distribution of Na^+ and K^+. All the values are mean of triplicates ± SD. Different letters indicate significantly different values (DMRT, $p \leq 0.05$).

A. Na^+ (% DW)			
Treatments	**Young leaf**	**Old leaf**	**Developing sink**
WS	0.158^{d} (± 0.03)	0.342^{e} (± 0.04)	0.47^{b} (±0.02)
TU	0.156^{d} (± 0.04)	0.364^{e} (± 0.06)	0.42^{bc} (±0.05)
H_2O_2	0.104^{d} (± 0.01)	0.499^{d} (± 0.01)	0.49^{b} (±0.03)
NaCl	0.796^{a} (± 0.04)	0.889^{b} (± 0.05)	0.80^{a} (±0.02)
NT	0.625^{b} (± 0.02)	1.031^{a} (± 0.07)	0.37^{c} (±0.02)
NH	0.489^{c} (± 0.04)	0.698^{c} (± 0.03)	0.40^{c} (±0.01)
B. K^+ (% DW)			
WS	3.175^{b} (± 0.58)	4.014^{b} (± 0.24)	1.694^{c} (±0.04)
TU	4.089^{a} (± 0.20)	3.842^{b} (± 0.11)	2.062^{a} (±0.09)
H_2O_2	3.690^{ab} (± 0.16)	5.674^{a} (± 0.16)	2.196^{a} (±0.09)
NaCl	1.574^{c} (± 0.12)	1.446^{e} (± 0.32)	1.286^{d} (±0.04)
NT	3.232^{b} (± 0.29)	2.078^{d} (± 0.18)	1.946^{b} (±0.23)
NH	3.349^{b} (± 0.22)	2.938^{c} (± 0.35)	1.972^{b} (±0.22)

The increased accumulation of Na^+ with a concomitant decrease in the K^+ was observed in all studied organs (Table 3.3.2). Upto 50, 23 and 47% decrease in K^+ content was observed for YL, OL and sink tissue respectively under NaCl treatment relative to WS-control. Although K^+ homeostasis was turned out to be improved in all tissues (YL, OL and DI) under NH treatment as compared to NaCl alone, NT maintained the K^+ homeostasis in sink and DI leaves. The OL under NT treatments were observed to have highest Na^+ and least K^+ content among all treatments. The maximum reversal for K^+ depletion was seen in YL under NT and NH treatment conditions corresponding to 105.34 and 112.77%, respectively relative to NaCl

alone treatment. Similarly, as compared to WS controls an improved K^+ content was also noticed in the plants under TU- and H_2O_2 treatments, with an exception for OL under TU-treatment, where K^+ levels stay unaltered (Table 3.3.2).

3.3.1.3. Improved photosynthetic responses under TU and H_2O_2 foliar spray

The improved chlorophyll content and improved yield parameters under NT and NH treatments indicated the relative improved photosynthesis and source sink coordination. Various parameters related to stomatal conductance and PS-2 stability were analyzed (Table 3.3.3).

Table-3.3.3: Quantification of various parameters related to photosynthetic efficiency under different treatment conditions. The values represent mean of ten biological replicate ± SE. Different letter indicates significantly different values (DMRT, $p \leq 0.05$).

Treatments	Photosynthetic rate (µMol CO_2 m^{-2} s^{-1})	WUE	F_v/F_m	ETR	PS-II yield	NPQ (AU unit)
WS	6.2^{b} (± 0.7)	2.1^{a} (± 0.2)	0.720^{a} (±0.03)	51.7^{ab} (± 1.8)	0.124^{b} (± 0.00)	2.1^{ab} (± 0.03)
TU	7.1^{ab} (± 0.5)	2.3^{a} (± 0.1)	0.734^{a} (± 0.01)	58.4^{a} (± 3.4)	0.144^{a} (± 0.01)	1.8^{b} (± 0.18)
H_2O_2	7.5^{a} (± 0.4)	2.4^{a} (± 0.7)	0.715^{a} (± 0.01)	60.5^{a} (± 6.5)	0.153^{a} (± 0.02)	2.4^{a} (± 0.53)
NaCl	1.9^{d} (± 0.5)	0.8^{c} (± 0.03)	0.614^{b} (± 0.04)	24.3^{d} (± 1.7)	0.087^{d} (±0.003)	1.6^{b} (± 0.04)
NT	3.4^{c} (± 0.2)	1.3^{b} (± 0.1)	0.705^{a} (± 0.04)	48.9^{bc} (± 8.2)	0.136^{ab} (± 0.01)	1.8^{b} (± 0.02)
NH	3.9^{c} (± 1.1)	1.4^{b} (± 0.2)	0.717^{a} (± 0.01)	42.0^{c} (± 3.2)	0.102^{c} (± 0.01)	2.1^{ab} (± 0.49)

The major effects of salinity were observed in rate of photosynthetic (PR) and water use efficiency (WUE) which got reduced by 69.35 and 61.90%, respectively relative to WS

control. On the contrary, restoration of photosynthetic efficiency was observed with improvement in these parameters showing about 78.95 and 62.5% increase in NT and 105.26 and 75% increase in NH, relative to plants subjected to NaCl without any treatment. Further, effects of treatments over PS-II stability were analyzed based on the chlorophyll fluorescence. Various parameters defying the PS-II stability like quantum yield of fluorescence (F_v/F_m) non photochemical quenching (NPQ), electron transport rate (ETR), and quantum yield of photosystem II (PS-II yield) were reported to decreased by 15%, 30%, 53% respectively in plants subjected to NaCl treatment. Although invariable electron transport rate was found under NT, the decrease in ETR under NH was restricted to only 19% over 53% under NaCl alone treatment (Table 3.3.3). Further 31.25% increase in NPQ activation was observed for NH as compared to NaCl alone. Both the treatments protect the PS-2 from irreversible damage as can be seen by F_v/F_m ratio (Table 3.3.3). The positive effect of the TU and H_2O_2 foliar sprays was also observed over photosynthesis and PS-II yield, under control condition which got increased upto 14.52 and 20.97% and 16.13and 23.39% compared to WS-control. Additionally, the NPQ port of energy dissipation under NH was found up regulated (22%) as compared to control.

3.3.1.4. Restoration of source-sink equipoise under TU and H_2O_2 foliar spray

The negative impacts of salinity not only affect photosynthetic efficiency of the plant, but also destabilize the metabolic homeostasis of source sink equilibrium. The dysregulation of source sink equilibrium is mediated via inactivation of various key enzymes regulating source (SPS and FBPase) and sink (SuSy, AI and NI) strength. For instance, the activity of the SPS was decreased by 46.21, 26.51 and 26% respectively in YL, OL and DI organs in NaCl treated plants as compared to WS-control (Fig 3.3.4 B). Akin to SPS activity, the activity of FBPase was also found to be decreased in NaCl treated plants, corresponding to 56.04, 45.05 and 68.86% decrease in YL, OL and DI organs relative to WS-control (Fig 3.3.4

A). The TU and H_2O_2 mediated source strength protection was evident by improved activities of SPS and FBPase particularly in YL corresponding to 74.37 and 40.09% respective increase under NT and 93.47and 32.85% respective increase under NH treatments (Fig 3.3.4 A, B).

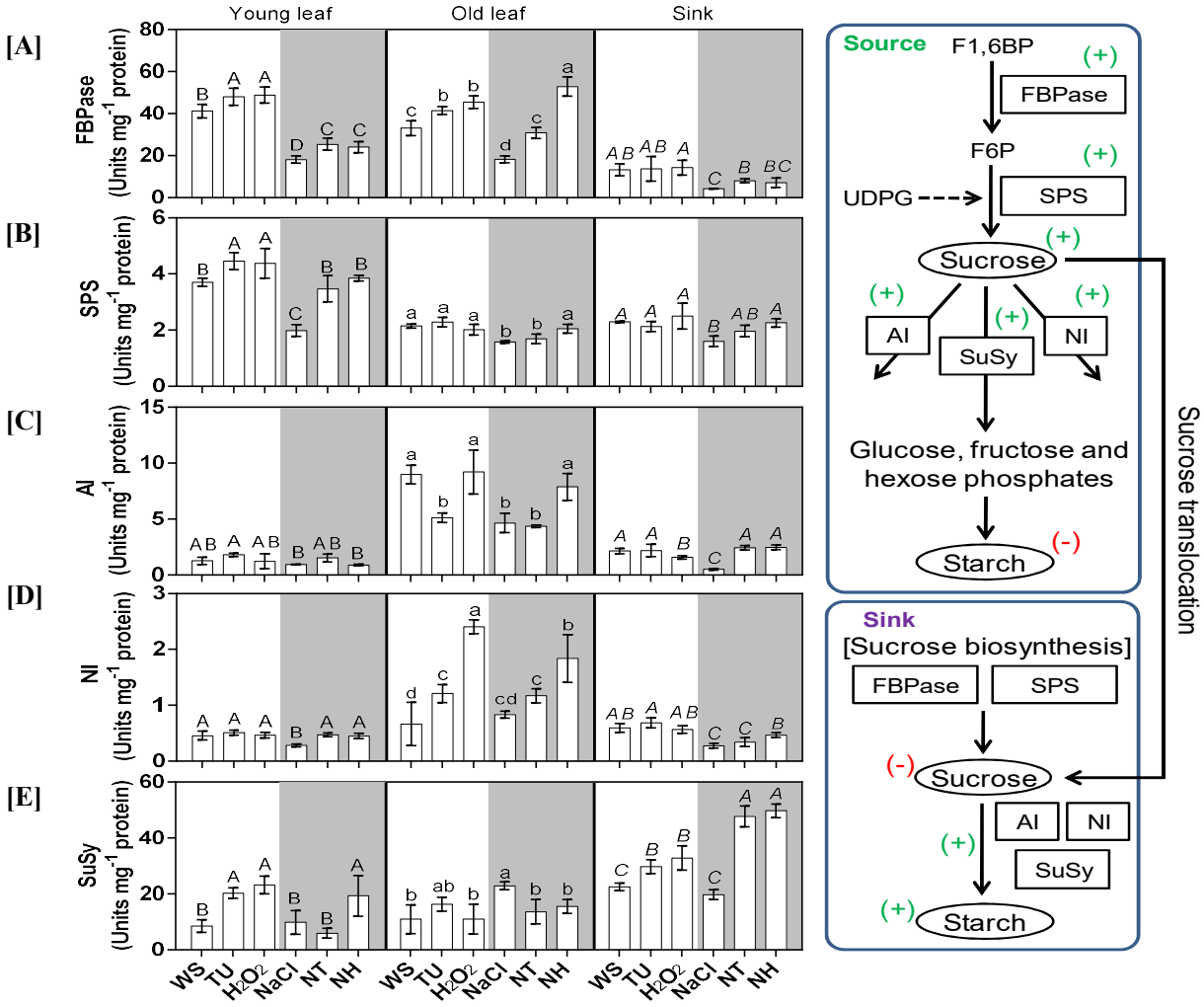

Fig. 3.3.4: Quantification of enzymatic activities involved in regulating source sink equilibrium under different treatment conditions. Quantification of enzymatic activities like FBPase (Fructose 1,6 bis-phosphatase; A); SPS (Sucrose phosphate synthetase; B); AI (Acid soluble invertase; C); NI (Neutral invertase; D) and SuSy (Sucrose synthase; E). All values represent mean of triplicates ± SD. Different letters indicate significantly different values (DMRT, $p \leq 0.05$). The overview of sucrose biosynthesis/breakdown pathway (refer

section 1 for more details) operated in source and sink organs were represented in right-hand panel (F). The quantified enzymes and metabolites of the present study were represented in rectangles and ovals respectively. The increase and decrease in the levels of enzymatic activity/metabolites were denoted as positive (+) and negative (−) labels respectively.

The SPS activity in OL was differentially regulated under TU and H_2O_2 treatments, with about 29.71% increase in SPS activity in OL under NH treatment was observed as compared to NaCl treated plants. On the contrary, no such reversal in SPS activity of OL was observed under NT treatment. The significant increase in the activity of FBPase was also seen in all three tested organs under NH and NT treatments relative to NaCl alone. The TU and H_2O_2 mediated increase in the SPS and FBPase activity was also evident under control conditions. Further, a relative increase of upto 20.22 % and 18.06% in SPS activity along with 16.48% and 18.50% increase in FBPase activity was observed in young leaves (YL) compared to WS-control. Additionally, the sucrose synthesis in the sink tissue remained unchanged under TU and H_2O_2 treatments relative to WS-control. AS compared to WS-Control, about 26.51% and 68.86% respective decrease in the SPS and FBPase activity in developing inflorescence (DI) was also observed in NaCl treated plants. On the other hand, an improved SPS activity corresponding to 29.75% and 22.60% increase under NH and NT treatments respectively relative to NaCl was also observed. The same trend was also followed by FBPase which got increased up to 71.84% and 93.93 respectively under NH and NT treatments as compared to NaCl alone.

Sucrose redistribution mediated by sucrose synthase (SuSy) invertase was also analyzed and reported (Fig 3.3.4 E). In general, the invertase activities were found to be repressed under NaCl relative to WS-control in both source (YL) and sink (DI) tissue (Fig 3.3.4 C, D). Upto 38.10 and 24.11% decrease in YL and 53.95 and76.46% decreases in DI for AI and NI respectively was observed under NaCl treatment compared to WS-control.

Although, upto 69.38% increase was observed in AI activity in OL under H_2O_2 treatment (Fig3.3.4 D), the activity of AI remained unaltered under TU treatment. On the contrary, NI activity was found to be increased in OL, corresponding to 40.44 and 120.97% increase under both NH and NT treatments respectively relative to NaCl treatment (Fig 3.3.4 C). The activities of NI and SuSy were observed as major determinant of the sink strength. As compared to NaCl, a significant improvement in the activities of AI and SuSy respectively in sink tissue (DI) was observed, corresponding to (381.99 and 141.38%) increase in NT and (397.74 and 151.54%) in NH treatment. The sink strength correlated with that of SuSy activity was showing up to 32.09 and 45.08% increase under TU and H_2O_2 treatments as compared to WS-control. A 12.25% decrease in the SuSy activity was also observed under NaCl treatment relative to WS-control. Further upto 141.38% and 151.54% increase in SuSy activity was reported under NT and NH treated plants respectively relative to NaCl alone.

The sucrose content in the leaves (OL and YL) and starch content in developing seeds were quantified as an indicator of source leaf capacitance for sucrose synthesis and sink strength to store it as starch. Salinity negatively affected the source sink coordination as evident by 27.65% and 48.48% decrease in YL sucrose and developing seeds starch content respectively as compared to WS-control (Table 3.3.4). Conversely, a significant increase the sucrose level was observed in both YL and DI organs corresponding to, 46.27 and 66.76% in NT and 58.71 and 66.47% in NH, respectively relative to NaCl-treated plants. Just opposite to source, the reverse trend for sucrose accumulation was observed in NaCl-treated DI, showing upto 32.32% increase as compared to WS control. On the contrary, as compared to NaCl alone treatment relative low sucrose got accumulated in the DI under NH and NT treatments corresponding to 40.46and 19.08%, respectively (Table 3.3.4). Similarly, increased starch content was observed in YL (53.42%) and OL (48.48%) in NaCl treated plants compared to WS-control. Besides, a significant decrease in starch content was also

observed in YL under NT (29.96%) and NH (26.72%). Additionally, the active involvement of OL for sucrose synthesis under H_2O_2 treatment was observed as evident by about 54.49% increase in sucrose and 24.75% decrease in starch content relative to WS-control (Table 3.3.4). The similar trend was followed under NH where upto 30.35% more sucrose and 41.84% less starch gets accumulated in OL compared to NaCl alone treatment.

Table-3.3.4: Quantification of sucrose [A] and starch [B] content. All the values are mean of triplicates ± SD. Different letters indicate significantly different values (DMRT, $p \leq 0.05$).

A. Sucrose (mg g^{-1} DW)			
Treatments	**Young leaf**	**Old leaf**	**Developing sink**
WS	62.93^{ab} (± 7.80)	43.07^{c} (± 8.40)	19.80^{b} (± 1.87)
TU	69.93^{a} (± 8.80)	39.80^{c} (± 3.47)	26.00^{a} (± 2.93)
H_2O_2	73.47^{a} (±14.67)	66.53^{a} (± 5.40)	19.27^{b} (± 2.20)
NaCl	45.53^{b} (± 5.87)	43.93^{c} (± 3.07)	26.20^{a} (± 2.40)
NT	66.60^{a} (± 13.00)	55.07^{b} (± 3.20)	21.20^{ab} (± 3.13)
NH	72.27^{a} (± 6.33)	57.27^{b} (± 4.33)	15.60^{b} (± 4.80)
B. Starch (mg g^{-1} DW)			
WS	10.73^{b} (± 0.8)	13.20^{b} (± 1.07)	44.00^{ab} (± 1.93)
TU	9.87^{b} (± 0.53)	11.67^{bc} (± 0.40)	48.60^{a} (± 6.07)
H_2O_2	11.93^{b} (± 1.07)	9.93^{c} (± 0.80)	48.80^{a} (± 2.73)
NaCl	16.47^{a} (± 1.06)	19.60^{a} (± 3.33)	22.67^{c} (± 5.20)
NT	11.53^{b} (± 2.13)	13.00^{b} (± 2.00)	37.80^{b} (±5.33)
NH	12.07^{b} (± 1.33)	11.40^{bc} (± 0.40)	37.73^{b} (±1.47)

3.3.1.5. Deciphering treatment-variable interlinkage through PCA clustering

In order to identify the principal component mediating amelioration and yield improvement under salt stress, principal component analysis (PCA) was executed with integral dataset of source leaves and sink tissue (Fig. 3.3.5). The PCA-1 was represented as different attributes under study while PCA-2 represented various treatments. The components revealed significant variation between treatments under study. Two different loading plots,

signifying the source and sink specific clustering of attributes with treatments were generated. The loading plot for source strength showed about 67.44% variance as PC1 and 12.2% PC2 (Fig. 3.3.5 A). On the basis of data clustering three independent groups were formed in source leaves. The first group contained photosynthesis, enzymes and metabolites related to source sink metabolic homeostasis and found to be shared in WS, TU and H_2O_2 treatments. The second groups showed the activity of GR as major determinant and found to be associated with NH and NT treatments. The third group was not accomplice with any of the variables studied in the PCA analysis and represented NaCl stress (Fig. 3.3.5 A).

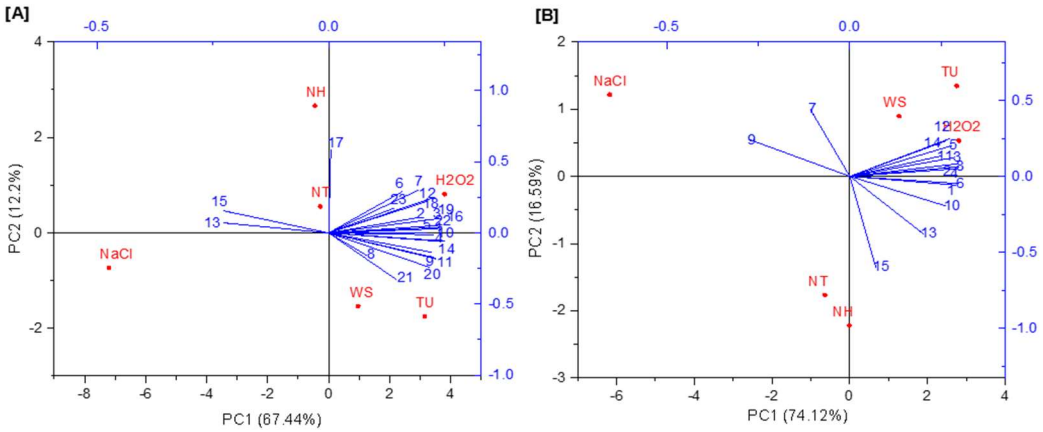

Source strength variables			
1	Leaf length	13	Starch
2	Leaf width	14	Chlorophyll
3	F_v/F_m	15	Na^+
4	Electron transfer rate (ETR)	16	K^+
5	Quantum yield of photosynthesis (PS-II)	17	Glutathione reductase (GR)
6	Non photochemical quenching (NPQ)	18	ASA/DHA
7	qP	19	Sucrose phosphate synthetase (SPS)
8	qN	20	Fructose 1,6 bis phosphatase (FBPase)
9	Photosynthesis rate	21	Acid Invertase (AI)
10	Transpiration rate	22	Neutral Invertase (NI)
11	Water use efficiency (WUE)	23	Sucrose synthase (SuSy)
12	Sucrose		

Sink strength variables			
1	Panicle number	9	Na^+
2	Panicle length	10	K^+
3	Plant height	11	Sucrose phosphate synthetase (SPS)
4	Yield per plant	12	Fructose 1,6 bis phosphatase (FBPase)
5	Harvest Index	13	Acid Invertase (AI)
6	1000 seed weight	14	Neutral Invertase (NI)
7	Sucrose	15	Sucrose synthase (SuSy)
8	Starch		

Fig. 3.3.5: Treatment-variable interaction identification based on Principal Component Analysis (PCA). PCA analysis that includes majority of the analysed parameter in source leaves and sink tissues under different treatments. Two individual biplots were generated to identify the responsive variables for source and sink-strength and represented as young leaf (source; A) and developing inflorescence (sink; B). Lines originating from central point of biplots indicate positive or negative correlations of different variables; where their closeness

indicates correlation strength with particular treatment. The variables were represented in the form of numeric values along with their details in associated tables.

Similarly, the loading plot for sink strength variables showed about 74.12 % variance by PC1 and 16.59% variance by PC2 (Fig. 3.3.5 B). Similar to source loading plot, three major groups were also recognized for explaining the variable treatment interaction in sink strength. The first group which define most of the vigour and yield associated parameters was found to be associated with WS, TU and H_2O_2 treatments. The second group predominantly identified as regulators of source sink metabolic homeostasis which includes various enzymes and metabolites and found to be accompanied with NH and NT treatments. The third group demonstrated Na^+ and sucrose as decisive parameter affiliated with NaCl treatment.

3.3.2. Discussion

Similar to nutrient media supplementation, the ameliorative capabilities of TU and H_2O_2 against salt stress was also apparent in the pot study as improved plant phenotype which includes both plant vigour (Fig. 3.3.1A), as well as yield per plant (Table 3.3.1, Fig. 3.3.1B), in control as well as NaCl stress conditions, corroborating their practical use in agrarian system. Taken into account of plant size, possible decay under the spontaneous sunlight and earlier reported working concentrations in various crops, the final dose for foliar spray was selected as TU (6.5 mM) and H_2O_2 (1 mM). The protective effect is mainly due to efficient management of ionic and redox homeostasis along with photosynthesis supported by better K^+ retention, improved AsA/DHA ratio and improved photosynthesis under NH and NT treatments. Besides, the regulatory roles of ROS and K^+ as signalling mediators have potential to alter the growth responses. Corresponding to improved K^+ retention, decreased Na^+ accumulation was also observed under both NH and NT treatments, particularly in YL and DI which depicting the main organs for photosynthesis and reproduction, respectively (Table 3.3.2). The improved K^+ retention and low Na^+ in these organs mediated its protective

effect by protecting photosynthesis from metabolic inhibitions Earlier studies also reported the photosynthetic inhibition and growth reduction under K^+ depleted conditions [219]. The results of this study were in line, where lower Na^+ accumulation along with improved K^+ retention (Table 3.3.2) could protect the photosystems from oxidative damage and improved the photosynthetic rate (Table 3.3.3) leading to overall plant growth and vigor. The instability of K^+/Na^+ ratio is a major factor by which Na^+ enforce intoxication in plants. An increased K^+ content in YL and DI may correlate well with that of maintenance of K^+/Na^+ ratio in these tissues. Further the ion accumulation in the OL showed a different pattern under TU and H_2O_2 under salt stress. The TU treatment increased the Na^+ accumulation in the OL and there by restricting the Na build up in young flag leaf to avoid Na mediated disruption of photosynthetic. Salt exclusion from young leaves and increased accumulation in leaf sheath was reported as protective salt tolerance mechanism in rice [266]. On the contrary, and H_2O_2 mediated increased K^+ accumulation in the YL and OL contributes its part in salinity stress amelioration. A relative low accretion of Na^+ in the developing sink tissue in early reproductive expansion phase of panicle may salvage the grain weight loss and panicle sterility [267].

Although, reduced superoxide production and activation of antioxidant system (Fig. 3.3.3) under NT and NH treatment suggested better management of ROS, an increased $O_2^{-\bullet}$ load under H_2O_2 treatment may be correlated with that of pro-oxidant behaviour of H_2O_2leading to mild oxidative stress (Fig. 3.3.3 A). Further, a significant improvement of the plant performance under TU [131] treatment even under control condition can be attributed to improved photosynthetic efficiency and synchronized regulation of source sink relationship. On the other hand, H_2O_2 can activate signalling pathways to stimulate cell proliferation and differentiation [268] along with activation of antioxidant machinery which may delimit the photo oxidation. The present study showed that most of the yield associated parameters like

harvest index, seed yield per plant, 1000 seed weight and panicle length were negatively affected via salt stress (Fig. 3.3.2; Table 3.3.1).

The reduction in the yield associated parameters was correlated well with that of limited CO_2 fixation and redistribution towards sink tissues. The decreased stomatal conductance with metabolic limitation of CO_2 fixation limits the photosynthetic efficiency of the plants under salt stress, whereas size and number of available sinks limits yield potential. Decrease in chlorophyll content under salinity may be considered as a typical oxidative stress symptom owing to delayed synthesis and enhanced breakdown of chlorophyll [269] and reported in many studies. In the present study both chlorophyll content and photosynthetic rate were found to be significantly improved under TU and H_2O_2 treatments relative to NaCl alone, suggesting limitation of photo-oxidation and photo-inhibition of the photosystem. The TU mediated direct scavenging of ROS was also reported earlier [131], which helps in reducing the ROS load, as evidenced in the histochemical staining of the leaf segments for superoxide radical. On the contrary H_2O_2 treatment found to increase the ROS load and there acts as pro-oxidant by activation of downstream antioxidant machinery. Glutathione reductase is one of import enzymes of the antioxidant machinery, which ultimately helps to maintain the redox buffers i.e., ascorbate and glutathione in their reduced form (Fig. 3.3.3 B, C). Although salinity mediated improved GR activity in rice was observed in the present study which was coincided with that of previous reports [218, 270]. Previous report also proclaimed an increased GR activity governs the sensitivity of the two contrasting pea's genotypes [271]. An improved activity of GR under H_2O_2 treatment even under NaCl deficient conditions, revealed the invigoration of antioxidant machinery for ensuing salt stress. The finding of this study corroborated well with previous finding where H_2O_2 mediated regulation over GR expression was reported in rice root [272].

Most of the parameters defining PS-II efficiency (F_v/F_m, photosynthesis rate, ETR, WUE and quantum yield of PSII) were uniformly reformed under NH and NT treatments relative to plants subjected to NaCl treatment (Table. 3.3.3). The photosynthetic efficiency of the PS-II was evaluated and found that F_v/F_m, that is an evaluation of maximum PSII efficiency and indicator of irreversible damage to photocentre was not affected much under the salinity stress as compared to other parameters like ETR, NPQ, photosynthesis rate. The F_v/F_m ratio is quite stable towards mild stress and only affected under severe stress [273]. The activation of NPQ port of energy dissipation mediates its protective effect via protecting PSII from over reduction and ROS mediated irreversible damage. Dissipation of excess energy by NPQ was pinpointed as NH-specific strategy (Table 3.3.3) for the protection of photosystem from photoinhibition. This is supported by H_2O_2 regulation of xanthophylls cycle, harmonized with increased NPQ and depressed ROS level under salt stress. Further the impairment of the PSII efficiency under stress condition may be considered due to metabolic limitation of reductants (ATP, NADPH) utilization and inactivation of D1 protein [274] which eventually lead to decrease in ETR. Upto 50 % increase in the ETR under NH and NT treatments showed a limitation over salt induced metabolic inhibition (Table. 3.3.3). The result of the study was in line with the previous finding where increased leaf H_2O_2 content was reported to rescued the acceptor side of PSI from over reduction thereby suppressing the ROS generation in the chloroplast while maintain the ETR and NPQ at high rate [275]. The maintenance of PSII efficiency under TU treatment may be attributed to decreased ROS load in the chloroplast, owing to its ROS scavenging capacity and enhanced protein synthesis [131] Additionally, thiourea mediated improved energy [276] and hormonal homeostasis co-ordinated with redox dependent transcriptional regulation over target genes in *Brassica* under salt stress was also reported [277].

Since both the treatments (NT and NH) showed an improved photosynthetic efficiency and yield parameters, suggesting a co-ordinated regulation of the source sink relationship. The source sink relationship has two components; synthesis of the sucrose in the leaf tissue (source capacity) and capacity of newly developed seeds tissue to assimilate/utilize the sucrose (sink strength). About 27.65 % decrease in the sucrose and 48.48% decrease in starch content in YL and DI respectively under salt stress reflects the negative effect of the salinity over source capacity and sink strength. Besides, the underutilized sucrose facilitated the formation of transient starch in the young leaf under salt stress. The improved leaf sucrose and seed starch content at the expanse of less transient starch formation in YL, reflects the status of source and sink strength under NH and NT treatments. Both the treatments were found to sustain the increased net photosynthetic rate coupled with enhanced SPS and FBPase activity. The co-ordinated action of SPS and FBPase together channelized the assimilated carbon flux for sucrose synthesis in cytosol. Previous reports with SPS null mutant [133] and cytosolic FBPase over-expression [278] revealed their importance in the sucrose biosynthesis in *Arabidopsis*. Further, SPS overexpression in sugarcane transgenic lines was reported to increase sucrose synthesis and accumulation with improved plant height and cane number compared to non-transgenic control. Our results were in agreement with previous reports where H_2O_2 [279] and TU [131] treatments were found to increase the sucrose synthesis by increased SPS and FBPase activity. In addition, de-regulation between co-ordinated activity of FBPase and SPS activities, suggested the impairment of sucrose synthesis in OL under NT thereby facilitating the onset of senescence. On the other hand, coordinated activity of SPS and FBPase along with increased AI and NI activities under NH treatment relieved the feedback inhibition and hence support the active sucrose biosynthesis in both YL and OL organs.

Additionally, the foliar application of H_2O_2 has been shown to improve the sugar dynamics with high sucrose content and less starch content in the old leaf as compared to NaCl treatment, The activity of the SPS and FBPase were also found to be increased significantly suggesting an active participation of the old leaf as photo synthetically active tissue. the positive effect of H_2O_2 foliar spray under salinity may be correlated with that of increase in mRNA transcripts of genes involved in oligosaccharide synthesis; d-myo-inositol 3-phosphate synthase 2 and galactinol synthase genes in soybean plants [280]. The increase in the oligosaccharides under H_2O_2 treatment further maintain the RWC content of the leaf and improve the photosynthetic efficiency. Further the increase in the activities of invertases (NI and AI) suppresses the feedback inhibition of the sucrose by breaking it into glucose and fructose or vacuolar sequestration particularly in the OL under NH treatment. H_2O_2 mediated increase in the invertase activity was also reported by [279] in melon fruits. Although no individual level of hexose sugars was analysed in the current study, the hexose sugar mediated signalling was also reported downstream to cytosolic NI to regulate to mitochondrial ROS homeostasis [143].

Sucrose import and its utilisation in the developing grains is an indispensable step regulating crop yield under control as well as stress conditions. The improved sink strength under NH and NT treatments were coordinated with that of enhanced activities of SuSy and AI. In both NH- and NT- treated sink organs, a preferential activation of SuSy and AI over NI was observed for breaking down the sucrose into simpler units for the synthesis of structural and non-structural carbohydrate. The elevated starch content in the developing sink will not only empower the sink strength but also, improves the comprehensive fitness of the plant. On the other hand, the increased NI activity in OL organ, can provide hexoses, thereby limiting the ROS level and maintain the energy supply in plants

under stress conditions. Our result corroborated with other studies where overexpression of SuSy or depression in AI in transgenic lines of rice have been shown to have a positive or negative effect over grain weight, respectively. The importance of the AI was also evident for the expansion of cotton fibre and *Arabidopsis* root elongation [139]. Recently OS Vin2-1 mutant was reported to have reduced seed size and grain weight as a consequence of impaired sink strength [140]. The enhancement of the Susy and AI activity in the sink tissue will be associated with effective utilization of the sucrose in the sink tissue, suggested by increased starch and less sucrose content in the grain.

Although, no significant change in the absolute sucrose and starch concentration was observed under TU and H_2O_2 treatments (Table 3.3.4), the higher activities of SPS and FBPase in YL along with improved SuSy activity in DI organs acts as stimulus for co-ordinating upregulation of source sink metabolic homeostasis in TU and H_2O_2 treated plants. The principal component analysis also identified GR and SuSy as major determinant of the source- and sink- strength respectively for NT- and NH –mediated protective effects (Fig. 3.3.5). Glutathione reductase is an important enzyme for maintaining reducing redox conditions by regeneration of GSH and AsA in plants. The overlapping response under TU and H_2O_2 treatments for most of the parameters related to growth and yield under both control and NaCl stress conditions notably improves their adaptability to be administered under the realistic field scenario. Collectively, the use of TU and H_2O_2 as PBR can be seen as a powerful approach sustaining the crop productivity by enhancing the source sink strength in plants under NaCl stress conditions without involving any genetic manipulations.

Thus, the foliar supplementation studies highlighted the agronomic feasibility of using TU and H_2O_2 based technology for improving plant growth and yield under the salt-affected field. Besides, it also described the nodal points of source-sink relationship which can be modulated through redox-dependent manner.

Chapter 4
Conclusions and Future Perspectives

4.1. Conclusions

Soil salinity, being one of the major abiotic constraints, limits plant growth and productivity. Plant bioregulators (PBRs) have remarkable properties for strengthening the plant defense, significantly under stress conditions. The present study was focused towards comparative analysis of ameliorative potential of two PBRs of contrasting chemistry: thiourea (TU; a non-biological ROS scavenger) and hydrogen peroxide (H_2O_2; an important stable biological ROS) for their competence to alleviate NaCl stress in rice.

Based on these studies, the following important conclusions were drawn and summarised in the form graphical representation (Fig. 4.1 A and B).

- Thiourea and H_2O_2, in spite of having the opposite mode of regulation on ROS levels, maintained the reducing redox status in rice plants.
- Thiourea and H_2O_2 treatments resulted in better growth phenotype of rice plants due to improved K^+ retention, PS-II efficiency and increased enzymatic antioxidants.
- Thiourea and H_2O_2 treatments activated the expression levels of key salt-stress related genes and the levels of photosynthesis related proteins.
- GC-MS based metabolomics data indicated activation of the salicylic acid signalling, GABA-shunt pathways, shikimic acid and Mal-Asp shuttle pathways under treatment conditions.
- The increased and decreased accumulation of sucrose and starch in source tissue (young leaf) and, vice versa in sink tissue (developing inflorescence), clearly showed a synchronized pattern between source-sink relationship in the treated rice plants under salt stress.

- Foliar supplementation on field-grown rice plants resulted in enhanced growth, yield and better source-sink relationship.

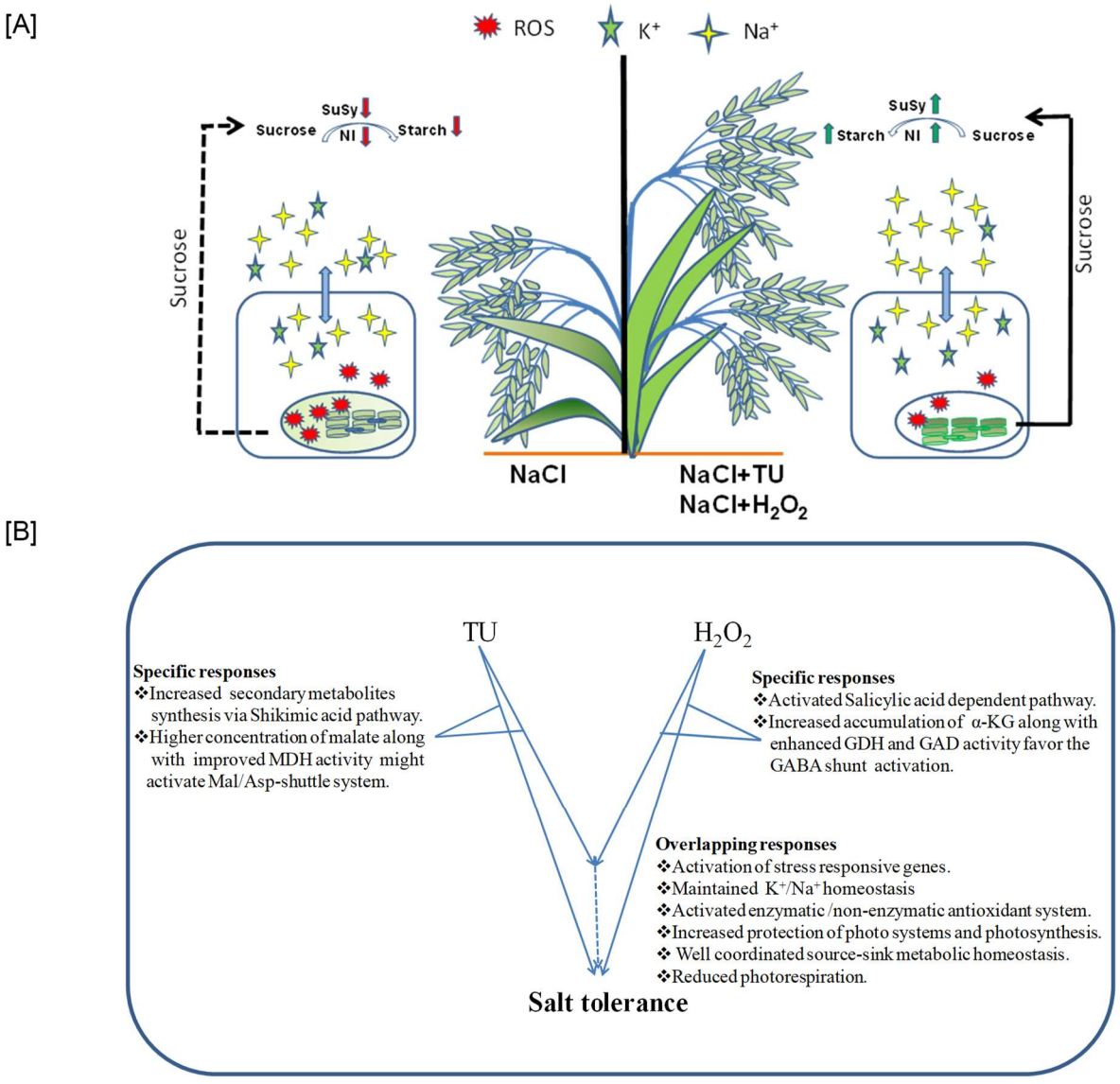

Fig. 4.1: Proposed mechanisms for TU and H_2O_2 mediated salt tolerance in rice

4.2. Future perspectives

Food security, in the event of climatic change and associated environmental stresses in conjunction with increasing human population, is a challenge which has to be managed by genetic and non-genetic approaches. Habituated to their sessile nature and vulnerability to stress environment, plants have to develop appropriate adaptive responses which are indispensable for sustaining plant growth and survival. An integrated knowledge of the action of PBRs gained from laboratories, greenhouse facilities, and realistic field conditions, is required to formulate efficient approaches for boosting plant defense mechanism towards stress tolerance.

- PBRs act as a "central" regulator in mitigating salinity induced damage in crop plants. More field-based studies will have to be undertaken to extend/validate the PBRs strategy for enhancing the rice productivity under field stress scenario.
- Modulated redox status of cells and proteins is critical in regulating plant functions under salt stress conditions, and henceforth the identification & characterization of the redox proteins will be of significant interest to understand salt stress induced responses.
- Future studies are essential to apply the knowledge into an agronomic-groundwork whereby the complex regulatory and functional modulations in the cellular proteome can be used to enrich our knowledge of stress responses for better survival and improved yield under salt stress.

References

1. Zörb C, Geilfus CM, Dietz KJ. Salinity and crop yield. Plant Biol. 2019 Jan;21:31-8.
2. Wani SH, Kumar V, Shriram V, Sah SK. Phytohormones and their metabolic engineering for abiotic stress tolerance in crop plants. Crop J. 2016 Jun 1;4(3):162-76.
3. KC KB, Fraser ED. Strategies to boost global food production: Modelling socioeconomic policy scenarios. Cogent Food Agric. 2017 Jan 1;3(1):1309739.
4. Isayenkov SV, Maathuis FJ. Plant salinity stress: many unanswered questions remain. Front Plant Sci. 2019 Feb 15;10:80.
5. Kamran M, Parveen A, Ahmar S, Malik Z, Hussain S, Chattha MS, Saleem MH, Adil M, Heidari P, Chen JT. An overview of hazardous impacts of soil salinity in crops, tolerance mechanisms, and amelioration through selenium supplementation. Int J Mol Sci. 2020 Jan;21(1):148.
6. Shokat S, Großkinsky DK. Tackling salinity in sustainable agriculture-What developing countries may learn from approaches of the developed world. Sustainability. 2019 Jan;11(17):4558.
7. Kotula L, Garcia Caparros P, Zörb C, Colmer TD, Flowers TJ. Improving crop salt tolerance using transgenic approaches: An update and physiological analysis. Plant Cell Environ. 2020 Dec;43(12):2932-56.
8. Srivastava AK, Pasala R, Minhas PS, Suprasanna P. Plant bioregulators for sustainable agriculture: integrating redox signaling as a possible unifying mechanism. Adv Agron. 2016 Jan 1;137:237-78.
9. Kumar P, Sharma PK. Soil Salinity and Food Security in India. Front Sustain Food Syst. 2020 Oct 6; 4: 533781.
10. Munns R, Tester M. Mechanisms of salinity tolerance. Annu Rev Plant Biol. 2008 Jun 2;59:651-81.

11. Masoud AA, Koike K, Atwia MG, El-Horiny MM, Gemail KS. Mapping soil salinity using spectral mixture analysis of landsat 8 OLI images to identify factors influencing salinization in an arid region. Int J Appl Earth Obs Geoinf. 2019 Nov 1;83:101944.
12. Ivushkin K, Bartholomeus H, Bregt AK, Pulatov A, Kempen B, De Sousa L. Global mapping of soil salinity change. Remote Sens Environ. 2019 Sep 15;231:111260.
13. Zaman M, Shahid SA, Heng L. Guideline for salinity assessment, mitigation and adaptation using nuclear and related techniques. Springer Nature; 2018.
14. Mandal S, Raju R, Kumar A, Kumar P, Sharma PC. Current status of research, technology response and policy needs of salt-affected soils in India–A Review. J Indian Soc Coastal Agric Res. 2018;36(2):40-53.
15. Panta S, Flowers T, Lane P, Doyle R, Haros G, Shabala S. Halophyte agriculture: success stories. Environ Exp Bot. 2014 Nov 1;107:71-83.
16. Razzaq A, Ali A, Safdar LB, Zafar MM, Rui Y, Shakeel A, Shaukat A, Ashraf M, Gong W, Yuan Y. Salt stress induces physiochemical alterations in rice grain composition and quality. J Food Sci. 2020 Jan;85(1):14-20.
17. Hanin M, Ebel C, Ngom M, Laplaze L, Masmoudi K. New insights on plant salt tolerance mechanisms and their potential use for breeding. Front Plant Sci. 2016 Nov 29;7:1787.
18. Robin AH, Matthew C, Uddin MJ, Bayazid KN. Salinity-induced reduction in root surface area and changes in major root and shoot traits at the phytomer level in wheat. J Exp Bot. 2016 Jun 1;67(12):3719-29.
19. Demidchik V, Maathuis FJ. Physiological roles of nonselective cation channels in plants: from salt stress to signalling and development. New Phytol. 2007 Aug;175(3):387-404.

20. Byrt CS, Zhao M, Kourghi M, Bose J, Henderson SW, Qiu J, Gilliham M, Schultz C, Schwarz M, Ramesh SA, Yool A. Non-selective cation channel activity of aquaporin AtPIP2; 1 regulated by Ca^{2+} and pH. Plant Cell Environ. 2017 Jun;40(6):802-15.
21. Adams E, Shin R. Transport, signaling, and homeostasis of potassium and sodium in plants. J Integr Plant Biol. 2014 Mar;56(3):231-49.
22. Gong HJ, Randall DP, Flowers TJ. Silicon deposition in the root reduces sodium uptake in rice (*Oryza sativa* L.) seedlings by reducing bypass flow. Plant Cell Environ. 2006 Oct;29(10):1970-79.
23. Oomen RJ, Benito B, Sentenac H, Rodríguez-Navarro A, Talón M, Véry AA, Domingo C. HKT2; 2/1, a K^+-permeable transporter identified in a salt-tolerant rice cultivar through surveys of natural genetic polymorphism. Plant J. 2012 Sep;71(5):750-62.
24. Gao LW, Yang SL, Wei SW, Huang DF, Zhang YD. Supportive role of the Na^+ transporter CmHKT1; 1 from *Cucumis melo* in transgenic *Arabidopsis* salt tolerance through improved K^+/Na^+ balance. Plant Mol Biol. 2020 Jul;103:561-80.
25. Khan I, Mohamed S, Regnault T, Mieulet D, Guiderdoni E, Sentenac H, Véry AA. Constitutive contribution by the rice OsHKT1;4 Na^+ transporter to xylem sap desalinization and low Na^+ accumulation in young leaves under low as high external Na^+conditions. Front Plant Sci. 2020 Jul 30;11:1130.
26. Long L, Zhao JR, Guo DD, Ma XN, Xu FC, Yang WW, Gao W. Identification of NHXs in *Gossypium* species and the positive role of GhNHX1 in salt tolerance. BMC Plant Biol. 2020 Dec;20:1-3.
27. Pehlivan N, Sun L, Jarrett P, Yang X, Mishra N, Chen L, Kadioglu A, Shen G, Zhang H. Co-overexpressing a plasma membrane and a vacuolar membrane sodium/proton antiporter significantly improves salt tolerance in transgenic *Arabidopsis* plants. Plant Cell Physiol. 2016 May 1;57(5):1069-84.

28. Zeng Y, Li Q, Wang H, Zhang J, Du J, Feng H, Blumwald E, Yu L, Xu G. Two NHX-type transporters from *Helianthus tuberosus* improve the tolerance of rice to salinity and nutrient deficiency stress. Plant Biotechnol J. 2018 Jan;16(1):310-21.
29. Niu M, Xie J, Chen C, Cao H, Sun J, Kong Q, Shabala S, Shabala L, Huang Y, Bie Z. An early ABA-induced stomatal closure, Na^+ sequestration in leaf vein and K^+ retention in mesophyll confer salt tissue tolerance in *Cucurbita* species. J Exp Bot. 2018 Sep 14;69(20):4945-60.
30. Penella C, Landi M, Guidi L, Nebauer SG, Pellegrini E, San Bautista A, Remorini D, Nali C, López-Galarza S, Calatayud A. Salt-tolerant rootstock increases yield of pepper under salinity through maintenance of photosynthetic performance and sinks strength. J Plant physiol. 2016 Apr 1;193:1-1.
31. Vrbka L, Vondrášek J, Jagoda-Cwiklik B, Vácha R, Jungwirth P. Quantification and rationalization of the higher affinity of sodium over potassium to protein surfaces. Proc Natl Acad Sci U S A. 2006 Oct 17;103(42):15440-4.
32. Assaha DV, Ueda A, Saneoka H, Al-Yahyai R, Yaish MW. The role of Na^+ and K^+ transporters in salt stress adaptation in glycophytes. Front Physiol. 2017 Jul 18;8:509.
33. Blaha G, Stelzl U, Spahn CM, Agrawal RK, Frank J, Nierhaus KH. Preparation of functional ribosomal complexes and effect of buffer conditions on tRNA positions observed by cryoelectron microscopy. Methods Enzymol. 2000:292–306.
34. Himabindu Y, Chakradhar T, Reddy MC, Kanygin A, Redding KE, Chandrasekhar T. Salt-tolerant genes from halophytes are potential key players of salt tolerance in glycophytes. Environ Exp Bot. 2016 Apr 1;124:39-63.
35. Lamers J, Van Der Meer T, Testerink C. How plants sense and respond to stressful environments. Plant Physiol. 2020 Apr 1;182(4):1624-35.

36. Tracy FE, Gilliham M, Dodd AN, Webb AA, Tester M. NaCl-induced changes in cytosolic free Ca^{2+} in *Arabidopsis thaliana* are heterogeneous and modified by external ionic composition. Plant Cell Environ. 2008 Aug;31(8):1063-73.
37. Qiu QS, Guo Y, Dietrich MA, Schumaker KS, Zhu JK. Regulation of SOS1, a plasma membrane Na^+/H^+ exchanger in *Arabidopsis thaliana*, by SOS2 and SOS3. Proc Natl Acad Sci U S A. 2002 Jun 11;99 (12):8436-41.
38. Wang WR, Liang JH, Wang GF, Sun MX, Peng FT, Xiao YS. Overexpression of PpSnRK1α in tomato enhanced salt tolerance by regulating ABA signaling pathway and reactive oxygen metabolism. BMC Plant Biol. 2020 Dec;20(1):1-5.
39. Suprasanna P, Ghuge SA, Patade VY, Mirajkar SJ, Nikalje GC. Genomic roadmaps for augmenting salinity stress tolerance in crop plants. In Salinity Responses and Tolerance in Plants, Volume 2 2018 (pp. 189-216). Springer, Cham.
40. Hossain MS, Dietz KJ. Tuning of redox regulatory mechanisms, reactive oxygen species and redox homeostasis under salinity stress. Front Plant Sci. 2016 May 10;7:548.
41. Foyer CH, Noctor G. Redox homeostasis and antioxidant signaling: a metabolic interface between stress perception and physiological responses. Plant Cell. 2005 Jul 1;17(7):1866-75.
42. Foyer CH. Reactive oxygen species, oxidative signaling and the regulation of photosynthesis. Environ Exp Bot. 2018 Oct 1;154:134-42.
43. Halliwell B. Reactive species and antioxidants. Redox biology is a fundamental theme of aerobic life. Plant Physiol. 2006 Jun 1;141(2):312-22.
44. Das K, Roychoudhury A. Reactive oxygen species (ROS) and response of antioxidants as ROS-scavengers during environmental stress in plants. Front Environ Sci. 2014 Dec 2;2:53.

45. Hasanuzzaman M, Bhuyan MH, Zulfiqar F, Raza A, Mohsin SM, Mahmud JA, Fujita M, Fotopoulos V. Reactive oxygen species and antioxidant defense in plants under abiotic stress: revisiting the crucial role of a universal defense regulator. Antioxidants. 2020 Aug;9(8):681.
46. Decros G, Baldet P, Beauvoit B, Stevens R, Flandin A, Colombié S, Gibon Y, Pétriacq P. Get the balance right: ROS homeostasis and redox signalling in fruit. Front Plant Sci. 2019 Sep 18;10:1091.
47. Mittler R. ROS are good. Trends Plant Sci. 2017 Jan 1;22(1):11-9.
48. Farmer EE, Mueller MJ. ROS-mediated lipid peroxidation and RES-activated signaling. Annu Rev Plant Biol. 2013 Apr 29;64:429-50.
49. Winger AM, Taylor NL, Heazlewood JL, Day DA, Millar AH. The cytotoxic lipid peroxidation product 4-hydroxy-2-nonenal covalently modifies a selective range of proteins linked to respiratory function in plant mitochondria. J Biol Chem. 2007 Dec 28;282(52):37436-47.
50. Yamauchi Y, Sugimoto Y. Effect of protein modification by malondialdehyde on the interaction between the oxygen-evolving complex 33 kDa protein and photosystem II core proteins. Planta. 2010 Apr;231(5):1077-88.
51. Mano JI, Nagata M, Okamura S, Shiraya T, Mitsui T. Identification of oxidatively modified proteins in salt-stressed *Arabidopsis*: a carbonyl-targeted proteomics approach. Plant Cell Physiol. 2014 Jul 1;55(7):1233-44.
52. Avery SV. Molecular targets of oxidative stress. Biochem J. 2011 Mar 1;434(2):201-10.
53. Biswas M, Terada R, Mano JI. Inactivation of carbonyl-detoxifying enzymes by H_2O_2 is a trigger to increase carbonyl load for initiating programmed cell death in plants. Antioxidants. 2020 Feb;9(2):141.

54. Lounifi I, Arc E, Molassiotis A, Job D, Rajjou L, Tanou G. Interplay between protein carbonylation and nitrosylation in plants. Proteomics. 2013 Feb;13(3-4):568-78.

55. Spampinato CP. Protecting DNA from errors and damage: an overview of DNA repair mechanisms in plants compared to mammals. Cell Mol Life Sci. 2017 May;74(9):1693-709.

56. Nisa MU, Huang Y, Benhamed M, Raynaud C. The plant DNA damage response: signaling pathways leading to growth inhibition and putative role in response to stress conditions. Front Plant Sci. 2019 May 17;10:653.

57. Gill SS, Anjum NA, Gill R, Yadav S, Hasanuzzaman M, Fujita M, Mishra P, Sabat SC, Tuteja N. Superoxide dismutase—mentor of abiotic stress tolerance in crop plants. Environ Sci Pollut Res Int. 2015 Jul;22(14):10375-94.

58. Leonowicz G, Trzebuniak KF, Zimak-Piekarczyk P, Ślesak I, Mysliwa-Kurdziel B. The activity of superoxide dismutases (SODs) at the early stages of wheat deetiolation. PLoS One. 2018 Mar 20;13(3):e0194678.

59. Wang FZ, Wang QB, Kwon SY, Kwak SS, Su WA. Enhanced drought tolerance of transgenic rice plants expressing a pea manganese superoxide dismutase. J Plant Physiol. 2005 Apr 22;162(4):465-72.

60. Guan Q, Liao X, He M, Li X, Wang Z, Ma H, Yu S, Liu S. Tolerance analysis of chloroplast OsCu/Zn-SOD overexpressing rice under NaCl and $NaHCO_3$ stress. PLoS One. 2017 Oct 11;12(10):e0186052.

61. Sen A, Puthur JT. Influence of different seed priming techniques on oxidative and antioxidative responses during the germination of *Oryza sativa* varieties. Physiol Mol Biol Plants. 2020 Feb 7:1-5.

62. Mehla N, Sindhi V, Josula D, Bisht P, Wani SH. An introduction to antioxidants and their roles in plant stress tolerance. In Reactive oxygen species and antioxidant Systems in Plants: role and regulation under abiotic stress 2017 (pp. 1-23). Springer, Singapore.
63. Sofo A, Scopa A, Nuzzaci M, Vitti A. Ascorbate peroxidase and catalase activities and their genetic regulation in plants subjected to drought and salinity stresses. Int J Mol Sci. 2015 Jun;16(6):13561-78.
64. Palma JM, Mateos RM, López-Jaramillo J, Rodríguez-Ruiz M, González-Gordo S, Lechuga-Sancho AM, Corpas FJ. Plant catalases as NO and H_2S targets. Redox Biol. 2020 May 25:101525.
65. Arias-Moreno DM, Jiménez-Bremont JF, Maruri-López I, Delgado-Sánchez P. Effects of catalase on chloroplast arrangement in *Opuntia streptacantha* chlorenchyma cells under salt stress. Sci Rep. 2017 Aug 17;7(1):1-4.
66. Moriwaki T, Yamamoto Y, Aida T, Funahashi T, Shishido T, Asada M, Prodhan SH, Komamine A, Motohashi T. Overexpression of the *Escherichia coli* catalase gene, katE, enhances tolerance to salinity stress in the transgenic indica rice cultivar, BR5. Plant Biotechnol Rep. 2008 Apr 1;2(1):41-6.
67. Zhou YB, Liu C, Tang DY, Yan L, Wang D, Yang YZ, Gui JS, Zhao XY, Li LG, Tang XD, Yu F. The receptor-like cytoplasmic kinase STRK1 phosphorylates and activates CatC, thereby regulating H_2O_2 homeostasis and improving salt tolerance in rice. Plant Cell. 2018 May 1;30(5):1100-18.
68. Liu JX, Feng K, Duan AQ, Li H, Yang QQ, Xu ZS, Xiong AS. Isolation, purification and characterization of an ascorbate peroxidase from celery and overexpression of the AgAPX1 gene enhanced ascorbate content and drought tolerance in *Arabidopsis*. BMC Plant Biol. 2019 Dec19: 488.

69. Kozuleva MA, Ivanov BN, Vetoshkina DV, Borisova-Mubarakshina MM. Minimizing an electron flow to molecular oxygen in photosynthetic electron transfer chain: An evolutionary view. Front Plant Sci. 2020 Mar 13;11:211.

70. Dvorak P, Krasylenko Y, Zeiner A, Samaj J, Takac T. Signaling toward ROS-scavenging enzymes in plants. Front Plant Sci. 2020;11:2178.

71. Teixeira FK, Menezes-Benavente L, Margis R, Margis-Pinheiro M. Analysis of the molecular evolutionary history of the ascorbate peroxidase gene family: inferences from the rice genome. J Mol Evol. 2004 Dec;59(6):761-70.

72. Sukweenadhi J, Kim YJ, Rahimi S, Silva J, Myagmarjav D, Kwon WS, Yang DC. Overexpression of a cytosolic ascorbate peroxidase from *Panax ginseng* enhanced salt tolerance in *Arabidopsis thaliana*. Plant Cell Tissue Organ Cult. 2017 May 1;129(2):337-50.

73. Sun WH, Duan M, Shu DF, Yang S, Meng QW. Over-expression of StAPX in tobacco improves seed germination and increases early seedling tolerance to salinity and osmotic stresses. Plant Cell Rep. 2010 Aug;29(8):917-26.

74. Trivedi DK, Gill SS, Yadav S, Tuteja N. Genome-wide analysis of glutathione reductase (GR) genes from rice and *Arabidopsis*. Plant Signal Behav. 2013 Feb 1;8(2):e23021.

75. Hasanuzzaman M, Nahar K, Anee TI, Fujita M. Glutathione in plants: biosynthesis and physiological role in environmental stress tolerance. Physiol Mol Biol Plants. 2017 Apr 1;23(2):249-68.

76. Achary VM, Reddy CS, Pandey P, Islam T, Kaul T, Reddy MK. Glutathione reductase a unique enzyme: molecular cloning, expression and biochemical characterization from the stress adapted C4 plant, *Pennisetum glaucum* (L.) R Br. Mol Biol Rep. 2015 May;42(5):947-62

77. Ding S, Lu Q, Zhang Y, Yang Z, Wen X, Zhang L, Lu C. Enhanced sensitivity to oxidative stress in transgenic tobacco plants with decreased glutathione reductase activity leads to a decrease in ascorbate pool and ascorbate redox state. Plant Mol Biol. 2009 Mar;69(5):577-92.
78. Borgohain P, Saha B, Agrahari R, Chowardhara B, Sahoo S, van der Vyver C, Panda SK. Sl NAC2 overexpression in *Arabidopsis* results in enhanced abiotic stress tolerance with alteration in glutathione metabolism. Protoplasma. 2019 Jul;256(4):1065-77.
79. Meyer Y, Belin C, Delorme-Hinoux V, Reichheld JP, Riondet C. Thioredoxin and glutaredoxin systems in plants: molecular mechanisms, crosstalks, and functional significance. Antioxid Redox Signal. 2012 Oct 15;17(8):1124-60.
80. Jedelská T, Luhová L, Petřivalský M. Thioredoxins: Emerging Players in the Regulation of Protein S-Nitrosation in Plants. Plants. 2020 Nov;9(11):1426.
81. Liebthal M, Maynard D, Dietz KJ. Peroxiredoxins and redox signaling in plants. Antioxid Redox Signal. 2018 Mar 1;28(7):609-24.
82. Dietz KJ. Peroxiredoxins in plants and cyanobacteria. Antioxid Redox Signal. 2011 Aug 15;15(4):1129-59.
83. Lindermayr, C.; Saalbach, G.; Durner, J. Proteomic Identification of S-Nitrosylated Proteins in *Arabidopsis*. Plant Physiol. 2005, 137, 921–930.
84. Zhang HH, Xu N, Teng ZY, Wang JR, Ma S, Wu X, Li X, Sun GY. 2-Cys Prx plays a critical role in scavenging H_2O_2 and protecting photosynthetic function in leaves of tobacco seedlings under drought stress. J Plant Interact. 2019 Jan 1;14(1):119-28.
85. Cha JY, Barman DN, Kim MG, Kim WY. Stress defense mechanisms of NADPH-dependent thioredoxin reductases (NTRs) in plants. Plant Signal Behav. 2015;10(5):e1017698.

86. Hasanuzzaman M, Bhuyan MH, Anee TI, Parvin K, Nahar K, Mahmud JA, Fujita M. Regulation of ascorbate-glutathione pathway in mitigating oxidative damage in plants under abiotic stress. Antioxidants. 2019 Sep;8(9):384.

87. Pignocchi C, Kiddle G, Hernández I, Foster SJ, Asensi A, Taybi T, Barnes J, Foyer CH. Ascorbate oxidase-dependent changes in the redox state of the apoplast modulate gene transcript accumulation leading to modified hormone signaling and orchestration of defense processes in tobacco. Plant Physiol. 2006 Jun 1;141(2):423-35.

88. Uarrota VG, Stefen DL, Leolato LS, Gindri DM, Nerling D. Revisiting carotenoids and their role in plant stress responses: From biosynthesis to plant signaling mechanisms during stress. In Antioxidants and antioxidant enzymes in higher plants 2018 (pp. 207-232). Springer, Cham.

89. Carocho M, Ferreira IC. A review on antioxidants, prooxidants and related controversy: natural and synthetic compounds, screening and analysis methodologies and future perspectives. Food Chem Toxicol. 2013 Jan 1;51:15-25.

90. Chen S, Wu F, Li Y, Qian Y, Pan X, Li F, Wang Y, Wu Z, Fu C, Lin H, Yang A. NtMYB4 and NtCHS1 are critical factors in the regulation of flavonoid biosynthesis and are involved in salinity responsiveness. Front Plant Sci. 2019 Feb 21;10:178.

91. Minh LT, Khang DT, Ha PT, Tuyen PT, Minh TN, Quan NV, Xuan TD. Effects of salinity stress on growth and phenolics of rice (*Oryza sativa* L.). Int Lett Nat Sci. 2016;57.

92. Ashraf MH, Harris PJ. Photosynthesis under stressful environments: an overview. Photosynthetica. 2013 Jun 1;51(2):163-90.

93. Laloi C, Havaux M. Key players of singlet oxygen-induced cell death in plants. Front Plant Sci. 2015 Feb 4;6:39.

94. Serrato AJ, de Dios Barajas-López J, Chueca A, Sahrawy M. Changing sugar partitioning in FBPase-manipulated plants. J Exp Bot. 2009 Jul 1;60(10):2923-31.

95. Kosová K, Vítámvás P, Urban MO, Prášil IT, Renaut J. Plant abiotic stress proteomics: the major factors determining alterations in cellular proteome. Front Plant Sci. 2018 Feb 8;9:122.

96. Sasi S, Venkatesh J, Daneshi RF, Gururani MA. Photosystem II extrinsic proteins and their putative role in abiotic stress tolerance in higher plants. Plants. 2018 Dec;7(4):100.

97. Huang S, Van Aken O, Schwarzländer M, Belt K, Millar AH. The roles of mitochondrial reactive oxygen species in cellular signaling and stress response in plants. Plant Physiol. 2016 Jul 1;171(3):1551-9.

98. Rhoads DM, Umbach AL, Subbaiah CC, Siedow JN. Mitochondrial reactive oxygen species. Contribution to oxidative stress and interorganellar signaling. Plant Physiol. 2006 Jun 1;141(2):357-66.

99. Sweetlove LJ, Foyer CH. Roles for reactive oxygen species and antioxidants in plant mitochondria. In Plant mitochondria: from genome to function 2004 (pp. 307-320). Springer, Dordrecht.

100. Che-Othman MH, Millar AH, Taylor NL. Connecting salt stress signalling pathways with salinity-induced changes in mitochondrial metabolic processes in C3 plants. Plant Cell Environ. 2017 Dec;40(12):2875-905.

101. Vanlerberghe GC. Alternative oxidase: a mitochondrial respiratory pathway to maintain metabolic and signaling homeostasis during abiotic and biotic stress in plants. Int J Mol Sci. 2013 Apr;14(4):6805-47.

102. Analin B, Mohanan A, Bakka K, Challabathula D. Cytochrome oxidase and alternative oxidase pathways of mitochondrial electron transport chain are important for the

photosynthetic performance of pea plants under salinity stress conditions. Plant Physiol Biochem. 2020 Sep 1;154:248-59.

103. Smith CA, Melino VJ, Sweetman C, Soole KL. Manipulation of alternative oxidase can influence salt tolerance in *Arabidopsis thaliana*. Physiol Plant. 2009 Dec;137(4):459-72.

104. Zhang X, Takano T, Liu S. Identification of a mitochondrial ATP synthase small subunit gene (RMtATP6) expressed in response to salts and osmotic stresses in rice (*Oryza sativa* L.). J Exp Bot. 2006 Jan 1;57(1):193-200.

105. Martí MC, Jiménez A, Sevilla F. Thioredoxin network in plant mitochondria: cysteine S-posttranslational modifications and stress conditions. Front Plant Sci. 2020 Sep 23;11:1476.

106. Kosová K, Vítámvás P, Urban MO, Prášil IT, Renaut J. Plant abiotic stress proteomics: the major factors determining alterations in cellular proteome. Front plant Sci. 2018 Feb 8;9:122.

107. Busch FA. Photorespiration in the context of Rubisco biochemistry, CO_2 diffusion and metabolism. Plant J. 2020 Feb;101(4):919-39.

108. Sandalio LM, Romero-Puertas MC. Peroxisomes sense and respond to environmental cues by regulating ROS and RNS signalling networks. Ann Bot. 2015 Sep 1;116(4):475-85.

109. Su T, Li W, Wang P, Ma C. Dynamics of peroxisome homeostasis and its role in stress response and signaling in plants. Front Plant Sci. 2019 Jun 4;10:705.

110. Zhang H, Han B, Wang T, Chen S, Li H, Zhang Y, Dai S. Mechanisms of plant salt response: insights from proteomics. J Proteome Res. 2012 Jan 1;11(1):49-67.

111. Wu D, Cai S, Chen M, Ye L, Chen Z, Zhang H, Dai F, Wu F, Zhang G. Tissue metabolic responses to salt stress in wild and cultivated barley. PLoS one. 2013 Jan 31;8(1):e55431.

112. Sanchez DH, Siahpoosh MR, Roessner U, Udvardi M, Kopka J. Plant metabolomics reveals conserved and divergent metabolic responses to salinity. Physiol Plant. 2008 Feb;132(2):209-19.

113. Saddhe AA, Manuka R, Penna S. Plant sugars: homeostasis and transport under abiotic stress in plants. Physiol Plant. 2020 Nov:1-17.

114. Che-Othman MH, Jacoby RP, Millar AH, Taylor NL. Wheat mitochondrial respiration shifts from the tricarboxylic acid cycle to the GABA shunt under salt stress. New Phytol. 2020 Feb;225(3):1166-80.

115. Jacoby RP, Taylor NL, Millar AH. The role of mitochondrial respiration in salinity tolerance. Trends Plant Sci. 2011 Nov 1;16(11):614-23.

116. Patterson JH, Newbigin ED, Tester M, Bacic A, Roessner U. Metabolic responses to salt stress of barley (*Hordeum vulgare* L.) cultivars, Sahara and Clipper, which differ in salinity tolerance. J Exp Bot. 2009 Oct 1;60(14):4089-103.

117. Hossain MS, Persicke M, ElSayed AI, Kalinowski J, Dietz KJ. Metabolite profiling at the cellular and subcellular level reveals metabolites associated with salinity tolerance in sugar beet. J Exp Bot. 2017 Dec 16;68(21-22):5961-76.

118. Zuther E, Koehl K, Kopka J. Comparative metabolome analysis of the salt response in breeding cultivars of rice. In Advances in molecular breeding toward drought and salt tolerant crops 2007 (pp. 285-315). Springer, Dordrecht.

119. Bandehagh A, Taylor NL. Can alternative metabolic pathways and shunts overcome salinity induced inhibition of central carbon metabolism in crops? Front Plant Sci. 2020;11.

120. Michaeli S, Fromm H. Closing the loop on the GABA shunt in plants: are GABA metabolism and signaling entwined? Front Plant Sci. 2015 Jun 9;6:419.

121. Zhao Y, Yu H, Zhou JM, Smith SM, Li J. Malate circulation: linking chloroplast metabolism to mitochondrial ROS. Trends Plant Sci. 2020 May 1;25(5):446-54.

122. Chang TG, Zhu XG. Source–sink interaction: a century old concept under the light of modern molecular systems biology. J Exp Bot. 2017 Jul 20;68(16):4417-31.

123. Rossi M, Bermudez L, Carrari F. Crop yield: challenges from a metabolic perspective. Curr Opin Plant Biol. 2015 Jun 1;25:79-89.

124. Munns R, Gilliham M. Salinity tolerance of crops–what is the cost? New Phytol. 2015 Nov;208(3):668-73.

125. Zhang Y, Kaiser E, Zhang Y, Yang Q, Li T. Short-term salt stress strongly affects dynamic photosynthesis, but not steady-state photosynthesis, in tomato (*Solanum lycopersicum*). Environ Exp Bot. 2018 May 1;149:109-19.

126. Moradi F, Ismail AM. Responses of photosynthesis, chlorophyll fluorescence and ROS-scavenging systems to salt stress during seedling and reproductive stages in rice. Ann Bot. 2007 Jun 1;99(6):1161-73.

127. Dall'Osto L, Cazzaniga S, North H, Marion-Poll A, Bassi R. The *Arabidopsis* aba4-1 mutant reveals a specific function for neoxanthin in protection against photooxidative stress. Plant Cell. 2007 Mar; 19(3):1048-64.

128. Hubbart S, Smillie IR, Heatley M, Swarup R, Foo CC, Zhao L, Murchie EH. Enhanced thylakoid photoprotection can increase yield and canopy radiation use efficiency in rice. Commun Biol. 2018 Mar 22;1(1):1-2.

129. Albacete AA, Martínez-Andújar C, Pérez-Alfocea F. Hormonal and metabolic regulation of source–sink relations under salinity and drought: from plant survival to crop yield stability. Biotechnol Adv. 2014 Jan 1;32(1):12-30.

130. Gangola MP, Ramadoss BR. Sugars play a critical role in abiotic stress tolerance in plants. In Biochemical, physiological and molecular avenues for combating abiotic stress tolerance in plants 2018 Jan 1 (pp. 17-38). Academic Press.

131. Pandey M, Srivastava AK, D'Souza SF, Penna S. Thiourea, a ROS scavenger, regulates source-to-sink relationship to enhance crop yield and oil content in *Brassica juncea* (L.). PLoS One. 2013 Sep 18;8(9):e73921.

132. Fabre D, Yin X, Dingkuhn M, Clément-Vidal A, Roques S, Rouan L, Soutiras A, Luquet D. Is triose phosphate utilization involved in the feedback inhibition of photosynthesis in rice under conditions of sink limitation? J Exp Bot. 2019 Oct 15;70(20):5773-85.

133. Sun J, Zhang J, Larue CT, Huber SC. Decrease in leaf sucrose synthesis leads to increased leaf starch turnover and decreased RuBP regeneration-limited photosynthesis but not Rubisco-limited photosynthesis in *Arabidopsis*null mutants of SPSA1. Plant Cell Environ. 2011 Apr;34(4):592-604.

134. Anur RM, Mufithah N, Sawitri WD, Sakakibara H, Sugiharto B. Overexpression of sucrose phosphate synthase enhanced sucrose content and biomass production in transgenic sugarcane. Plants. 2020 Feb;9(2):200.

135. Cho MH, Jang A, Bhoo SH, Jeon JS, Hahn TR. Manipulation of triose phosphate/phosphate translocator and cytosolic fructose-1, 6-bisphosphatase, the key components in photosynthetic sucrose synthesis, enhances the source capacity of transgenic *Arabidopsis* plants. Photosynth Res. 2012 Mar;111(3):261-8.

136. Mitchell MC, Pritchard J, Okada S, Zhang J, Venables I, Vanhercke T, Ral JP. Increasing growth and yield by altering carbon metabolism in a transgenic leaf oil crop. Plant Biotechnol J. 2020 Oct;18(10):2042-52.

137. Nielsen TH, Rung JH, Villadsen D. Fructose-2, 6-bisphosphate: a traffic signal in plant metabolism. Trends Plant Sci. 2004 Nov 1;9(11):556-63.

138. Peng J, Zhang L, Liu J, Luo J, Zhao X, Dong H, Ma Y, Sui N, Zhou Z, Meng Y. Effects of soil salinity on sucrose metabolism in cotton fiber. PloS one. 2016 May 26;11(5):e0156398.

139. Wang L, Li XR, Lian H, Ni DA, He YK, Chen XY, Ruan YL. Evidence that high activity of vacuolar invertase is required for cotton fiber and *Arabidopsis* root elongation through osmotic dependent and independent pathways, respectively. Plant Physiol. 2010 Oct 1;154(2):744-56.

140. Lee DW, Lee SK, Rahman MM, Kim YJ, Zhang D, Jeon JS. The role of rice vacuolar invertase2 in seed size control. Mol Cells. 2019 Oct;42(10):711.

141. Chourey PS, Taliercio EW, Carlson SJ, Ruan YL. Genetic evidence that the two isozymes of sucrose synthase present in developing maize endosperm are critical, one for cell wall integrity and the other for starch biosynthesis. Mol Genet Genomics. 1998 Jul 1;259(1):88-96.

142. Xu SM, Brill E, Llewellyn DJ, Furbank RT, Ruan YL. Overexpression of a potato sucrose synthase gene in cotton accelerates leaf expansion, reduces seed abortion, and enhances fiber production. Mol Plant. 2012 Mar 1;5(2):430-41.

143. Xiang L, Li Y, Rolland F, Van den Ende W. Neutral invertase, hexokinase and mitochondrial ROS homeostasis: emerging links between sugar metabolism, sugar signaling and ascorbate synthesis. Plant Signal Behav. 2011 Oct 1;6(10):1567-73.

144. Michelet L, Zaffagnini M, Morisse S, Sparla F, Pérez-Pérez ME, Francia F, Danon A, Marchand C, Fermani S, Trost P, Lemaire SD. Redox regulation of the Calvin–Benson cycle: something old, something new. Front Plant Sci. 2013 Nov 25;4:470.

145. Benitez-Alfonso Y, Jackson D. Redox homeostasis regulates plasmodesmal communication in *Arabidopsis* meristems. Plant Signal Behav. 2009 Jul 1;4(7):655-9.

146. Krügel U, Veenhoff LM, Langbein J, Wiederhold E, Liesche J, Friedrich T, Grimm B, Martinoia E, Poolman B, Kühn C. Transport and sorting of the *Solanum tuberosum* sucrose transporter SUT1 is affected by posttranslational modification. Plant Cell. 2008 Sep 1;20(9):2497-513.

147. Hou LY, Ehrlich M, Thormählen I, Lehmann M, Krahnert I, Obata T, Cejudo FJ, Fernie AR, Geigenberger P. NTRC Plays a Crucial Role in Starch Metabolism, Redox Balance, and Tomato Fruit Growth. Plant Physiol. 2019 Nov 1;181(3):976-92.

148. Voss-Fels KP, Stahl A, Hickey LT. Q&A: Modern crop breeding for future food security. BMC Biol. 2019 Dec;17(1):1-7.

149. Singh RK, Redoña E, Refuerzo L. Varietal improvement for abiotic stress tolerance in crop plants: special reference to salinity in rice. In Abiotic stress adaptation in plants 2009 (pp. 387-415). Springer, Dordrecht.

150. Ammar MH, Pandit A, Singh RK, Sameena S, Chauhan MS, Singh AK, Sharma PC, Gaikwad K, Sharma TR, Mohapatra T, Singh NK. Mapping of QTLs controlling Na^+, K^+ and Cl^- ion concentrations in salt tolerant indica rice variety CSR27. J Plant Biochem Biotechnol. 2009 Jul;18(2):139-50.

151. Turan S, Cornish K, Kumar S. Salinity tolerance in plants: breeding and genetic engineering. Aust J Crop Sci. 2012 Sep;6(9):1337.

152. Tonosaki K, Osabe K, Kawanabe T, Fujimoto R. The importance of reproductive barriers and the effect of allopolyploidization on crop breeding. Breed Sci. 2016:15114

153. Suprasanna P, Mirajkar SJ, Bhagwat SG. Induced mutations and crop improvement. In Plant biology and biotechnology 2015 (pp. 593-617). Springer, New Delhi.

154. Wani SH, Dutta T, Neelapu NR, Surekha C. Transgenic approaches to enhance salt and drought tolerance in plants. Plant Gene. 2017 Sep 1;11:219-31.

155. Yoon Y, Seo DH, Shin H, Kim HJ, Kim CM, Jang G. The Role of stress-responsive transcription factors in modulating abiotic stress tolerance in plants. Agronomy. 2020 Jun;10(6):788.

156. Bolognesi B, Lehner B. Protein overexpression: reaching the limit. Elife. 2018 Aug 10;7:e39804

157. Cobo JM, Fort J, Isern N. The spread of domesticated rice in eastern and southeastern Asia was mainly demic. J Archaeol Sci. 2019 Jan 1;101:123-30.

158. Fukagawa NK, Ziska LH. Rice: Importance for Global Nutrition. J NutrSciVitaminol (Tokyo). 2019;65(Supplement):S2-S3.

159. Food and Agriculture Organization of the United Nations (FAO). "India at a glance." (2019).

160. Radanielson AM, Gaydon DS, Li T, Angeles O, Roth CH. Modeling salinity effect on rice growth and grain yield with ORYZA v3 and APSIM-Oryza. Eur J Agron. 2018 Oct 1;100:44-55.

161. Asch F, Wopereis MC. Responses of field-grown irrigated rice cultivars to varying levels of floodwater salinity in a semi-arid environment. Field Crops Res. 2001 Apr 20;70(2):127-37.

162. Tukey HB, Carlson RF. Breaking the dormancy of peach seed by treatment with thiourea. Plant Physiol. 1945 Oct;20(4):505.

163. Kaya C, Ashraf M, Sönmez O. Promotive effect of exogenously applied thiourea on key physiological parametersand oxidative defense mechanism in salt-stressed *Zea mays* L. plants. Turk J Botany. 2015 Sep 18;39(5):786-95.

164. Hassanein RA, Amin AA, Rashad ES, Ali H. Effect of thiourea and salicylic acid on antioxidant defense of wheat plants under drought stress. Int J Chem Tech Res. 2015;7(01):346-54.

165. Wakchaure GC, Minhas PS, Ratnakumar P, Choudhary RL. Optimising supplemental irrigation for wheat (*Triticumaestivum* L.) and the impact of plant bio-regulators in a semi-arid region of Deccan Plateau in India. Agric Water Manag. 2016 Jul 1;172:9-17.

166. Seleiman MF, Kheir AM. Saline soil properties, quality and productivity of wheat grown with bagasse ash and thiourea in different climatic zones. Chemosphere. 2018 Feb 1;193:538-46.

167. Kaya C, Sarioglu A, Akram NA, Ashraf M. Thiourea-mediated nitric oxide production enhances tolerance to boron toxicity by reducing oxidative stress in bread wheat (*Triticumaestivum* L.) and durum wheat (*Triticum durum* Desf.) plants. J Plant Growth Regul. 2019;38(3):1094-1109.

168. Upadhyay MK, Majumdar A, Barla A, Bose S, Srivastava S. Thiourea supplementation mediated reduction of grain arsenic in rice (*Oryza sativa* L.) cultivars: A two year field study. J Hazard Mater. 2021 Apr 5;407:124368.

169. Srivastava AK, Pandey M, Ghate T, Kumar V, Upadhyay MK, Majumdar A, Sanjukta AK, Agrawal AK, Bose S, Srivastava S, Suprasanna P. Chemical intervention for enhancing growth and reducing grain arsenic accumulation in rice. Environ Pollut. 2021 Feb 13:116719.

170. Yadav P, Srivastava S. Effect of thiourea application on root, old leaf and young leaf of two contrasting rice varieties (*Oryza sativa* L.) grown in arsenic contaminated soil. Environ Technol Innov. 2021 Feb 1;21:101368.

171. Petrov VD, Van Breusegem F. Hydrogen peroxide—a central hub for information flow in plant cells. AoB plants. 2012 Jan 1;2012.

172. Niu L, Liao W. Hydrogen peroxide signaling in plant development and abiotic responses: crosstalk with nitric oxide and calcium. Front Plant Sci. 2016 Mar 4;7:230.

173. Hossain MA, Bhattacharjee S, Armin SM, Qian P, Xin W, Li HY, Burritt DJ, Fujita M, Tran LS. Hydrogen peroxide priming modulates abiotic oxidative stress tolerance: insights from ROS detoxification and scavenging. Front Plant Sci. 2015 Jun 16;6:420.

174. Ishibashi Y, Koda Y, Zheng SH, Yuasa T, Iwaya-Inoue M. Regulation of soybean seed germination through ethylene production in response to reactive oxygen species. Ann Bot. 2013 Jan 1;111(1):95-102.

175. Bhattacharjee S. Heat and chilling induced disruption of redox homeostasis and its regulation by hydrogen peroxide in germinating rice seeds (*Oryza sativa* L., Cultivar Ratna). Physiol Mol Biol Plants. 2013 Apr;19(2):199-207.

176. Hu Y, Ge Y, Zhang C, Ju T, Cheng W. Cadmium toxicity and translocation in rice seedlings are reduced by hydrogen peroxide pretreatment. Plant Growth Regul. 2009 Sep;59(1):51-61.

177. Sun Y, Wang H, Liu S, Peng X. Exogenous application of hydrogen peroxide alleviates drought stress in cucumber seedlings. S Afr J Bot. 2016 Sep 1;106:23-8.

178. dos Santos Araújo G, de Oliveira Paula-Marinho S, de Paiva Pinheiro SK, de Castro Miguel E, de Sousa Lopes L, Marques EC, de Carvalho HH, Gomes-Filho E. H_2O_2 priming promotes salt tolerance in maize by protecting chloroplasts ultrastructure and primary metabolites modulation. Plant Sci. 2021 Feb 1;303:110774.

179. Hasanuzzaman M, Nahar K, Gill SS, Alharby HF, Razafindrabe BH, Fujita M. Hydrogen peroxide pretreatment mitigates cadmium-induced oxidative stress in *Brassica napus* L.: an intrinsic study on antioxidant defense and glyoxalase systems. Front Plant Sci. 2017 Feb 10;8:115.

180. Sayed S, Gadallah M. Hydrogen peroxide supplementation alleviates the deleterious effects of cadmium on photosynthetic pigments and oxidative stress and improves growth, yield and pods quality of pea (*Pisum sativum* l.) plants. Acta Physiol Plant. 2019 Jul;41(7):1-2.

181. Silva PC, AzevedoNeto AD, Gheyi HR, Ribas RF, Silva CR, Cova AM. Salt tolerance induced by hydrogen peroxide priming on seed is related to improvement of ion homeostasis and antioxidative defense in sunflower plants. J Plant Nutr. 2020 Dec 12:1-5.

182. Abdel Latef AA, Kordrostami M, Zakir A, Zaki H, Saleh OM. Eustress with H_2O_2 facilitates plant growth by improving tolerance to salt stress in two wheat cultivars. Plants. 2019 Sep;8(9):303.

183. Yoshida S, Forno DA, Cock JH. Laboratory manual for physiological studies of rice. Laboratory manual for physiological studies of rice. 1971.

184. Beauchamp C, Fridovich I. Superoxide dismutase: improved assays and an assay applicable to acrylamide gels. Anal Biochem. 1971 Nov 1;44(1):276-87.

185. Nakano Y, Asada K. Hydrogen peroxide is scavenged by ascorbate-specific peroxidase in spinach chloroplasts. Plant cell Physiol. 1981 Aug 1;22(5):867-80.

186. Aebi H. Catalase. In Methods of enzymatic analysis 1974 Jan 1 (pp. 673-684). Academic press.

187. Smith IK, Vierheller TL, Thorne CA. Assay of glutathione reductase in crude tissue homogenates using 5, 5′-dithiobis (2-nitrobenzoic acid). Anal Biochem. 1988 Dec 1;175(2):408-13.

188. Srivastava S, Mishra S, Tripathi RD, Dwivedi S, Gupta DK. Copper-induced oxidative stress and responses of antioxidants and phytochelatins in *Hydrillaverticillata* (Lf) Royle. Aquat Toxicol. 2006 Dec 30;80(4):405-15.

189. Gillespie KM, Chae JM, Ainsworth EA. Rapid measurement of total antioxidant capacity in plants. Nat Protoc. 2007 Apr;2(4):867-70.

190. Hodges DM, DeLong JM, Forney CF, Prange RK. Improving the thiobarbituric acid-reactive-substances assay for estimating lipid peroxidation in plant tissues containing anthocyanin and other interfering compounds. Planta. 1999 Feb; 207(4):604-11.

191. Bradford MM. A rapid and sensitive method for the quantitation of microgram quantities of protein utilizing the principle of protein-dye binding. Anal Biochem. 1976 May 7;72(1-2):248-54.

192. Gayen D, Barua P, Lande NV, Varshney S, Sengupta S, Chakraborty S, Chakraborty N. Dehydration-responsive alterations in the chloroplast proteome and cell metabolomic profile of rice reveals key stress adaptation responses. Environ Exp Bot. 2019 Apr 1;160:12-24.

193. Roessner-Tunali U, Hegemann B, Lytovchenko A, Carrari F, Bruedigam C, Granot D, Fernie AR. Metabolic profiling of transgenic tomato plants overexpressing hexokinase reveals that the influence of hexose phosphorylation diminishes during fruit development. Plant Physiol. 2003 Sep 1;133(1):84-99.

194. Wang QJ, Sun H, Dong QL, Sun TY, Jin ZX, Hao YJ, Yao YX. The enhancement of tolerance to salt and cold stresses by modifying the redox state and salicylic acid content via the cytosolic malate dehydrogenase gene in transgenic apple plants. Plant Biotech J. 2016 Oct;14(10):1986-97.

195. Ritambhara G, Kumar KS, Dubey RS. Salinity induced behavioral changes in malate dehydrogenase and glutamate dehydrogenase activities in rice seedlings of differing salt tolerance. Plant Sci. 2000;156:23-34.

196. Jalil SU, Ahmad I, Ansari MI. Functional loss of GABA transaminase (GABA-T) expressed early leaf senescence under various stress conditions in *Arabidopsis thaliana*. Curr Plant Biol. 2017 Jun 1;9:11-22..

197. Bournonville CFG, Díaz-Ricci JC. Quantitative determination of superoxide in plant leaves using a modified NBT staining method. Phytochem Anal. 2011 May;22(3):268-71.

198. Gillespie KM, Ainsworth EA. Measurement of reduced, oxidized and total ascorbate content in plants. Nat Protoc. 2007 Apr;2(4):871-4.

199. Zhao X, Chen T, Feng B, Zhang C, Peng S, Zhang X, Fu G, Tao L. Non-photochemical quenching plays a key role in light acclimation of rice plants differing in leaf color. Front Plant Sci. 2017 Jan 10;7:1968.

200. Mirajkar SJ, Suprasanna P, Vaidya ER. Spatial distribution and dynamics of sucrose metabolising enzymes in radiation induced mutants of sugarcane. Plant Physiol Biochem. 2016 Mar 1;100:85-93.

201. Lázaro JJ, Chueca A, Gorgé JL, Mayor F. Fructose-1, 6-diphosphatase from spinach leaf chloroplasts: purification and heterogeneity. Phytochemistry. 1974 Nov 1;13(11):2455-61.

202. Xia J, Wishart DS. Using MetaboAnalyst 3.0 for comprehensive metabolomics data analysis. Curr Protoc Bioinformatics. 2016 Sep;55(1):14-0.

203. Wang Y, Li K, Li X. Auxin redistribution modulates plastic development of root system architecture under salt stress in *Arabidopsis thaliana*. J Plant Physiol. 2009 Oct 15;166(15):1637-45.

204. Jiang K, Schwarzer C, Lally E, Zhang S, Ruzin S, Machen T, Remington SJ, Feldman L. Expression and characterization of a redox-sensing green fluorescent protein

(reduction-oxidation-sensitive green fluorescent protein) in *Arabidopsis*. Plant Physiol. 2006 Jun 1;141(2):397-403.

205. Overvoorde P, Fukaki H, Beeckman T. Auxin control of root development. Cold Spring Harbor perspectives in biology. 2010 Jun 1;2(6):a001537.

206. Fu Y, Yang Y, Chen S, Ning N, Hu H. *Arabidopsis* IAR4 modulates primary root growth under salt stress through ROS-mediated modulation of auxin distribution. Front Plant Sci. 2019 Apr 25;10:522.

207. Su C, Liu L, Liu H, Ferguson BJ, Zou Y, Zhao Y, Wang T, Wang Y, Li X. H_2O_2 regulates root system architecture by modulating the polar transport and redistribution of auxin. J Plant Biol. 2016 Jun;59(3):260-70.

208. Ashrafi E, Razmjoo J, Zahedi M, Pessarakli M. Screening alfalfa for salt tolerance based on lipid peroxidation and antioxidant enzymes. Agronomy J. 2015 Jan;107(1):167-73.

209. Sikder RK, Wang X, Jin D, Zhang H, Gui H, Dong Q, Pang N, Zhang X, Song M. Screening and evaluation of reliable traits of upland cotton (*Gossypium hirsutum* L.) genotypes for salt tolerance at the seedling growth stage. J Cotton Res. 2020 Dec;3:1-3

210. AbdElgawad H, Zinta G, Hegab MM, Pandey R, Asard H, Abuelsoud W. High salinity induces different oxidative stress and antioxidant responses in maize seedlings organs. Front Plant Science. 2016 Mar 8;7:276.

211. Sandhu D, Cornacchione MV, Ferreira JF, Suarez DL. Variable salinity responses of 12 alfalfa genotypes and comparative expression analyses of salt-response genes. Sci Rep. 2017 Feb 22;7(1):1-8.

212. Guler NS, Pehlivan N. Exogenous low-dose hydrogen peroxide enhances drought tolerance of soybean (*Glycine max* L.) through inducing antioxidant system. Acta Biol Hung. 2016 Jun;67(2):169-83.

213. Roy PR, Tahjib-Ul-Arif M, Akter T, Ray SR, Sayed MA. Exogenous ascorbic acid and hydrogen peroxide alleviates salt-induced oxidative stress in rice (*Oryza sativa* L.) by enhancing antioxidant enzyme activities and proline content. Adv Environ Biol. 2016 Oct 1;10(10):148-55.

214. Li JT, Qiu ZB, Zhang XW, Wang LS. Exogenous hydrogen peroxide can enhance tolerance of wheat seedlings to salt stress. Acta Physiol Plant. 2011 May 1;33(3):835-42.

215. Srivastava AK, Srivastava S, Penna S, D'Souza SF. Thiourea orchestrates regulation of redox state and antioxidant responses to reduce the NaCl-induced oxidative damage in Indian mustard (Brassica juncea (L.) Czern.). Plant Physiol Biochem. 2011 Jun 1;49(6):676-86.

216. Gondim FA, Gomes-Filho E, Costa JH, Alencar NL, Prisco JT. Catalase plays a key role in salt stress acclimation induced by hydrogen peroxide pretreatment in maize. Plant Physiol Biochem. 2012 Jul 1;56:62-71.

217. Caverzan A, Bonifacio A, Carvalho FE, Andrade CM, Passaia G, Schünemann M, dos Santos Maraschin F, Martins MO, Teixeira FK, Rauber R, Margis R. The knockdown of chloroplastic ascorbate peroxidases reveals its regulatory role in the photosynthesis and protection under photo-oxidative stress in rice. Plant Sci. 2014 Jan 1;214:74-87.

218. Wu TM, Lin WR, Kao CH, Hong CY. Gene knockout of glutathione reductase 3 results in increased sensitivity to salt stress in rice. Plant Mol Biol. 2015 Apr;87(6):555-64.

219. Wu H, Zhang X, Giraldo JP, Shabala S. It is not all about sodium: revealing tissue specificity and signalling roles of potassium in plant responses to salt stress. Plant Soil. 2018 Oct;431(1):1-7.

220. Marschner H. Marschner's mineral nutrition of higher plants. Academic press; 2011 Aug 8.

221. Almeida DM, Oliveira MM, Saibo NJ. Regulation of Na^+ and K^+ homeostasis in plants: towards improved salt stress tolerance in crop plants. Genet Mol Biol. 2017;40(1):326-45.

222. Ahanger MA, Tomar NS, Tittal M, Argal S, Agarwal RM. Plant growth under water/salt stress: ROS production; antioxidants and significance of added potassium under such conditions. Physiol Mol Biol Plants. 2017 Oct;23(4):731-44.

223. Wang S, Cao M, Ma X, Chen W, Zhao J, Sun C, Tan L, Liu F. Integrated RNA sequencing and QTL mapping to identify candidate genes from *Oryza rufipogon* associated with salt tolerance at the seedling stage. Front Plant Science. 2017 Aug 15;8:1427.

224. Yakhin OI, Lubyanov AA, Yakhin IA, Brown PH. Biostimulants in plant science: a global perspective. Front Plant Science. 2017 Jan 26;7:2049.

225. Nareshkumar A, Subbarao S, Vennapusa AR, Ashwin V, Banarjee R, Kulkarni MJ, Ramu VS, Udayakumar M. Enzymatic and non-enzymatic detoxification of reactive carbonyl compounds improves the oxidative stress tolerance in cucumber, tobacco and rice seedlings. J Plant Growth Regul. 2020 Sep;39(3):1359-72.

226. Yamauchi Y, Hasegawa A, Mizutani M, Sugimoto Y. Chloroplastic NADPH-dependent alkenal/one oxidoreductase contributes to the detoxification of reactive carbonyls produced under oxidative stress. FEBS Lett. 2012 Apr 24;586(8):1208-13.

227. Luo Y, Liu HY, Fan YZ, Wang W, Zhao YY. Comparative chloroplast proteome analysis of exogenously supplied trehalose to wheat seedlings under heat stress. Photosynthetica. 2018 Dec;56(4):1123-33.

228. Zhu J, Fan Y, Shabala S, Li C, Lv C, Guo B, Xu R, Zhou M. Understanding mechanisms of salinity tolerance in barley by proteomic and biochemical analysis of near-isogenic lines. Int J Mol Sci. 2020 Jan;21(4):1516.

229. Nguyen HT, Shim IS, Kobayashi K, Usui K. Regulation of ammonium accumulation during salt stress in rice (*Oryza sativa* L.) seedlings. Plant Prod Sci. 2005;8(4):397-404.

230. Tercé-Laforgue T, Clément G, Marchi L, Restivo FM, Lea PJ, Hirel B. Resolving the role of plant NAD-glutamate dehydrogenase: III. Overexpressing individually or simultaneously the two enzyme subunits under salt stress induces changes in the leaf metabolic profile and increases plant biomass production. Plant Cell Physiol. 2015 Oct 1;56(10):1918-29.

231. Wang B, Xie G, Liu Z, He R, Han J, Huang S, Liu L, Cheng X. Mutagenesis reveals that the OsPPa6 gene is required for enhancing the alkaline tolerance in rice. Front Plant Sci. 2019 Jun 11;10:759.

232. Huihui Z, Xin L, Yupeng G, Mabo L, Yue W, Meijun A, Guanjun L, Nan X, Guangyu S. Physiological and proteomic responses of reactive oxygen species metabolism and antioxidant machinery in mulberry (*Morus alba* L.) seedling leaves to NaCl and $NaHCO_3$ stress. Ecotoxicol Environ Saf. 2020 Apr 15;193:110259.

233. Lakra N, Kaur C, Singla-Pareek SL, Pareek A. Mapping the 'early salinity response'triggered proteome adaptation in contrasting rice genotypes using iTRAQ approach. Rice. 2019 Dec;12(1):1-22.

234. Wani AS, Ahmad A, Hayat S, Fariduddin Q. Salt-induced modulation in growth, photosynthesis and antioxidant system in two varieties of *Brassica juncea*. Saudi J Biol Sci. 2013 Apr 1;20(2):183-93.

235. Khelil A, Menu T, Ricard B. Adaptive response to salt involving carbohydrate metabolism in leaves of a salt-sensitive tomato cultivar. Plant Physiol Biochem. 2007 Aug 1;45(8):551-9.

236. Brankova L, Ivanov S, Alexieva V. The induction of microsomal NADPH: cytochrome P450 and NADH: cytochrome b5 reductases by long-term salt treatment of cotton (*Gossypiumhirsutum* L.) and bean (*Phaseolus vulgaris* L.) plants. Plant Physiol Biochem. 2007 Sep 1;45(9):691-5.

237. Jimbo H, Yutthanasirikul R, Nagano T, Hisabori T, Hihara Y, Nishiyama Y. Oxidation of translation factor EF-Tu inhibits the repair of photosystem II. Plant Physiol. 2018 Apr 1;176(4):2691-9.

238. Rausch T, Wachter A. Sulfur metabolism: a versatile platform for launching defence operations. Trends Plant Sci. 2005 Oct 1;10(10):503-9.

239. Nechushtai R, Conlan AR, Harir Y, Song L, Yogev O, Eisenberg-Domovich Y, Livnah O, Michaeli D, Rosen R, Ma V, Luo Y. Characterization of *Arabidopsis* NEET reveals an ancient role for NEET proteins in iron metabolism. Plant Cell. 2012 May 1;24(5):2139-54.

240. Calderón A, Ortiz-Espín A, Iglesias-Fernández R, Carbonero P, Pallardó FV, Sevilla F, Jiménez A. Thioredoxin (Trxo1) interacts with proliferating cell nuclear antigen (PCNA) and its overexpression affects the growth of tobacco cell culture. Redox Biol. 2017 Apr 1;11:688-700.

241. Zhang Z, Liu X, Li R, Yuan L, Dai Y, Wang X. Identification and functional analysis of a protein disulfide isomerase (AtPDI1) in *Arabidopsis thaliana*. Front Plant Sci. 2018 Jul 19;9:913.

242. Neto AD, Prisco JT, Enéas-Filho J, Medeiros JV, Gomes-Filho E. Hydrogen peroxide pre-treatment induces salt-stress acclimation in maize plants. J Plant Physiol. 2005 Oct 14;162(10):1114-22.

243. Sathiyaraj G, Srinivasan S, Kim YJ, Lee OR, Parvin S, Balusamy SR, Khorolragchaa A, Yang DC. Acclimation of hydrogen peroxide enhances salt tolerance by activating defense-related proteins in *Panax ginseng* CA Meyer. Mol Biol Rep. 2014 Jun 1;41(6):3761-71.

244. Hugouvieux V, Dutilleul C, Jourdain A, Reynaud F, Lopez V, Bourguignon J. *Arabidopsis* putative selenium-binding protein1 expression is tightly linked to cellular sulfur demand and can reduce sensitivity to stresses requiring glutathione for tolerance. Plant Physiol. 2009 Oct 1;151(2):768-81.

245. Hu R, Zhu Y, Wei J, Chen J, Shi H, Shen G, Zhang H. Overexpression of PP2A-C5 that encodes the catalytic subunit 5 of protein phosphatase 2A in *Arabidopsis* confers better root and shoot development under salt conditions. Plant Cell Environ. 2017 Jan;40(1):150-64.

246. Máthé C, Garda T, Freytag C. The role of serine-threonine protein phosphatase pp2a in plant oxidative stress signaling—facts and hypotheses. Int J Mol Sci. 2019 Jan;20(12):3028.

247. Das P, Manna I, Sil P, Bandyopadhyay M, Biswas AK. Exogenous silicon alters organic acid production and enzymatic activity of TCA cycle in two NaCl stressed indica rice cultivars. Plant Physiol Biochem. 2019 Mar 1;136:76-91.

248. Abogadallah GM. Differential regulation of photorespiratory gene expression by moderate and severe salt and drought stress in relation to oxidative stress. Plant Sci. 2011 Mar 1;180(3):540-7.

249. Amthor JS, Bar-Even A, Hanson AD, Millar AH, Stitt M, Sweetlove LJ, Tyerman SD. Engineering strategies to boost crop productivity by cutting respiratory carbon loss. Plant Cell. 2019 Feb 1;31(2):297-314.

250. Sánchez-Martín JA, Heald JI, Kingston-Smith AL, Winters AN, Rubiales D, Sanz M, Mur LA, Prats E. A metabolomic study in oats (*Avena sativa*) highlights a drought tolerance mechanism based upon salicylate signalling pathways and the modulation of carbon, antioxidant and photo-oxidative metabolism. Plant Cell Environ. 2015 Jul;38(7):1434-52.

251. Jayakannan M, Bose J, Babourina O, Rengel Z, Shabala S. Salicylic acid improves salinity tolerance in *Arabidopsis* by restoring membrane potential and preventing salt-induced K^+ loss via a GORK channel. J Exp Bot. 2013 May 1;64(8):2255-68

252. Pandey M, Srivastava AK, Suprasanna P, D'Souza SF. Thiourea mediates alleviation of UV-B stress-induced damage in the Indian mustard (*Brassica juncea* L.) J Plant Interact. 2012 Jun 1;7(2):143-50.

253. Goswami L, Sengupta S, Mukherjee S, Ray S, Mukherjee R, Majumder AL. Targeted expression of L-myo-inositol 1-phosphate synthase from *Porteresiacoarctata* (Roxb.) Tateoka confers multiple stress tolerance in transgenic crop plants. J Plant Biochem Biotechnol 2014 Jul 1;23(3):316-30.

254. Nisa ZU, Chen C, Yu Y, Chen C, Mallano AI, Xiang-bo D, Xiao-li S, Yan-ming Z. Constitutive overexpression of myo-inositol-1-phosphate synthase gene (GsMIPS2) from *Glycine soja* confers enhanced salt tolerance at various growth stages in *Arabidopsis*. Journal of Northeast Agricultural University (English Edition). 2016 Jun 1;23(2):28-44.

255. Lu YA, Sharkey TD. The importance of maltose in transitory starch breakdown. Plant Cell Environ. 2006 Mar;29(3):353-66.

256. Thalmann M, Santelia D. Starch as a determinant of plant fitness under abiotic stress. New Phytol. 2017 May;214(3):943-51.

257. Valerio C, Costa A, Marri L, Issakidis-Bourguet E, Pupillo P, Trost P, Sparla F. Thioredoxin-regulated β-amylase (BAM1) triggers diurnal starch degradation in guard cells, and in mesophyll cells under osmotic stress. J Exp Bot. 2011 Jan 1;62(2):545-55.

258. Chen HJ, Chen JY, Wang SJ. Molecular regulation of starch accumulation in rice seedling leaves in response to salt stress. Acta Physiol Plant. 2008 Mar 1;30(2):135-42.

259. Ahanger MA, Qin C, Begum N, Maodong Q, Dong XX, El-Esawi M, El-Sheikh MA, Alatar AA, Zhang L. Nitrogen availability prevents oxidative effects of salinity on wheat growth and photosynthesis by up-regulating the antioxidants and osmolytes metabolism, and secondary metabolite accumulation. BMC Plant Biol. 2019 Dec;19(1):1-2.

260. Garg BK, Burman U, Kathju S. Influence of thiourea on photosynthesis, nitrogen metabolism and yield of clusterbean (*Cyamopsistetragonoloba* (L.) Taub.) under rainfed conditions of Indian arid zone. Plant Growth Regul. 2006 Mar;48(3):237-45.

261. Bayliak MM, Lylyk MP, Vytvytska OM, Lushchak VI. Assessment of antioxidant properties of alpha-keto acids in vitro and in vivo. Eur Food Res Technol. 2016 Feb 1;242(2):179-88.

262. Al-Quraan NA, Locy RD, Singh NK. Implications of paraquat and hydrogen peroxide-induced oxidative stress treatments on the GABA shunt pathway in *Arabidopsis thaliana* calmodulin mutants. Plant Biotechnol Rep. 2011 Jul;5(3):225-34.

263. Ramos-Ruiz R, Martinez F, Knauf-Beiter G. The effects of GABA in plants. Cogent Food Agric. 2019 Jan 1;5(1):1670553.

264. Sudhir P, Murthy SD. Effects of salt stress on basic processes of photosynthesis. Photosynthetica. 2004 Dec 1;42(2):481-6.

265. Lemoine R, La Camera S, Atanassova R, Dédaldéchamp F, Allario T, Pourtau N, Bonnemain JL, Laloi M, Coutos-Thévenot P, Maurousset L, Faucher M. Source-to-sink transport of sugar and regulation by environmental factors. Front Plant Sci. 2013 Jul 24;4:272.

266. Neang S, de Ocampo M, Egdane JA, Platten JD, Ismail AM, Skoulding NS, Kano-Nakata M, Yamauchi A, Mitsuya S. Fundamental parenchyma cells are involved in Na^+ and Cl^-removal ability in rice leaf sheath. Funct Plant Biol. 2019 Jul 23;46(8):743-55.

267. Asch F, Dingkuhn M, Dörffling K, Miezan K. Leaf K/Na ratio predicts salinity induced yield loss in irrigated rice. Euphytica. 2000 May;113(2):109-18.

268. Hasan SA, Irfan M, Masrahi YS, Khalaf MA, Hayat S. Growth, photosynthesis, and antioxidant responses of *Vigna unguiculata* L. treated with hydrogen peroxide. Cogent Food Agric. 2016 Dec 31;2(1):1155331.

269. Santos CV. Regulation of chlorophyll biosynthesis and degradation by salt stress in sunflower leaves. Sci Hortic. 2004 Dec 31;103(1):93-9.

270. Wu TM, Lin WR, Kao YT, Hsu YT, Yeh CH, Hong CY, Kao CH. Identification and characterization of a novel chloroplast/mitochondria co-localized glutathione reductase 3 involved in salt stress response in rice. Plant Mol Biol. 2013 Nov 1;83(4-5):379-90.

271. Hernandez JA, Jiménez A, Mullineaux P, Sevilia F. Tolerance of pea (*Pisum sativum* L.) to long-term salt stress is associated with induction of antioxidant defences. Plant Cell Environ. 2000 Aug;23(8):853-62.

272. Tsai YC, Hong CY, Liu LF, Kao CH. Expression of ascorbate peroxidase and glutathione reductase in roots of rice seedlings in response to NaCl and H_2O_2. J Plant Physiol. 2005 Mar 14;162(3):291-9.

273. Tsai YC, Chen KC, Cheng TS, Lee C, Lin SH, Tung CW. Chlorophyll fluorescence analysis in diverse rice varieties reveals the positive correlation between the seedlings salt tolerance and photosynthetic efficiency. BMC Plant Biology. 2019 Dec;19(1):1-7.

274. Nishiyama Y, Allakhverdiev SI, Murata N. Protein synthesis is the primary target of reactive oxygen species in the photoinhibition of photosystem II. Physiol Plant 2011 May;142(1):35-46.

275. Güler NS, Pehlivan N. Role of H_2O_2 on photosynthetic characteristics of soybean genotypes under low water input. Sakarya Üniversitesi Fen Bilimleri Enstitüsü Dergisi. 2020 Feb 1;24(1):183-8.

276. Srivastava AK, Ramaswamy NK, Mukopadhyaya R, Jincy MC, D'souza SF. Thiourea modulates the expression and activity profile of mtATPase under salinity stress in seeds of *Brassica juncea*. Ann Bots. 2009 Feb 1;103(3):403-10.

277. Srivastava AK, Sablok G, Hackenberg M, Deshpande U, Suprasanna P. Thiourea priming enhances salt tolerance through co-ordinated regulation of microRNAs and hormones in *Brassica juncea*. Sci Rep. 2017 Apr 6;7(1):1-5.

278. Cho MH, Jang A, Bhoo SH, Jeon JS, Hahn TR. Manipulation of triose phosphate/phosphate translocator and cytosolic fructose-1, 6-bisphosphatase, the key components in photosynthetic sucrose synthesis, enhances the source capacity of transgenic *Arabidopsis* plants. Photosynth Res. 2012 Mar;111(3):261-8.

279. Ozaki K, Uchida A, Takabe T, Shinagawa F, Tanaka Y, Takabe T, Hayashi T, Hattori T, Rai AK, Takabe T. Enrichment of sugar content in melon fruits by hydrogen peroxide treatment. J Plant Physiol. 2009 Apr 1;166(6):569-78.

280. Ishibashi Y, Yamaguchi H, Yuasa T, Iwaya-Inoue M, Arima S, Zheng SH. Hydrogen peroxide spraying alleviates drought stress in soybean plants. J Plant Physiol. 2011 Sep 1;168(13):1562-7.

Appendix

Table-3.2.4: Metabolite score table. Identified metabolites were given a score calculated on the basis of PCA scores (refer sec.2.19)

S.NO.	Metabolites	Control	TU	H_2O_2	NaCl	NaCl + TU	NaCl + H_2O_2
1.	Propanedioic acid	0.50	0.65	-0.17	-0.32	-0.67	-0.83
2.	N-Methyltrifluoroacetamide	0.79	0.16	-0.04	0.20	0.41	0.35
3.	4-Hydroxybutanoic	2.01	-0.61	-0.31	-0.67	-0.29	-0.61
4.	Diethylene	2.01	-0.61	-0.31	-0.36	-0.29	-0.61
5.	L-Serine,	1.23	-0.21	-0.19	-0.33	-0.21	-0.41
6.	Ethanolamine,	0.07	0.62	-0.11	-0.55	-0.63	-0.72
7.	Silanol,	1.01	-0.17	-0.12	-0.18	0.06	-0.07
8.	L-Threonine,	-0.30	-0.01	0.05	0.03	0.07	0.12
9.	L- Glycine,	-0.81	0.16	0.17	0.15	0.43	0.60
10.	Butanedioic	0.68	-0.07	-0.08	0.06	0.09	0.01
11.	Glyceric	-0.30	0.48	-0.05	-0.37	-0.56	-0.59
12.	L-Aspartic acid	-1.50	-0.27	0.25	0.53	0.30	0.55
13.	Malic acid	-1.20	0.33	0.26	0.52	0.62	0.88
14.	Salicylic acid	-0.83	-0.03	0.15	0.35	0.25	0.40
15.	meso-Erythritol,	0.51	0.01	-0.10	-0.18	-0.20	-0.29
16.	L-5-Oxoproline,	-1.43	-0.31	0.22	0.16	0.20	0.43
17.	Pyroglutamic acid	-1.19	-0.07	0.10	-0.03	-0.33	-0.20
18.	1-Deoxypentitol,	1.37	0.30	-0.28	-0.64	-0.65	-0.93
19.	2,3,4-Trihydroxybutyric	2.01	-0.61	-0.31	-0.50	-0.29	-0.61

20.	2,3-Dihydroxy-2-methylpropanoic	1.83	-0.51	-0.28	-0.37	-0.25	-0.54
21.	L-Threonic	-0.06	0.48	-0.08	-0.29	-0.56	-0.62
22.	D-Erythro-Pentitol,	1.99	-0.64	-0.30	-0.43	-0.21	-0.52
23.	Cyclooctasiloxane,	1.64	0.03	-0.31	-0.47	-0.59	-0.90
24.	D-Arabinose,	-0.75	0.20	0.03	0.08	-0.43	-0.38
25.	L-(-)-Arabitol,	-0.29	-0.01	0.03	0.00	-0.03	0.01
26.	Adonitol	1.20	0.32	-0.26	-0.40	-0.62	-0.87
27.	Xylitol,	-1.06	0.03	0.08	-0.24	-0.37	-0.27
28.	4-Ketoglucose,	2.00	-0.62	-0.31	-0.61	-0.26	-0.58
29.	2,6-Dihydroxybenzoic	0.71	0.60	-0.20	-0.40	-0.67	-0.86
30.	Ribonic	0.71	-0.07	-0.08	0.09	0.11	0.03
31.	L-Fucitol,	1.57	0.10	-0.30	-0.50	-0.61	-0.91
32.	Inososе,	1.94	-0.39	-0.32	-0.55	-0.44	-0.77
33.	Shikimic acid	-1.09	0.04	0.21	0.53	0.42	0.63
34.	Citric acid	-1.44	-0.32	0.17	0.00	-0.15	0.03
35.	D-(+)-Ribono-1,4-lactone,	1.32	0.33	-0.28	-0.45	-0.66	-0.93
36.	2-Ketoglutaric	0.91	0.26	-0.20	-0.31	-0.52	-0.72
37.	Quininic acid	-1.28	0.01	0.24	0.52	0.45	0.69
38.	D-Fructose,	-1.07	0.39	0.24	0.57	0.63	0.86
39.	D-(+)-Talose,	-1.12	-0.02	0.21	0.32	0.37	0.58
40.	D-Mannose,	1.77	-0.14	-0.32	-0.51	-0.54	-0.86
41.	Butanal,	2.01	-0.61	-0.31	-0.37	-0.29	-0.61

42.	Methyl	1.65	-0.48	-0.21	-0.44	0.02	-0.21
43.	Ribitol,	1.09	0.14	-0.22	-0.32	-0.49	-0.70
44.	D-Gluconic acid	1.94	-0.60	-0.29	-0.56	-0.24	-0.54
45.	Palmitic acid	-1.13	-0.03	0.09	-0.19	-0.34	-0.23
46.	Myo-Inositol,	-1.82	-0.54	0.27	0.21	0.20	0.49
47.	Pentenoic acid	-0.77	0.33	0.19	0.38	0.53	0.71
48.	D-(+)-Galactose,	0.99	-0.13	-0.11	-0.30	0.15	0.03
49.	Glucopyranose,	1.91	-0.47	-0.31	-0.66	-0.36	-0.67
50.	D-Glucose,	-1.11	0.05	0.21	0.20	0.43	0.64
51.	Gluconic acid	2.01	-0.61	-0.31	-0.45	-0.29	-0.61
52.	Stearic acid	-0.22	0.37	-0.05	-0.43	-0.49	-0.52
53.	beta-D-(+)-Talopyranose,	1.15	-0.23	-0.15	-0.40	0.02	-0.14
54.	D-(+)-Galacturonic	1.97	-0.59	-0.30	-0.69	-0.28	-0.59
55.	Octasiloxane,	0.03	0.06	0.03	-0.11	0.20	0.22
56.	Lactulose,	-0.33	0.10	0.09	0.00	0.28	0.36
57.	Sucrose,	-1.54	-0.27	0.25	0.46	0.32	0.58
58.	Maltose,	-0.36	0.22	0.11	0.30	0.40	0.50
59.	D-(+)-Turanose,	2.02	-0.61	-0.31	-0.48	-0.29	-0.62
60.	Galactinol,	0.25	0.63	-0.13	-0.36	-0.64	-0.76
61.	Tris(2,4-di-tert-butylphenyl)	2.01	-0.61	-0.31	-0.47	-0.29	-0.61
62.	3-.alpha.-Mannobiose,	0.97	0.52	-0.23	-0.49	-0.67	-0.90
63.	L-Rhamnose,	-0.59	0.27	0.01	-0.11	-0.46	-0.43

64.	D-Glucuronic	-0.54	0.38	-0.01	-0.38	-0.52	-0.51
65.	Amphetamine,	-0.37	-0.02	0.05	0.11	0.00	0.06
66.	Glycerol,	-0.55	0.36	-0.01	-0.18	-0.51	-0.50
67.	Xylose,	-1.80	-0.55	0.26	0.38	0.13	0.41
68.	L-(+)-Threose,	-0.53	0.39	-0.01	-0.19	-0.52	-0.52
69.	D-(-)-Erythrose,	-0.44	0.11	0.11	0.24	0.31	0.41
70.	Acetin,	-0.43	0.43	-0.03	-0.21	-0.54	-0.55
71.	1,2,3-Butanetriol,	-0.43	0.43	-0.03	-0.21	-0.54	-0.55
72.	L-Asparagine,	-0.43	0.43	-0.03	-0.21	-0.54	-0.55
73.	D-Psicofuranose,	-0.70	0.25	0.02	-0.12	-0.45	-0.42
74.	D-(+)-Cellobiose,	-0.43	0.43	-0.03	-0.21	-0.54	-0.55
75.	L-Valine,	-0.38	0.04	0.08	0.18	0.21	0.30
76.	Erythritol,	-0.38	0.04	0.08	0.18	0.21	0.30
77.	Trimethylsilyl	-0.38	0.04	0.08	0.18	0.21	0.30
78.	Dulcitol,	-0.38	0.04	0.08	0.18	0.21	0.30
79.	Deoxyglucose,	-0.61	0.07	0.13	0.27	0.30	0.43
80.	Trimethylsilyl-di(timethylsiloxy)-silane	-0.61	0.07	0.13	0.27	0.30	0.43
81.	Methylsuccinic	-0.61	0.07	0.13	0.27	0.30	0.43
82.	Pentanedioic	-0.84	0.10	0.05	-0.05	-0.37	-0.30
83.	Propanetriol,	-0.40	0.10	0.10	0.22	0.29	0.38

Thesis Highlight

Name of the Student: Manish Pandey **Name of the CI/OCC**: B.A.R.C.

Enrolment No.: LIFE01201504006 **Thesis Title:** Study of redox associated molecular changes under salt stress in rice (*Oryza sativa* L.)

Discipline: Life Sciences **Sub-Area of Discipline**: Biochemistry

Date of viva voce: 28th may 2021

Maintenance of the redox homeostasis was considered as central component for plant's adaptation under salt stress. Fine tuning of the redox homeostasis can be achieved with the application of low doses of plant bioregulators (PBRs), which boosted the built-in defense and confer stress tolerance in plants. The differential regulation of redox homeostasis conferring the salinity tolerance under contrasting PBRS; thiourea (TU, non-physiological thiol-based ROS scavenger) and H_2O_2 (a physiologically produced ROS), was evaluated. In spite of having the opposite mode of regulation on ROS levels, both TU and H_2O_2 were able to induce the reducing redox status as indicated by the higher levels of Trolox equivalent and higher fluorescence intensity of redox-sensitive dyes. Additionally, the activation of antioxidant system along with improved K^+ retention was found to co-relate with plant growth and survival under stress. The analysis at gene, protein and metabolite levels helped in the identification of specific as well as common components associated with NT and NH treatments mediated amelioration of NaCl stress in rice. The activation of salt stress responsive genes (*OsHAK* and *OsLEA*), protection of photosystems and ATP synthase together with alternate pathways mediated metabolites shuffling in mitochondria like, activation of GABA-shunt and Mal/Asp shuttle system under "NaCl+H2O2" and "NaCl+TU" treatments respectively substantiated the improved plant growth under stress conditions.

Further, the study was advanced for field evaluation of TU and H2O2 for their efficacy and agronomic feasibility under realistic field conditions. A positive upregulation of source-sink equilibrium along with improved yield associated parameters were observed in the plants subjected to TU and H2O2 foliar applications. Taken together, the findings concluded that both TU and H2O2 can maintain the reduced redox status that serve as "core" regulator for enhancing plant growth and minimizing yield gap, under both lab as well as field conditions.